Aus dem Universitätsklinikum Münster

Institut für Translationale Neurologie

Direktor: Univ-Prof. Dr. med. Dr. rer. nat. Dr. h.c. Sven Meuth

The Role of KCNQ-Channels in the Pathophysiology of Multiple Sclerosis

INAUGURAL – DISSERTATION

zur

Erlangung des doctor medicinae

der Medizinischen Fakultät

der Westfälischen Wilhelms-Universität Münster

vorgelegt von Delank, Anna-Katharina

aus Bochum, Deutschland

2020

Gedruckt mit Genehmigung der Medizinischen Fakultät der Westfälischen Wilhelms-Universität Münster

Dekan: Univ.-Prof. Dr. med. Frank Ulrich Müller

1. Berichterstatter: Univ-Prof. Dr. med. Dr. rer. nat. Dr. h.c. Sven Meuth

2. Berichterstatter: Univ.-Prof. Dr. med. Dr. phil. Udo Dannlowski

Tag der mündlichen Prüfung: 04.12.2020

Aus dem Universitätsklinikum Münster

Institut für Translationale Neurologie

- Direktor: Univ-Prof. Dr. med. Dr. rer. nat. Dr. h.c. Sven Meuth -

Referent: Univ-Prof. Dr. med. Dr. rer. nat. Dr. h.c. Sven Meuth

Korreferent: Univ.-Prof. Dr. med. Dr. phil. Udo Dannlowski

ZUSAMMENFASSUNG

The Role of KCNQ-Channels in the Pathophysiology of Multiple Sclerosis

Delank, Anna-Katharina

Multiple Sklerose (MS) ist eine demyelinisierende Autoimmunerkrankung des zentralen Nervensystems. Durch den autoreaktiven Angriff auf Myelinscheiden kommt es zu Neurodegeneration mit Veränderungen der neuronalen Erregbarkeit und Reizweiterleitung. Ziel dieser Dissertation ist es, den Einfluss von KCNQ-Kanälen auf diese pathophysiologischen Veränderungen zu untersuchen. KCNQ-Kanäle sind spannungsabhängige Kalium Kanäle, die das Membranpotential hyperpolarizieren und somit die neuronale Aktivität regulieren. Das Antikonvulsivum Retigabine nutzt diesen Mechanismus und setzt durch Öffnen der KCNQ-Kanäle die neuronale Erregbarkeit herab. Es konnte gezeigt werden, dass eine prophylaktische Retigabine Therapie eine Verbesserung des Outcomes einer experimentellen autoimmunen Enzephalitis (EAE), einem MS-Tiermodell, erzielte. Da das Antikonvulsivum die Proliferation und Cytokinproduktion von murinen Splenozyten nicht beeinflusste, vermuten wir keinen Einfluss von KCNQ-Kanälen auf die zugrundeliegende Immunreaktion von EAE/MS. Mit Hilfe des Cuprizone-Modells untersuchten wir den Einfluss der Kanäle auf Neurodegeneration und konnten zeigen, dass mit Retigabine behandelte Mäuse weniger Auffälligkeiten in Verhaltensexperimenten zeigten. Dies weist auf ein besseres Lern- und Erinnerungsvermögen der Tiere hin, welches durch die neurodegenerativen Vorgänge stark beeinflusst sein kann. Daher ergeben sich Hinweise auf eine neuroprotektive Eigenschaft von Retigabine und konsekutiv auf einen Einfluss von KCNQ-Kanälen in der Pathophysiologie von MS.

Die tierexperimentellen Arbeiten sind am 04.08.16, 08.05.17 und 26.02.19 durch das Landesamt für Natur, Umwelt und Verbraucherschutz genehmigt worden (84-02.04.2015.A585, 84-02.04.2016.A307, 81-02.04.2018.A266).

Tag der mündlichen Prüfung: 04.12.2020

Eidesstattliche Erklärung

Ich gebe hiermit die Erklärung ab, dass ich die Dissertation mit dem Titel:

„The Role of KCNQ-Channels in the Pathophysiology of Multiple Sclerosis"

in dem Institut für Translationale Neurologie
des Universitätsklinikums Münster
unter Anleitung von Herrn Univ-Prof. Dr. med. Dr. rer. nat. Dr. h.c. Sven Meuth

1. selbstangefertigt
2. nur unter Benutzung der im Literaturverzeichnis angegebenen Arbeiten angefertigt und sonst kein anderes gedrucktes oder ungedrucktes Material verwendet,
3. keine unerlaubte fremde Hilfe in Anspruch genommen,
4. sie weder in der gegenwärtigen noch in einer anderen Fassung einer in- oder ausländischen Fakultät als Dissertation, Semesterarbeit, Prüfungsarbeit oder zur Erlangung eines akademischen Grades vorgelegt habe.

Münster, den

Anna-Katharina Delank

Inhaltsverzeichnis

1. Introduction

1.1 Multiple Sclerosis

Multiple Sclerosis (MS) is an inflammatory and demyelinating disorder of the central nervous system (CNS). It is widely considered as autoimmune disease with an inflammatory and neurodegenerative component, resulting in neuronal damage with axonal transection and demyelination (1–4). It is the most common cause of neurological disabilities in young patients in Europe and North America, with an average age at onset of 20 - 40 years (5). Different genetic and environmental risk factors are discussed as potential hallmarks, but the main cause of the disease is still to be unraveled (6). The symptoms of MS are diverse and the clinical development is depending on sex, age and genetics, as the intrinsic buffering systems for inflammatory stressors alter with these factors (7). Most frequent symptoms are visual disturbance, paresthesia, ataxia, bladder dysfunction, fatigue and cognitive deficits (3). In general, MS can involve all neurological systems like motor, sensory, visual and autonomic ones (6). The categorization of MS is depending on the clinical course. The first episode of neurological deficit is called clinically isolated syndrome (CIS) (6). Not all CISs progress into a manifested MS (4). Therefore, the diagnosis of MS needs a combination of confirmed CIS and magnet resonance imaging (MRI) showing lesions in the CNS disseminated in time and space, which is known as McDonald criteria (8). A common disease course is relapsing remitting MS (RRMS) with is defined by complete or partial recovery after a clinical episode (3,4). These episodes are clinical exacerbations with neurological symptoms related to myelin loss, that persist for at least 24 h in the absence of fever or inflammatory sings (9).

The treatment of MS is varying depending on the patient, severity of the disease, the disease course, preferences of the physician and costs (10). Exacerbations are normally treated with high-dose corticosteroids applied intravenously (11). Glucocorticoids do not affect the course of the disease but reduce the symptoms (10). Besides that kind of approach, disease modifying therapy (DMT) is used to influence the outcome of MS and moderate its progression (10). DMTs are directed against the inflammatory response, that is observed in the infiltration of immune cells in MS lesions (10). The first established DMTs were interferons and glatiramer acetate (12) and recently monoclonal antibodies as Alemtuzumab (anti-CD52-antibody), Natalizumab

(anti-α4-integrin-antibody) and Ocrelizumab (anti-CD20-antibody) are used (10). Despite therapeutic options, MS remains a progressing disease very heterogeneous in clinical course and severity. No curative treatment is availably so far and therefore, investigations focusing on the pathophysiology of this disease and possible therapeutic strategies are needed.

1.2 Pathophysiology of MS

MS is widely considered as autoimmune disease with an inflammatory and neurodegenerative component. The underlining pathophysiological mechanism is subject of ongoing investigations. The most accepted theory is, that T-cells react on myelin antigens, which are presented on antigen presenting cells like macrophages, microglia, astrocytes and cerebral endothelia cells (3). This leads to an immune reaction against the myelin-oligodendrocyte complex resulting in inflammatory and neurodegenerative lesions in the white and grey matter regions of the CNS (13,14). Since the underlying factors for the development of MS are still not fully understood, it remains unclear if neurodegeneration requires or causes the inflammatory process.

There are different theories for the development of autoimmunity in MS (4). Because many microbial proteins share homologies in the structure with the human myelin sheath it is thought, that they trigger an autoreactive reaction with myelin destruction as a consequence of a process called molecular mimicry (15). This theory supports the inflammatory onset of the disease. Since there is evidence that initial MS lesions can be independent from inflammation, another hypothesis suggests that damage occurs firstly to the CNS and then it is followed by an autoimmune reaction (inside-out hypothesis) (4,16,17). This theory hypothesizes, that macrophages and microglia, which are responsible to clean neurodegenerative lesion, are lacking the capacity to remove all myelin debris and the remaining fragments function as antigens in an autoimmune way, triggering further immune reactions (18,19). In general, different steps are needed for the manifestation of MS (20): priming of T-cells against self-antigens of the CNS and migration of those pro-inflammatory cells in the CNS with passing the blood brain barrier (BBB) (20). Therefore, the BBB, which usually separates neuronal structures from the vascular space marking the brain as immune privileged organ, needs to be damaged, e.g. by activated T-cells and their

proinflammatory cytokines (21). The entering $CD8^+$ T-cells, which are mainly responsible for the immune reaction in MS (22), cause an extensive damage to myelin sheath and axons (23,24) by reacting on self-antigens of the CNS like myelin oligodendrocyte glycoprotein (MOG), myelin basic protein (MBP), proteolipid protein (PLP) and lipids (4). Secondary to the lymphatic immune reaction, factors as oxidative stress, mitochondria dysfunction and subsequent ion channel dysfunction are supporting the inflammatory reaction (7). Brain resident immune cells get involved (7), leading to an overall immune reaction with oligodendrocyte death and degeneration of myelin and axons (20).

Demyelination, loss of oligodendrocytes, astrogliosis, destruction of thin caliber axons, axonal transection and impaired remyelination are hallmarks of the neurodegenerative process in MS (1,25). Demyelination is induced by leucocytes and produced cytokines, but inflammation is not essential for demyelination (26). Within the demyelination process, the metabolic supplementation of the neuronal membrane becomes insufficient resulting in myelin degeneration occurring without the presence of macrophages (14). Without myelin, the action potential (AP) conduction switches from saltatory to a continuous one which requires more energy supply (4). For continuous AP conduction more Na^+ channels along the axon are needed, which results in greater Na^+ influx (4,27). To reestablish the membrane potential by Na^+/K^+ ATPase more adenosine trisphosphate (ATP) and therefore more mitochondria are needed, with consequent higher H_2O_2 production (4,27). H_2O_2 can react to highly reactive radicals like OH•, which cause further damage to the cells (4). With insufficient energy supplementation, Na^+ ions start to accumulate intracellularly, which results in reverse activation of the Na^+/Ca^{2+} exchanger. The increasing intracellular Ca^{2+} can result in Ca^{2+} dependent cell death (28) and in increasing levels of excitotoxic amino acids like glutamate (29). In physiologic conditions, the increased glutamate transmission can be useful to restore the function of remaining neurons, which have lost their synaptic inputs, but in MS the glutamate transmission is exaggerated and triggers excitotoxic dendritic spine loss and neuron-to-neuron dysconnectivity which can result in neuronal death (30).

Chronic lesions in the brain show remyelination (31) because of increased numbers of promyelinating oligodendrocytes (11). This process is most active during acute inflammation, but also occurs during the progressive phase of MS (6) and it is stronger

in the cortex compared to white matter regions (31). The underlying process, namely, how remyelination is initiated, is the subject of ongoing investigations. Moreover, since the original status, the one before demyelination, might not be reestablished, it is an aim of ongoing research to assess how remyelination works and how this process can be pharmacologically supported. Therefore, different animal models are used to learn more about the pathophysiology and therapeutic options of MS.

1.3 Animal Models in MS Research

There are different limitations in human studies of MS research. The access to human tissue is limited, as biopsies are rarely performed and tissue deriving from autopsies is normally coming from a chronic stage of the disease (32,33). It is not possible to study the pathophysiology in patients (32), as not all stages of the disease can be addressed. Furthermore, the different pathophysiological mechanisms cannot be observed separately in human studies, as the disease is mainly diagnosed in a symptomatic stage (33). Therefore, animal models are essential in MS research. Animal experiments allow insides into pathophysiological mechanisms as well as therapeutic options due to standardization, reproducibility and easily modifications of the experimental setup (32–34). The most common used animal model for MS is the experimental autoimmune/allergic encephalitis (EAE), but there are also viral induced models of encephalitis like Theiler's immune encephalomyelitis virus, and chronic demyelinating models like the cuprizone model of de- and remyelination, and focal demyelination induced by lyso-phosphatidylcholin (32). For our studies we took advantage of the EAE model, as it is a well-established and best explored animal model in MS research, and the cuprizone model of de- and remyelination, to focus on neurodegeneration independent from inflammation.

1.3.1 Experimental Autoimmune Encephalitis

The EAE model is the most common used animal model for MS. It was established by River et al. in 1933 (35). EAE can be induced in primates and rodents by exposing the animals to CNS specific antigens, peptides derived from these antigens or CNS tissue homogenates (4). An active EAE immunizes animals with peptides from the CNS and the immune reaction is “boosted” using an adjuvant like Freud’s adjuvant with or without pertussis toxin, to promote the immune reaction. The peptides are functioning as CNS specific antigens with MOG, MBP, PLP and lipids as most commonly used ones (36). A MOG_{35-55} induced experimental outline in C57BL/6 mice causes an monophasic EAE with onset of symptoms about day 9-14 after immunization, a maximum score (d_{max}) at day 18-20 and slow symptom recovery (remission phase) (36). The ascending paralysis, starting with the tail tip, is accompanied by reduced body weight, food intake and social exploration (37). In EAE, lesions are usually found in the spinal cord, where neuronal loss is already observed at early stages (2). These lesions are induced by inflammation (38) thereby making it a useful model to study the impact of inflammation on neurodegeneration. Besides demyelination due to inflammation, synaptic plasticity and axonal remodeling play an important role in the development and remission of clinical symptoms in EAE (38). Those structural alterations can also be found in the brain, mainly, cortex, hippocampus, cerebellum, striatum and cortex (39). Synaptic plasticity leads to cortical hyperexcitability in the remission phase of EAE, which causes further neurodegeneration (40) indicating, that inflammation is not the only source of neuronal damage in EAE.

The EAE model contributes heavily to our understanding of inflammation in MS (41). The overall immune response in EAE is comparable to the inflammatory components of MS (25,42), but important differences need to be mentioned: While the immune response in MS patients is driven by major histocompatibility complex (MHC) I and $CD8^+$ T-cells, EAE shows a MHC II and $CD4^+$-driven immune reaction (41,43), with hints, that a MOG_{35-55} induced EAE in C57BL/6 mice also triggers a $CD8^+$ immune response (44,45). Because the neuronal damage is a consequence of EAE induction, no primary neurodegeneration independent from inflammation is observed in EAE (41,43). Furthermore, EAE is an induced model using genetically homogeneous strains of mice, while MS occurs in a heterogeneous group of patients, exposed to similar environmental and genetic factors, but characterized by different times of onset,

course and severity of the disease (43). The immune system of mice used for animal experiments is not exposed to other pathogens and environmental factors like the human immune system (43) and therefore, EAE can only represent some aspect of the pathophysiology of MS.

Nevertheless, it is a useful model to study therapeutic approaches for MS treatment. Recently, the number of therapies tested on EAE in the preclinical phase has increased (46). The EAE model is also used to investigate the mechanisms behind establishes MS therapies (41). Unfortunately not all treatments that were promising in EAE experiments, exerted the same effects in MS studies (41,46). Reasons for this outcome might be the different genetics, pathogenetics or kinetics like different biorhythms and differences of immune reactivity of mice compared to humans (41). Furthermore, in MS the BBB is insufficiently disrupted compared to the BBB of EAE animals making it harder for the tested compounds to reach their target (41). Because of the differences between EAE and MS, some authors consider EAE a misleading animal model for MS (47), but reflecting all results and advantages that we learned from EAE, it is still a valid animal model for MS (41,43).

1.3.2 Cuprizone Model of De- and Remyelination

The cuprizone model is an established animal model to study de- and remyelination independent from inflammation in rodents (48,49). Cuprizone is a copper chelator affecting mitochondria metabolism leading to increased production of oxidative agents resulting in oligodendrocyte death (34). Cuprizone is administered orally with the diet (0.2% mixed with the pellet chow). Acute demyelination is induced by administration for 5 weeks. By prolonging the diet for 12 weeks, chronic demyelination can be assessed (48). Demyelination occurs in white and grey matter (50) with a regional specificity varying along rostrocaudal and mediolateral gradients (51). After 3 weeks of cuprizone diet the corpus callosum (CC) shows significant demyelination (52), reaching full demyelination after 5 weeks of cuprizone diet (50). Demyelination of the cortex is delayed compared to the CC and it takes 6 weeks of cuprizone diet until achieving full demyelination (50). Remyelination starts directly after the demyelination process is completed, irrespective of diet continuation, but, as further cuprizone administration harms newly formed myelin sheaths it is recommended to stop the diet

(48,53). The first changes on messenger ribonucleic acid (mRNA) level and protein expression indicating remyelination can be observed within the first week after stopping cuprizone administration (34,48), defining the early phase of remyelination (54,55). The remyelination process is strengthened within the next 2-4 weeks (55) resulting in a full remyelination phase, 25 days after changing of the food (54).

The cuprizone model is well-established to study the process of de- and remyelination, which correlates well histologically with the neurodegenerative process observed in MS (41). It is easily reproducible, as it is independent from individual skills of the researcher, e.g. surgical skills (34). Furthermore, extensive investigations using the cuprizone model, revealed kinetics of de- and remyelination, with distinction in early and full remyelination, making it a useful model to study neurodegeneration (34,49,54,56). As the demyelinating process is independent from inflammation, the cuprizone model cannot reflect all aspects of MS (34). However, this can be used to focus on investigating the neurodegenerative aspects of the disease independent from inflammation.

1.3.3 Behavior Experiments in Animal Models of MS

A prominent symptom of MS in patients, besides sensomotoric impairment, is cognitive impairment (57–60). In order to represent a broader spectrum of pathophysiological changed in MS, behavior experiments can be used to assess cognitive impairment in animal models (61,62). A broad variety of experimental protocols is used in behavior research of rodents with different tests to evaluate motor function, learning abilities, memory impairment and emotionality and exploration (62,63). As there is no perfect behavior test fitting for all behavior related questions the choice of the experimental outline should consider different aspects e.g. if the animal is physiologically capable to solve the test and which motivation is the main driving force (e.g. fear, hunger, curiosity) (63). In addition, behavior tests are strongly depending on animal-experimenter interaction and the experience of the experimenter as well as automatized study protocols and blinded experimental setups should be taken into consideration to minimize bias (63).

It is important to assess motor- prior to cognitive impairment in order to ensure that the tested animals are capable of handling the experimental setup of the cognition

tests (62,64). Traditionally, motor coordination is tested using the rotarod test, which measures the ability of the tested animal to balance on a rotating rod (64,65). Other experimental set-ups e.g. the beam walking test, where the tested animal has to traverse elevated narrow beams in order to reach a safe platform, or footprint-analysis using paint to visualize the walking pattern, can also be utilized to investigate motor function (62,65). The open field test (OF) gives information about the locomotion activity as well as about anxiety of the animals (62). In this experimental set-up the tested animal is placed in an arena, which is divided in an open central part and the periphery next to the walls and the distance traveled by the mouse is tracked (62). An anxious animal avoids staying in the open center (62). Assessing anxiety levels in detail can be achieved by performing approach-avoid behavior tests (66). Mice prefer staying in dark, covered area as this reduces the risk of predation (66), which is in conflict with their natural curiosity and compulsion of exploration (62). This conflict is used in different experimental setups e.g. the light-dark box, where a box is divided into a dark side with black walls and a light side with bright walls and the time the animals spend in the corresponding sides is measured (66). A similar concept is used by the elevated plus maze (EPM) test, where a cross-shaped maze with two open arms and two closed arms with walls is used. By counting the entries into- and the time spent within the corresponding arms, anxiety-like behavior can be detected (62).

There are different experimental setups to investigate memory dysfunction and impaired learning abilities in rodents (62). The novel object recognition test (NOR) assesses short- and long-term memory impairment, by taking advantage of the preference of mice to explore the novelty (67,68). When mice are exposed to a novel and a familiar object at the same time, they recognize the familiar one and spend more time exploring the novel object (67). For further insights into learning and memory impairment, a Pavlovian fear conditioning can be used (69). This experimental setup presents an emotionally neutral conditioned stimulus together with an adverse unconditioned stimulus (70). After successful conditioning, the conditioned stimulus can evoke a fear related response (70). Pavlovian conditioning experiments and related modifications contribute to our understanding of fear learning and provide the basis for investigations focusing on memory-related brain units and underlying neuro-chemical reactions (71). Therefore, this test is a useful tool to study learning and memory consolidation in rodents (71).

1.3.3.1 Behavioral Correlates of EAE Mice

Already in the preclinical phase, when no motor deficits are detectable, EAE mice present an anxiety-like behavior and reduced social interactions (72) as well as lower attention rate and activity scores (73). They also suffer from memory impairment and memory extinction which occurs faster in EAE than in healthy mice (72). Olechowski et al. could demonstrate that the cognitive impairment is due to EAE induction as the mice present no impairment in experiments performed before immunization (73). It is thought, that the cognition impairment derives from decreased hippocampal grey matter volume and disturbed hippocampal integrity in EAE leading to hippocampus related learning problems (74). The behavioral changes can alter, within the time course of an EAE experiment, food intake and social interaction, which are reduced during the preclinical and acute phase, but improved during the recovery phase (37). The behavioral impairments do not depend on the motor impairment, as there are differences during the preclinical and recovery phase, whereas the motor functions are similar during these two phases (37). Therefore, other influencing factors like immune system activation with increased cytokine production may play a role in the underlying mechanisms (37). Taken together, EAE induces several behavioral changes which are varying during the preclinical, acute and recovery phase of the disease depending on underlying inflammatory and neurodegenerative processes (37,72,74).

1.3.3.2 Behavioral Correlates of Cuprizone Mice

Behavior experiments are a useful tool to assess the clinical manifestation of de- and remyelination in the cuprizone model. The demyelination process of cuprizone mice leads to impaired motor abilities and poorer coordination skills (75–78). The impaired bilateral senso-motoric behavior cannot be reversed by remyelination (79). There are debatable reports on the influence of cuprizone on behavior changes. Previous investigations described a decreased anxiety in cuprizone-fed mice (76), but recently, an increase in anxiety-like behavior and reduction of explorative activity was reported (77). Cuprizone affects cognitive learning abilities of mice (49,54,76). By using a Pavlovian fear conditioning, Cerina et al. could demonstrate that mice at full demyelination cannot discriminate between tones with frequencies of 2.5 kHz and 10 kHz (49,54). This impairment does not improve by withdrawal of the cuprizone diet with

consequent remyelination (49,54) indicating that the ongoing remyelination process does not reestablish original conditions.

1.4 Neuronal KCNQ-Channels

1.4.1 Excitability Changes of Neurons Observable in MS and its Animal Models

MS is affecting the cortical excitability in patients (80,81). Patients with RRMS present a generalized increased cortical hyperexcitability independent of the localization of new plaques and of the site of clinical manifestation (80). Impairment of interneuronal excitability correlates with the clinical manifestation of the disease (81). Early neurodegenerative changes during MS are determined by excitotoxity involving changes in neuronal excitability (82). Synaptic transmission operated by glutamate or gamma aminobutyric acid (GABA) is disturbed by neuroinflammation and –degeneration and results in excitotoxic neuronal damage and compensatory neuronal plasticity (82,83). Investigations using the EAE model demonstrated that a functional maladaptation of neurons result in cortical hyperexcitability indicating the start of neurodegeneration (40). By studying the neurodegenerative process in the cuprizone mouse model, a similar hyperexcitability could be observed in early remyelinated neurons (54,84) by our group. On the contrary demyelination and prolonged myelination for 25 days shifts the resting membrane potential (RMP) of neurons into hyperpolarization with decreased excitability (54,84). Therefore, the ongoing remyelination process observed in the cuprizone mouse model fails to restore normal neuronal functions (52,54). These excitability changes influence neuronal connections, like the thalamo-cortical connections (56,85). The sensory responsiveness of the thalamus is impaired after cuprizone induced demyelination and again, this impairment persists during remyelination (56).

Neuronal hyperexcitability is also observed in other neurodegenerative disease and their mouse models, e.g. Alzheimer's disease (86). Therefore, the underlying process and the consequences of neuronal hyperexcitability due to neurodegeneration are subject of ongoing research.

1.4.2 The Role of Ion Channels in the Pathophysiology of MS

Neuronal activity including excitability, AP generation and conduction and restoration of the RMP is depending on a number of ion channels expressed in the cell (87). Therefore, ion channels play an important role in neurological disorders and are key players in the pathophysiology of MS (88). Recent research demonstrates that different ion channels expressed either on neurons or immune cells are involved in pathophysiological changes during neuroinflammation and -degeneration (88,89). In addition, ion channels represent good targets for a cell-type and context-specific pharmacological therapy as they show an ubiquitous expression pattern and are mandatory for a number of different cell functions (89).

The involvement of Na^+-channels in the pathophysiology of MS is already established: Na^+-channels are upregulated during demyelination to restore nerve conductance (90,91). Especially Nav1.6-channels, which are usually expressed at nodes of Ranvier, alter their location along the axon to formally myelinated parts, resulting in continuous AP conduction (27,92,93). The upregulated expression of Na^+-channels leads to increasing intraneuronal Na^+ concentrations which require higher activity of the Na^+/K^+ ATPase to restore the membrane potential (27,94,95). Due to mitochondrial dysfunction, the required energy supplementation is missing and therefore, the Na^+/Ca^{2+} exchanger starts working thereby increasing the intraneuronal Ca^{2+} concentrations resulting in neuronal cell death (27,94–96). Because of this mechanism, pharmacological blocking of Na^+-channels was thought to be a promising therapeutic strategy in MS treatment (95), but trials with lamotrigine (Na^+-channel blocker) showed no amelioration of symptoms (89,97).

K^+-channels are key players in regulating neuronal excitability by initiating the repolarization after AP generation and by restoring the RMP. Demyelination of neurons leads to exposure and up/downregulation of different K^+-channels (89,98). Abnormal K^+ currents are associated with slow AP conduction, conduction failure and changes in repetitive discharge of neurons (89). Therefore the pharmacological modulation of K^+-channels might help improving AP generation in demyelinated neurons (99). The neurodegenerative process observed in the cuprizone mouse model was accompanied by a transient hyperexcitability of the neurons during the early remyelination phase (49,54) and also the EAE model shows an hyperexcitability of cortical neurons during the remission phase (40). Consequently, neuroinflammation

and -degeneration influence neuronal excitability by changed ion channel expression, which results in a maladaptive condition (7). KCNQ-channels are voltage gated K^+-channels that are colocalized with Nav1.6-channels at the distal part of the axon initial segment (AIS) and nodes of Ranvier (100–102). By creating outward K^+ currents they prevent subthreshold Na^+-currents (100) and hyperpolarize the membrane potential, preventing repetitive AP firing and controlling the excitability of neurons (103). Because of their colocalization with Nav1.6-channels, Hamada and Kole assessed, that KCNQ3-channels redistribute to demyelinated interneurons in contrast to Nav1.6-channels in the cuprizone model (93). Because of this altered expression pattern and their role in regulating neuronal excitability, we decided to target KCNQ-channels to understand their role in the pathophysiology of MS.

1.4.3 KCNQ-channels

KCNQ-channels (also known as Kv7-channels) are voltage gated K^+-channels which open by depolarization of the cell (104). There are five different subunits (KCNQ1-5) and four subunits form one K^+-channel with six transmembrane domains as homeric- or heteromeric channels in certain combinations (105). KCNQ1 is the only subunit that is expressed outside the CNS/PNS (104,105). This subunit is expressed on cardiac cells and on the inner ear cells (104,105). In the intestine KCNQ1 is involved in chloride secretion (105). The subunits from KCNQ2 to 5 are expressed in the PNS/CNS (106). KCNQ2 and KCNQ3 are forming heteromeric channels, which are expressed in the cortex and on cerebral deep grey matter as hippocampal and thalamic neurons (107–111). The subunit KCNQ4 is expressed on sensory hair cells of the inner ear and in the auditory pathway (105). Similar to KCNQ2/3, the subtype KCNQ5 is expressed in the brain in cortex and hippocampal neurons, where it can form heteromeric channels with KCNQ3 (105,112). The expression pattern and function of KCNQ-channels underline their role in controlling excitability of neurons. Mutations of KCNQ genes are associated with various excitability-related diseases. Mutations affecting KCNQ2 cause numerous neurological disorders of varying severity like various epileptic phenotypes e.g. benign familiar infant seizures and neonatal epileptic encephalopathy (113–119). The subtypes KCNQ2, 3 and 5 are matter of particular interest concerning hyperexcitability, as they generate a non-inactivating low threshold potassium current (I_M current) which regulates neuronal excitability (104,105,120). This current was first

described by Brown and Adams in a sympathetic neuron of a frog (121). The underlying KCNQ-channels of the I_M current are closed at a membrane potential more negative than -60 mV with a maximum conductance between -10 and +20 mV (121). They are inhibited by a variety of hormones and transmitters acting on G protein-coupled receptors like the muscarinic acetylcholine receptor, which is responsible for the original name I_M current/M-current (106,121). Inhibition of I_M leads to enhanced neuronal excitability (104,105). Pharmacologically, this inhibition can be induced by 10,10-bis(4-pyridinylmethyl)-9(10H)-anthracenone (XE991), a highly selective neuronal KCNQ-channel blocker (120,122). By blocking I_M with 10µM XE991 the firing pattern of neurons in brain slices changes from phasic to tonic (120) and by applying the drug to the AIS spontaneous firing occurs (100). XE991 is a structural variation of linopiridin (123), a I_M channel inhibitor with cognitive enhancing effects (124), which did not pass phase 3 trials for Alzheimer treatment (125). XE991 is considered an irreversible KCNQ-channel inhibitor (126). The inhibition kinetics are depending on the activation state of KCNQ-channels, which is most likely based on conformation changes of the subtypes, that form the channel (126).

Retigabine, known also as ezogabine, is a KCNQ-channel opener which shifts the activation of KCNQ2/3 to more negative potentials and therefore increases the rate of activation (127). Retigabine was synthetized from the former used central analgesic flupirtin, which showed anti-epileptic features in several test trials (127,128). By prolonging the opening time of KCNQ-channels, retigabine stabilizes the RMP and reduces neuronal excitability, a suitable effect when used in epilepsy treatment (127). Retigabine shows highest affinity on KCNQ3, compared to KCNQ2 (129–131), has only a small effect on KCNQ4 and no effect on KCNQ1 (122). Application of retigabine to the neocortex in human brain slices leads to suppression of spontaneous sharp waves (132). In the murine thalamus, retigabine triggers burst-firing and reduces the number of tonic APs (111). It also reduces the excitability of peripheral neurons (133). Effects on chronic pain mechanisms are described by means of increased firing threshold and reduced responsiveness of nociceptive neurons (134). In 2011 retigabine was approved for treatment of partial onset seizures with or without secondary generalization in adults with epilepsy (127). In general, retigabine provided a well-tolerated treatment with somnolence, dizziness, headache and fatigue as most common side-effects (127,135), but also a bluish pigmentation of ocular tissue, finger-

and toenails, as well as of the skin around lips and eyes could be observed (136,137). Because of its structural relation with the drug flupirtin, it was associated with acute drug induced liver failure (136) and the European medicine agency decided the withdrawal of flupirtin and retigabine from the market (138). Nevertheless, retigabine is a well-established compound for KCNQ-channel modulation in *in vivo* and *in vitro* experiments.

1.5 Aim of this Thesis

The pathophysiology of MS involves neurodegenerative and inflammatory aspects. Both can influence neuronal activity in forms of changes in neuronal excitability, AP conduction and interneuronal connections (82,83). Ion channels play an important role in regulating those neuronal function (87). Experiments using EAE and cuprizone treatment demonstrated hyperexcitability and together with the altered expression of KCNQ3 in demyelinated neurons (93), we hypothesize an involvement of KCNQ-channels in the pathophysiology of MS. Therefore, the project presented in this thesis used the pharmacological treatment of KCNQ-channels with retigabine or XE991 *in vitro* and *in vivo*. The project can be divided into three parts. The first part focused on the involvement of KCNQ-channels in EAE experiments by using a prophylactical treatment with retigabine. We can show, that retigabine ameliorated the progression of EAE in mice. To elucidate the underlying mechanism, the second part of this thesis dealt with the expression and function of KCNQ-channels in immune-related cell types. There is no effect of retigabine and XE991 administration on murine splenocytes, making an immune regulatory aspect of KCNQ-channels questionable. So thirdly, the role of KCNQ-channels in neurodegeneration was assessed by using the cuprizone model of de- and remyelination and a therapeutic treatment with retigabine and XE991 with performing behavior experiments as read-out. Here an improvement of retigabine-treated mice is observed, indicating neuroprotective functions of KCNQ-channels.

2. Materials

2.1 Instruments

A list of all instruments used in this work is provided in table 1.

2.2 Expendable Material and Reagents

A list of expendable material and reagents used in this work is provided in table 2.

2.3 Media and Buffers

If not mentioned otherwise, the pH was adjusted to 7.3 by titration with either NaOH or HCl 1 M each.

Ammonium-Chlorid-Potassium buffer (ACK-Buffer)

- 150 mM NH_4CL
- 10 mM $KHCO_3$
- 0.1 mM EDTA

Annexin binding buffer:

- 50 mM HEPES
- 700 mM NaCl
- 12.5 mM $CaCl_2$
- pH adjusted to 7.4

Washing medium for splenocyte culture

- DMEM
- 1 % FCS
- 1 % Glutamine
- 1 % P/S

Splenocyte complete medium

- DMEM
- 10 mM Hepes

- 25 µg/ml Gentamicin
- 50 µM Mercaptoethanol
- 5 % FSC
- 2 mM Glutamine
- 1 % NEAA

Magnetic-activated cell sorting (MACS) buffer

- PBS
- 0.5 % BSA
- 2 mM EDTA

Fluorescence-activated cell sorting (FACS) buffer

- PBS
- 0.1 % BSA
- 0.1 % NaN_3 10 %
- 2.5 mM EDTA

Erythrocyte lysis buffer

- ddH_2O
- 150 mM NH_4CL
- 10 mM $KHCO_3$
- 0.1 mM ETDA

2.4 Antibodies and Primer

Antibodies and primer used in this work are listed in table 3.

2.5 Software

A list of software used in this work can be found in table 4.

3. Methods

3.1 Animals and Experimental Design

All the work performed on animals, *in vitro* and *ex vivo*, was done according to the 2010/63/EU law of the European Parliament and of the Council of 04 August 2016, 08 May 2017 and 26 February 2019 and has been approved by local authorities (Landesamt für Natur, Umwelt und Verbraucherschutz, Nordrhein-Westfahlen; approval IDs: 84-02.04.2015.A585, 84-02.04.2016.A307, 81-02.04.2018.A266) All efforts were made to minimize the number of needed animals, and to avoid stress and suffering for the animals using the ARRIVE guidelines (139). Female C57BL/6J mice were used for all experiments. Mice were group-caged in a 12-h dark/light cycle with food and water available *ad libitum*.

3.1.1 Experimental Autoimmune Encephalitis (EAE)

Female C57BL/6J mice (8-12 weeks of age at the beginning of the experiment, 10 per group) were anesthetized with isoflurane and injected with the epitope 35-55 of Myelin Oligodendrocyte Glycoprotein (MOG_{35-55}) mixed with *M. Tuberculosis* and Freund´s adjuvant in both flanks of the animal (200 µl MOG_{35-55} per mouse) in order to evoke an immune response. Moreover, 100 ng Pertussis toxin per mouse were injected intraperitoneally on the same day. At day two after the immunization, 200µl of Pertussis toxin were injected intraperitoneally in order to render the blood brain barrier leaky and allow the activated immune cells to enter the CNS (140). The treatment using retigabine and the vehicle started the same day of the immunization and continued for 25 days. Animals of the treated group received a daily injection of 200µl of retigabine (1 mg/kg BW) and animals of the vehicle group were injected with 200µl of dimethyl sulfoxide (DMSO, 1:400 solution diluted in PBS). A daily monitoring of bodyweight (BW) and disease score according to table 5 was performed. Animals which lost more than 20% of their initial BW or reached a score 7 persisting for three days, were taken out from the experiment and eliminated by cervical dislocation.

Score:	**Clinical symptoms:**
1	Paralysis of the tip of the tail
2	Complete paralysis of the tail
3	Light ataxia and altered walking
4	Ataxia, problems of moving the hind limbs
5	Light paralysis of hind limbs
6	Complete paralysis of one leg
7	Complete paralysis of both legs
8	Paralysis of one arm
9	Tetraparesis and dyspnoe
10	death

Table 5: Disease score of EAE mice according to the clinical symptoms of the animals.

3.1.2 Cuprizone Diet

To introduce general experimental toxic demyelination, C57BL/6J female mice (8-12 weeks of age at the beginning of the experiment, 5-10 per group) were fed a diet containing 0.2 % cuprizone (bis-cyclohexanone oxaldihydrazone, Sigma-Aldrich Inc., Hamburg, Germany) mixed with standard rodent chow (48). This diet was maintained for 5 weeks. By stopping the diet and changing to normal rodent chow, we allowed spontaneous remyelination (48,54). In parallel to the beginning of this remyelination process, the animals received an additional daily treatment. Two groups of animals were injected with either 200 µl of retigabine (1 mg/kg BW), 100 µl of XE991 (0.75 µg/µl) or DMSO (1:400 diluted in PBS) serving as vehicle control. The treatment continued for either 7 or 25 days after reintroduction of normal food.

As control, mice matched for sex and age which were fed normal rodent chow were used. And in addition, all experiments were performed on mice which underwent the cuprizone diet until full demyelination after 5 weeks.

The following eight experimental groups were analyzed:

- Control mice (n=5, control)
- Cuprizone treated mice at full demyelination (n=5, cuprizone)
- Mice remyelinated for 7 days treated with Retigabine (n=10, remy 7 days + Ret)
- Mice remyelinated for 7 days treated with XE991 (n=10, remy 7 days + XE)
- Mice remyelinated for 7 days treated with vehicle (n=10, remy 7 days + veh)
- Mice remyelinated for 25 days treated with Retigabine (n=10, remy 25 days + Ret)
- Mice remyelinated for 25 days treated with XE991 (n=10, remy 25 days + XE)
- Mice remyelinated for 25 days treated with vehicle (n=10, remy 25 days + veh)

3.2 Behavior Experiments

We performed different behavior experiments to characterize the phenotype of the mice in different experimental animal models. EAE mice with mild symptoms and an average score of 4 performed a NOR test assessing memory impairment. The different groups of cuprizone-fed mice performed EMP and OF tests to assess locomotor activity and anxiety like behavior and NOR test as well as Auditory Pavlovian Conditioning to evaluate memory impairment and learning disabilities. The experiments were performed at the end of the treatment phase of the corresponding group as specified in the text.

3.2.1 Elevated Plus Maze (EPM)

To measure the anxiety level of the animals, EPM test (tracking software: EthoVision XT, Noldus IT, The Netherlands) was performed. The maze consists of a device shaped like a cross (25x25 cm, 30 cm above the ground) with two open arms and two arms covered with walls (closed arms). The movement of each animal was tracked for 5 minutes. The time spend in the open and the closed arms was analyzed as well as the entries into the corresponding arm.

3.2.2 Open Field Test (OF)

After an interval of 5 hours the same animals that were tested in the EPM underwent an OF test (tracking software from Noldus Ethovision, The Netherlands). Here, the locomotor activity and the anxiety level of the animals were measured by tracking the animal's exploration of the test setting. The animal was placed in an arena (35x40x40 cm) for 5 minutes. Distance, speed, time spent in center and in the periphery were measured and the number of rearings and groomings were recorded. Rearing describes an explorative behavior where the animal stands on the hind limbs looking up and represents curiosity while grooming is a behavior is which the mouse cleans its fur and represents a non-anxiety-like behavior.

3.2.3 Novel Object Recognition (NOR)

To assess cognitive abilities of the animals, a NOR test (tracking software from Noldus Ethovision, The Netherlands) was performed (68). The animals were placed in the arena where the OF experiment was carried out, ensuring that the animals were familiar with the experimental setup. In the first trial, the adaptation phase, two identical objects were placed in one half of the arena. This trial lasts 10 minutes and the time the animal spent exploring the objects was measured to ensure that the animal is familiar with the objects. Therefore, the total adaptation time was calculated as sum of: Time exploring object 1 + Time exploring object 2.

In the following test trials (30 minutes, 60 minutes and 24 h after the adaptation trial) one object was changed at every trial while the other one was left in place. Each animal had 5 minutes to explore both objects and it was measured if the animal spent more time with the familiar or the new object. Therefore, the NOR index was calculated as: Time spent exploring new object / (Time spent exploring new object + Time spent exploring old object). An index of 0.5 shows, that the animal spent the same time with both objects. An index of > 0.5 demonstrates, that the animal spent more time exploring the novel object and if the index is < 0.5, it spent more time with the familiar object (68,141).

3.2.4 Auditory Pavlovian Conditioning

After undergoing cuprizone diet and 7 or 25 days of remyelination with or without treatment after cuprizone withdrawn, the mice underwent a modified fear conditioning-protocol to test their ability to discriminate auditory stimuli (49,142,143). The test lasts for three consecutive days. During the first day, mice were adapted two times (with 6-hours interval) to the fear conditioning apparatus (TSE System GmbH, Bad Homburg Germany) while being exposed to six neutral tones (unconditioned stimulus, 2,5 kHz, 85 dB, 10 s duration). On the next day, they were exposed to the conditioned stimulus in three trials (10 kHz, 85 dB, 9 s duration). This stimulus was randomly coupled with a mild food shock (0.4 mA, 1 s duration). On the third day, animals were presented with both stimuli in the absence of foot shock and the percentage of immobility (freezing) of the animal after presenting the conditioned stimulus (10 kHz) was taken as read out for fear conditioned behavior (49,142,143).

3.3 In Vitro Experiments

For the *in vitro* experiments, organs and cells from naïve C57BL/6J mice were used as described in the following.

3.3.1 Isolation of Splenocytes

Animals (8 – 12 weeks old female mice) were sacrificed and the spleens were collected in a falcon containing 10 ml of wash medium and stored on ice. Next, the tissue was mechanically homogenized using a 40 µm cell filter, which was washed with 10 ml of wash medium. The suspension was centrifuged (1500 rpm, 4 °C for 5 minutes). After discarding the supernatant, the pellet containing the isolated splenocytes was resuspended in 5 ml erythrocyte lysis buffer (ACK buffer) and incubated at room temperature for 1 minute to destroy leftover erythrocytes which can generate false-positive signals when measuring immune cell reactivity. Afterwards, the reaction was stopped by adding 10 ml of wash medium. After another centrifugation (1500 rpm, 4 °C for 5 min), the supernatant was discarded, and the pellet was resuspended in 10 ml of splenocyte complete. Cells were transferred to another tube by washing through a 40

µm cell strainer to remove debris. The number of isolated cells was counted using a Casy Model TT cell counter (Innovatis AG, USA) and stored on ice until further use.

3.3.2 Isolation of Lymphocytes

To isolate lymphocytes from abdominal lymph nodes the same protocol described above for splenocyte isolation was used, without re-suspending in erythrocyte lysis buffer, as lymph nodes do not contain erythrocytes.

3.3.3 Retigabine Titration

The effect of retigabine and its vehicle DMSO on the viability of splenocytes was assessed by performing a cell viability assay. Different concentrations of the drug were added to isolated splenocytes and incubated for either 24 or 48 h.

To mimic inflammatory conditions, two 96-U bottom well plates were coated with purified anti-CD3 antibody (2 mg/ml, 50 µl per well) and stored in the fridge overnight. Furthermore, anti-CD28 antibody (1 mg/ml) was added to isolated splenocytes, which were adjusted to a concentration of $5x10^5$ cells /100 µl. For every animal, three technical repetitions were seeded for the following experimental conditions: stimulated, stimulated + retigabine, and stimulated + vehicle (DMSO). The stimulated condition is the positive control indicating the viability of splenocytes undergoing inflammation without interference of other variables. To investigate if retigabine influences this viability, different concentrations of this compound (1 µM, 5 µM, 10 µM, 30 µM, and 500 µM) were added to the splenocytes. The concentration of 500 µM served as proof of principle to show that retigabine has an effect on splenocyte viability in toxic concentrations. The corresponding volume of DMSO used to dilute retigabine (6 µl, 30 µl, 60 µl, or 100 µl) was added to stimulated splenocytes to assess if the vehicle alone influences splenocyte viability. The well plates were incubated at 37 °C in the dark for 24 h and 48 h. After incubation, the level of stimulation and proliferation of the cells was checked under the microscope (Inverted Zeiss Axioexaminer, Germany). After 24 or 48 h, the splenocytes of each well were resuspended and transferred into FACS tubes and, after adding 100 µl of FACS-buffer, the tubes were centrifuged (1800 rpm, 4 °C for 5 minutes). The supernatant was removed, and the cells were resuspended in the staining solution containing the marker dye for necrosis FVD, the viability dye

eFlour™ 780 and apoptotic cells marker dye annexin V (144). According to manufactures instructions, annexin V binds on phosphatidylserin, which is a component of the inner leaflet of the cell membrane. When a cell undergoes apoptosis, phosphatidylserine is exchanged to the outer leaflet of the cell membrane as a marker for phagocytosis. This is used by annexin V to mark apoptotic cells. The annexin V antibody was diluted in annexin binding buffer, which facilitates the binding of the antibody to phophatidylserin, in a ratio of 1:50. The splenocytes were resuspended in FACS buffer, incubated with the annexin V staining for 20 minutes at 4 °C. The FVD antibody was diluted in annexin binding buffer in a ratio of 1:10.000 and incubated with the cells for 20 minutes at 4 °C. The reactions were stopped by adding 1 ml of FACS buffer to the tubes which were then centrifuged (1800 rpm, 4 °C for 5 minutes) and the supernatant was discarded. Cells were resuspended in 300 µl of FACS buffer and the staining was analyzed by flow cytometry (Gallios™ Beckmann Coulter GmbH, Germany). Quantification of the results was performed by counting the percentage of unstained cells, namely, the cells which were not positive for the apoptosis and/or necrosis markers.

3.3.4 Proliferation Assay

To examine the effect of retigabine, the vehicle DMSO as well as of XE991 on splenocyte viability an eFlour 670 assay was performed. eFlour 670 is a fluorescent dye, that binds on intracellular proteins that contain primary amines. During mitosis, the dye distributes equally to the mother- and daughter cell, so that with every cell division the fluorescent intensity is halved. The fluorescence decrease can be measured via FACS (145). A 96 well plate with U bottom was coated with anti-CD3 antibody (1 mg/ml) the day before the experiment. Splenocytes were isolated as described above ($10x10^6$ cells per condition). Afterwards, they were centrifuged (1500 rpm, 4 °C for 5 minutes) and the supernatant was removed. The splenocytes were resuspended in PBS and the eFlour670 staining solution (1 µl eFlour670 in 500 µl PBS) was added. The tubes were incubated at 37 °C for 10 minutes in the dark. The reaction was stopped by adding splenocyte complete medium and the solution rested on ice for 5 minutes. The splenocytes were counted using the Casy Model TT cell counter and $8x10^5$ cells were separated for every condition. After centrifugation (1500 rpm, 4 °C for 5 minutes), the supernatant was discarded. The splenocytes were resuspended in a

solution of splenocyte complete medium together with anti-CD28 antibody and either 1 mM of retigabine or XE991 or DMSO in a ratio of 1:400. Stimulated splenocytes without treatment served as stimulation control. The splenocytes were seeded in triplicates using 200 µl per well. The plate was incubated at 37 °C for 4 days. After incubation, the level of stimulation/proliferation of the splenocytes was assessed by using a bright light microscope (Inverted Zeiss Axioexaminer, Germany). Properly stimulated splenocytes showed proliferation and formed cluster. The wells were resuspended and transferred into FACS tubes. Afterwards, 100 µl of FACS buffer were added and the tubes were centrifuged (1400 rpm, 4 °C for 5 minutes). The supernatant was removed, and the pellet resuspended in 300 µl of FACS buffer. The samples were analyzed using FACS (Gallios™ Beckmann Coulter GmbH, Germany).

3.3.5 Cytokine Quantification

The effect of retigabine and XE991 on the cytokine production of splenocytes was assessed by flowcytometric analysis using a LegendPlex Mouse Inflammation Panel multiplex assay kit (BioLegend, USA). In order to produce supernatant containing cytokines, freshly isolated splenocytes ($7.5x10^6$ cells per condition) were incubated on a 24-well plate coated with anti-CD3 antibody (1 mg/ml). After centrifuging the cells (1400 rpm at 4 °C for 5 minutes), the supernatant was discarded, and the pellets were resuspended in splenocyte complete medium containing either only anti-CD28 antibody or the antibody in a combination with retigabine (30 µM) or the vehicle DMSO (1:400 in PBS). The splenocytes were seeded and incubated at 7 °C for 2 days. After incubation the level of stimulation/proliferation was visually tested using the microscope (Inverted Zeiss Axioexaminer, Germany) and the splenocytes were resuspended and transferred into 1.5 ml Eppendorf tubes. The tubes were centrifuged (600 rpm, 4 °C for 6 minutes) and the supernatant containing the cytokines was transferred into new Eppendorf tubes. The supernatant was stored at -20 °C until performing the LegendPlex assay to detect the following cytokines: IL-2, IL-6, IL-10, IL-17 and TNF α.

The beads used to mark the cytokines listed in table 6 were sonicated and vortexed for 30 seconds prior to use. They were diluted by using an assay buffer to a 1x concentration. According to manufactures instruction the washing buffer was diluted using distillated water. The standard curve was prepared with the final concentrations

(in pg/ml) of 10.000 / 2.500 / 625 / 156.3 / 39.1 / 9.8 / 2.4 and 0. To perform the assay, 25 µl assay buffer were added to every well of a 96 V-bottom plate. The first two rows of the plate served for the standard curve by adding 25 µl standard buffer. The remaining wells were loaded with 25 µl of the cytokine supernatant. On top of every well 25µl mixed beads and 25 µl detection antibodies were added. The plate was protected from light with aluminum foil and mixed at 600 rpm by using a plate shaker for 2 h. Streptavidin-phycoerythrin (SA-PE) which detects biotinylated antibodies, was added to every well and the plate was covered and mixed for 30 minutes at 600 rpm. Afterwards, the plate was centrifuged (1g for 5 minutes) and the supernatant was removed by using a multichannel pipet. The washing buffer was added to every well and the plate was mixed on the plate shaker for 1 minute. After centrifugation, the supernatant was discarded, and the pellets were resuspended in washing buffer. The samples were directly transferred into FACS tubes and analyzed by FACS (Gallios™ Beckmann Coulter GmbH, Germany). The data was analyzed using the LEGENDplex™ data analysis software.

3.3.6 mRNA Isolation and cDNA Synthesis

For mRNA isolation the following organs were quickly removed from sacrificed C57BL/6J mice: brain, heart, lung, liver, spleen, spinal cord, muscle, thymus, kidney, lymph nodes and bladder. To lysate the cells and isolate the mRNA, 1 ml of Trizol was added to the tissue and the organs were mechanically homogenized using a mixer. The samples were incubated for 5 minutes at room temperature. To separate the mRNA from cell debris, 200 µl of Chloroform were added and the samples incubated at room temperature for 3 minutes. The tubes were centrifuged (1200 rpm, 4 °C for 15 minutes) in order to separate two phases. The upper, aqueous phase, which contained the isolated mRNA, was separated by pipetting and 500 µl of isopropanol were added to precipitate the mRNA. The samples were incubated at room temperature for 10 minutes. The tubes were centrifuged (7500 rpm, 4 °C for 5 minutes) and the supernatant was discarded. The pellet of mRNA was resuspended in 1 ml of ethanol. The samples were mixed and afterwards centrifuged at 7500 rpm, 4 °C for 5 minutes. The supernatant was removed, and the mRNA pellets dried at air. The pellets were dissolved in 30 µl of diethyl pyrocarbonate (DEPC) water (50 - 20 µl, depending on the size of the pellet) to inactivate RNase enzymes and incubated for 10 minutes at 57 °C.

The purity of the mRNA samples was measured using a NanoDrop™ spectrophotometer (Peqlab Erlangen, Germany) with a high purity considered at values between 1.0 – 2.0. For further investigations, 500 ng of the isolated mRNA per sample were used for cDNA synthesis by performing a polymerase chain reaction (PCR) using a reverse transcriptase, deoxyribonucleic acid trisphosphates (dNTPs) and random hexamers.

cDNA for expression analysis in neurons, microglia and astrocytes were kindly provided by the working group of Tobias Ruck from the Clinic of Neurology and Institute of Translational Neurology from Münster University. cDNA from oligodendrocyte progenitor cells (OPC) and oligodendrocytes differentiated for 24 and 48 h, were kindly provided by the working group of Tanja Kuhlmann from the Neuropathophysiology Department from Münster University.

3.3.7 PCR KCNQ

To investigate the expression pattern of KCNQ channels, conventional PCR using the cDNA created from different organs was performed. For every sample, the template was mixed with distillated water, 10xbuffer, dNTPs (10 mM), primer forward and reverse and the Taq polymerase. The PCR was performed for brain, heart, lung, liver, spleen, spinal cord, muscle, thymus, kidney, lymph nodes and bladder. Brain cDNA served as positive control for KCNQ2-5 and heart for KCNQ1. Water was used as negative control. The following cycling program was used:

- 94 °C 3 min
- 35 repetitions of:
    - 94 °C 30 s
    - 58 °C 1 min
    - 72 °C 1 min
- 72 °C 7 min
- 4 °C until further usage

As internal control, 18sRNA was chosen as a protein that is expressed in all used tissues. The following cycling program was used:

- 94 °C 3 min
- 35 repetitions of:
  - 94 °C 20 s
  - 60 °C 20 s
  - 72 °C 20 s
- 72 °C 2 min
- 4 °C until further usage

3.3.8 Gel Electrophoresis

To visualize the expression pattern of the different KCNQ subtypes we performed gel electrophoresis and separated the products of the KCNQ-PCR. Therefore, a 2 % Agarose gel was prepared by dissolving 2 g of Agarose powder in 100 ml of water and adding 5 µl of RedSafe™ to visualize the DNA. The gel was arranged with 15 chambers organized in a row. The first chamber contained 10 µl of a 50 base pair gene ladder, to measure the length of the KCNQ-DNA fragments. 20 µl of the KCNQ-DNA derived from the KCNQ-PCR, which was performed on cDNA from different tissues, were filled in the remaining chambers. The gel was set in an electrophoresis chamber (BIO-RAD, USA) with 110 V for 40 minutes. Afterwards, the different expression bands were visualized under fluorescent light and photographed (CCD camera from Biozym Scientific GmbH, GER).

3.3.9 Real-Time PCR (RT-PCR)

For the quantitative analysis of KCNQ expression, a real-time PCR (RT-PCR) was performed. Therefore, cDNA derived from different tissues (see chapter 3. Methods, Abstract: mRNA Isolation and cDNA Synthesis) was mixed with primers needed for DNA replication and a probe. This probe has a fluorescent reporter dye labeled at the 5´end and a non-fluorescent quencher dye at the 3´end. While both dyes are labeled to the probe, the fluorescent signal transmission is suppressed. During the elongation process of PCR, the polymerase separates the quencher dye from the reporter dye and the released reporter dye transmits a fluorescent signal (146). The time until the fluorescent signal is detectable is defined as ΔCT and corresponds with the

quantitative expression of KCNQ-channels in the tested tissue. A lower ΔCT value describes a high expression. To perform the RT-PCR, 2 µl of every sample containing KCNQ-cDNA derived from different organs (brain, heart, spleen, thymus, lymph node) were put into a 96 well V bottom plate. A master mix containing maxima probe/ ROX buffer 2x, RNase free water, 18 sRNA TaqMan primer and 1 µl of target primer was added (a list of all used KCNQ-TaqMan primers is provided under table 7). The RT-PCR was performed using the Real-Time PCR system Step One Plus (Applied Biosystem, Thermo Fisher Scientific, USA) with the following repetitions: The cycler was set to 50 °C for 1 minute, heated up to 95 °C for 10 minutes, and then cooled down to 60 °C for 1 minute. This protocol was repeated for a total time of 75 minutes.

3.4 Statistics

All results are presented as mean ± standard error of the mean (SEM). Statistical analysis was performed using GraphPad PRISM5 (Graphpadsoftware Inc., USA). Analysis of the variance between two or more groups was performed using one-way ANOVA or two-way ANOVA for multiple comparison, followed by Tuckey's, Dunn's or Bonferroni's post hoc test.

Behavior tests were performed and analyzed using EthoVision XT (Noldus, The Netherlands).

GraphPad and Adobe Illustrator (Adobe Inc., USA) were used for preparing graphs, data presentation and figure preparation.

4. Results

This project aims to investigate the role of KCNQ-channels in the pathophysiology of MS by using the animal model EAE for investigating neuroinflammation and neurodegeneration, and the cuprizone model for investigating effects of de- and remyelination. Therefore, a pharmacological treatment with the channel opener retigabine and its blocker XE991 was performed prophylactically and therapeutically in *in vivo* and *in vitro*.

4.1 The Effect of KCNQ-Channels on Experimental Autoimmune Encephalitis

To investigate if KCNQ-channels play a role in the pathophysiology of MS, we took advantage of the EAE mouse model. The mice were immunized, using the protocol described above (see chapter 3. Material, abstract 3.3.1 Experimental Autoimmune Encephalitis, compare scheme Fig. 1A). Ten mice were subjected to a prophylactic treatment with daily injections of retigabine (1mg/kg BW, blue curve, Fig. 1B), a KCNQ-channel opener, while the control group received a daily treatment using the vehicle DMSO (n = 10, orange curve, Fig. 1B). The time course of the disease was followed over 25 days and we observed that the variable “time” affected both groups (Two-Way ANOVA, time: $F_{(24,432)} = 62.38$, $p < 0.0001$, Fig. 1B), as both groups developed first symptoms at day 14, confirming the reliability of the experimental method. Until day 17 both groups presented a similar score development with first significant difference observed at day 18 (Two-Way ANOVA, treatment: $F_{(1,18)} = 7.84$, $p = 0.01$, Sidak’s multiple comparisons test: day 18: $p = 0.0009$, Fig. 1B). Mice of the control group steadily increased their scores until day 21, when they reached a plateau. From day 19 to day 24, retigabine-treated mice also showed increasing scores but with a significantly lower severity (Sidak’s multiple comparisons test: $p < 0.0001$). On the last day of observation (day 25), the difference between the scores of vehicle- and retigabine treated animals was still significant ($p = 0.0005$, Fig. 1B).

By comparing the cumulative scores, a significant difference between the control vehicle-treated (veh, orange bar, n = 10, 6.02 ± 0.26, orange bars, Fig. 1C) and the retigabine treated group (Ret, blue bar, n = 10, 3.54 ± 0.6, Unpaired t-test: t = 3.81, df = 18, p = 0.001, Fig 1C) is observed. Based on these results, retigabine appears to

ameliorate the disease score of EAE animals, suggesting that opening KCNQ-channels might beneficially modify the EAE course.

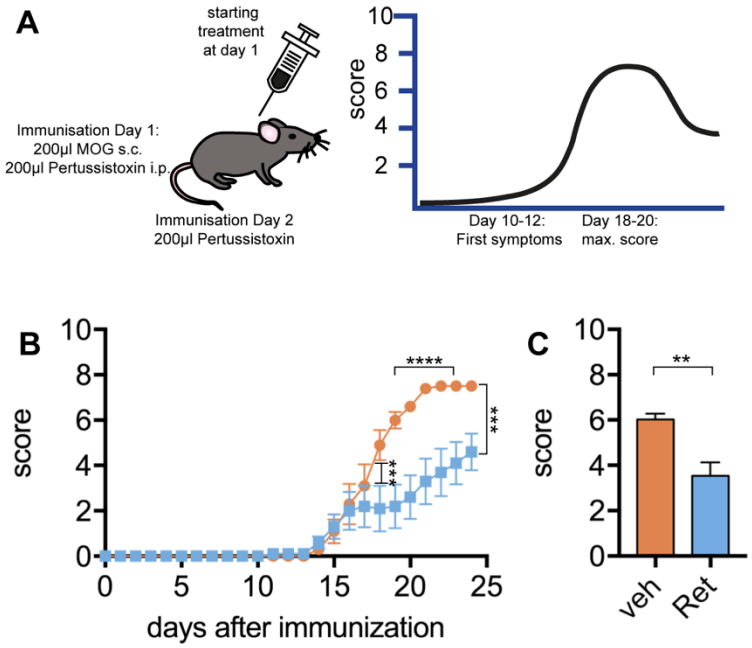

Figure 1: The effect of the KCNQ-channel opener retigabine on the outcome of EAE. **A** Schematic representation of the experimental outline. After immunization using Pertussis toxin and MOG_{35-55} the mice received an additional prophylactic treatment of retigabine or DMSO as vehicle. The expected disease course of an EAE without prophylactical treatment is indicated by the black graph showing the onset of symptoms at day 10-12 and a maximal score between day 18 and 20. **B** Dot-line graph showing the course of the scores for retigabine treated mice (blue line) compared to vehicle treated mice (orange line). **C** Bar graph showing the average cumulative score of EAE mice treated with retigabine (Ret, blue bar) and the vehicle (veh, orange bar).

4.2 Novel Object Recognition of EAE Mice treated with Retigabine

Induction of EAE does not only provoke an ascending paralysis starting at the hindlimbs, but also affects the cognition abilities of the mice (72–74). To explore a potential cognition impairment in our immunized mice and test if retigabine has an effect on short- and long-term memory abilities, we performed a NOR test as described above (see chapter 3. Methods, abstract 3.2.3 Novel Object Recognition, compare scheme in Fig. 2A). Exemplary spatial heat-maps indicating the regions of the arena where the animal spent most of the time are shown in Fig. 2B for the vehicle treated mice and in Fig. 2C for retigabine treated mice (red marking the area, where the animal spent most of the time).

Vehicle treated mice (veh, orange bars, n = 8, 66.63 ± 11.61 s) show a tendency to spend more time exploring the figures during the adaptation phase compared to retigabine treated mice (Ret, blue bars, n = 7, 56.57 ± 13.52 s), but this difference is not significant (Unpaired t-test: t = 0.57, df = 13, p = 0.58, Fig. 2D).

Testing the short-term memory 30 minutes (NOR index veh: 0.44 ± 0.06, vs. NOR index Ret: 0.7 ± 0.05, Bonferroni's multiple comparisons test: p = 0.19) and 60 minutes after the adaptation phase (NOR index veh: 0.44 ± 0.08, NOR index Ret: 0.66 ± 0.1, Bonferroni's multiple comparisons test: p = 0.3, Fig. 2E) did not show differences between the experimental groups. Repeating the NOR 24 h after the adaptation phase to test for long-term memory impairment showed that mice treated with retigabine performed significantly better than mice treated with the vehicle (NOR index veh: 0.28 ± 0.13, NOR index Ret: 0.66 ± 0.11, p = 0.01, Fig 2E). However, the general influence of the variable "time" is not a significant factor (Two-Way ANOVA, time: $F_{(2,26)} = 0.56$, p = 0.58), while the treatment influences the outcome of the NOR significantly (Two-Way ANOVA, treatment: $F_{(1,13)} = 16.4$, p = 0.001, Fig. 2D).

Taken together our results suggest an effect of retigabine on the long-term memory impairment of EAE mice.

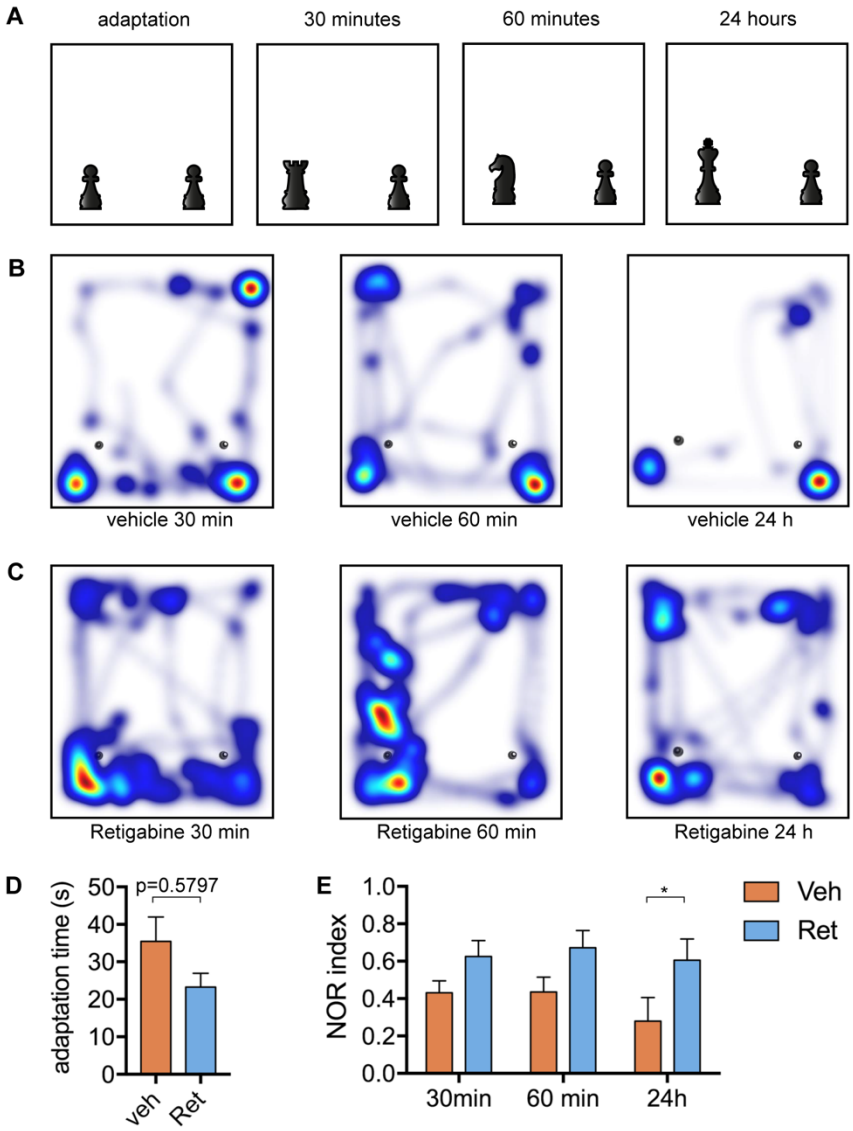

Figure 2: Effect of prophylactic treatment with retigabine on NOR test performed with EAE mice during the preclinical phase. **A** Schematic representation of the experimental setting. **B, C** Heatmaps showing the area where the mice spent most of the time during the experimental trial. The black dot on the left side of the arena symbolizes the novel object while the right object stayed the same. **D** Bar graph showing the average time mice spent exploring the objects during the adaptation trial. **E** Bar graph showing the NOR indexes for the different trial intervals of mice treated with retigabine (Ret, blue graphs) compared to vehicle treatment (veh, orange graphs).

4.3 Expression Pattern of KCNQ-Channels in Different Organs

The effect of retigabine on the EAE experiments proposes a possible role of KCNQ-channels in the pathophysiology of MS. To understand the underlying influence of KCNQ-channels on the disease, we performed conventional and RT-PCR to investigate the expression pattern of KCNQ-channel subtypes (KCNQ1-5) in different organs. We could corroborate findings from the literature by showing that KCNQ1 was

expressed in the heart (Fig. 3A) (104,105). This was confirmed by RT-PCR (Fig. 3B), where the ΔCT value of KCNQ1 in the heart was lower compared to the other tissues, but this difference failed in reaching significance threshold (heart: 15 ± 2.35, n = 5, vs. brain: 20.4 ± 2.08, n = 5, Kruskal-Wallis test: p = 0.07, Dunn's multiple comparisons test: heart vs. brain: p = 0.83; Fig. 3B). The conventional PCR of KCNQ2 showed that this subtype is mostly expressed in neuronal tissue like brain and spinal cord (Fig. 3A). Compared to the expression in immune-related tissue RT-PCR showed a significant difference in the ΔCT value of the brain (14.01 ± 1.03, n = 5, Kruskal-Wallis test: p = 0.02, Dunn's multiple comparisons test: brain vs. spleen: p = 0.03, brain vs. thymus: p = 0.04). The expression pattern of KCNQ3 showed that this subtype is expressed in neuronal tissue in accordance to the literature (104,106). In addition, there are also indications that the channel, or its splice variants, might be expressed in immune tissue like spleen, thymus and lymph nodes (Fig. 3A). RT-PCR comparing the ΔCT value of brain (14.37 ± 1.2, n = 5), spleen (20.61 ± 1.43, n = 3), thymus (18.83 ± 0.68, n = 4) and lymph nodes (18.15 ± 1.57, n = 4) showed no significance, while the KCNQ3 expression in brain was significantly higher compared to heart (22.77 ± 1.31, n = 5) and muscle (23.53 ± 0.88, n = 5, Kruskal-Wallis test: p = 0.003, Dunn's multiple comparisons test: brain vs. heart: p = 0.01, brain vs. muscle: p = 0.005, Fig. 3D). This strengthens the results from the conventional PCR. The subtype KCNQ4 is neither expressed in brain nor in immune tissue, while it seems to be expressed in the spinal cord. This subtype gave only clear positive results for muscle and bladder (Fig. 3A). Therefore, the expression pattern of KCNQ4 shows differences comparing all organs (Kruskal-Wallis test: p = 0.05, Dunn's multiple comparisons test: n.s.). The subtype KCNQ5 showed a clear expression pattern in brain and spinal cord in the conventional PCR corroborating the literature (106). No signal for immune related organs was observed (Fig. 3A). RT-PCR analysis showed a significant difference for ΔCT values of KCNQ5 in the brain (14.87 ± 1.04, n = 5) compared to heart (21.28 ± 1.48, Kruskal-Wallis test: p = 0.1, Dunn's multiple comparisons test: brain vs. heart: p = 0.05; Fig. 3F).

Taken together, these findings demonstrate, that the subtypes KCNQ2, 3 and 5 are expressed in neuronal tissue. In this respect, these subtypes get in focus for the possible impact of a pharmacological KCNQ-channel treatment and its influence on the pathophysiology of MS.

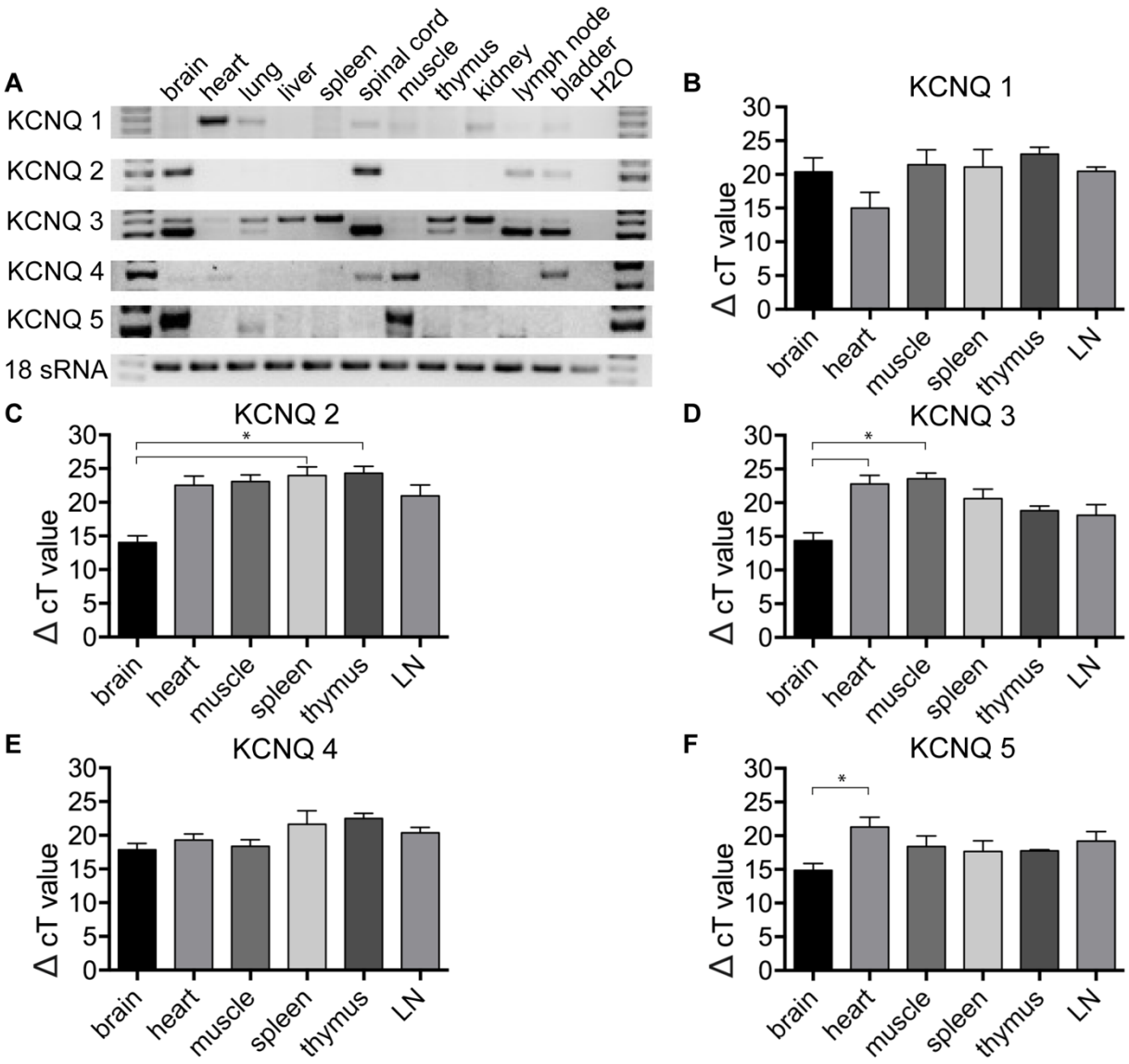

Figure 3: Expression pattern of the KCNQ-channel subtypes KCNQ1-5. **A** Conventional PCR showing the expression pattern of KCNQ1-5 in different organs. **B-F** Bar graphs showing the ΔCT value of different organs after performing RT-PCR for the different subtypes of KCNQ channels.

4.4 Retigabine Titration

Based on conventional and RT-PCR experiments, KCNQ3 seems to be expressed in immune related tissue. Thus, we decided to perform further immune assays assessing the impact of retigabine, as a KCNQ-channel opener, on immune cells (splenocytes). First, we examined the influence of retigabine on the viability of splenocytes. The influence of different concentrations of retigabine was assessed by performing FACS using annexin V to stain apoptotic splenocytes and FVD, which marks necrotic splenocytes (see Material and Methods for details on the assays).

After 24 h of incubation the only significant difference between the viability of stimulated splenocytes treated with retigabine and splenocytes treated with the vehicle was observed at a concentration of 500 µM, as expected (Two-Way ANOVA, treatment: $F_{(1,30)} = 16.03$, $p = 0.0004$, concentration: $F_{(4,30)} = 26.14$, $p < 0.0001$, $n = 4$, Fig. 4A). A similar result was observed after 48 h (Two-Way ANOVA, treatment: $F_{(1,30)} = 112.9$, $p < 0.0001$, concentration: $F_{(4,30)} = 158.9$, $p < 0.0001$, $n = 4$, Fig. 4A). Moreover, at this time point, splenocytes incubated with 1 µM retigabine showed a significantly higher viability compared to splenocytes incubated with 10 µM retigabine (Bonferroni's multiple comparisons test: Ret 1 µM vs. Ret 10 µM: $p = 0.004$) and to splenocytes incubated with 30 µM retigabine (Ret 1 µM vs. Ret 30 µM: $p < 0.0001$). Another significant difference in viability was observed between splenocytes incubated with 5 µM retigabine and 30 µM retigabine ($p = 0.0008$). This demonstrates that increasing concentrations of retigabine partially affected the viability of splenocytes.

Based on the results of this titration assay, we decided to use 30 µM retigabine for further immune assays, as it is a commonly used concentration for other *in vitro* assays (111) and 1 µM retigabine in order to exclude any effect of high but not toxic concentrations of the drug.

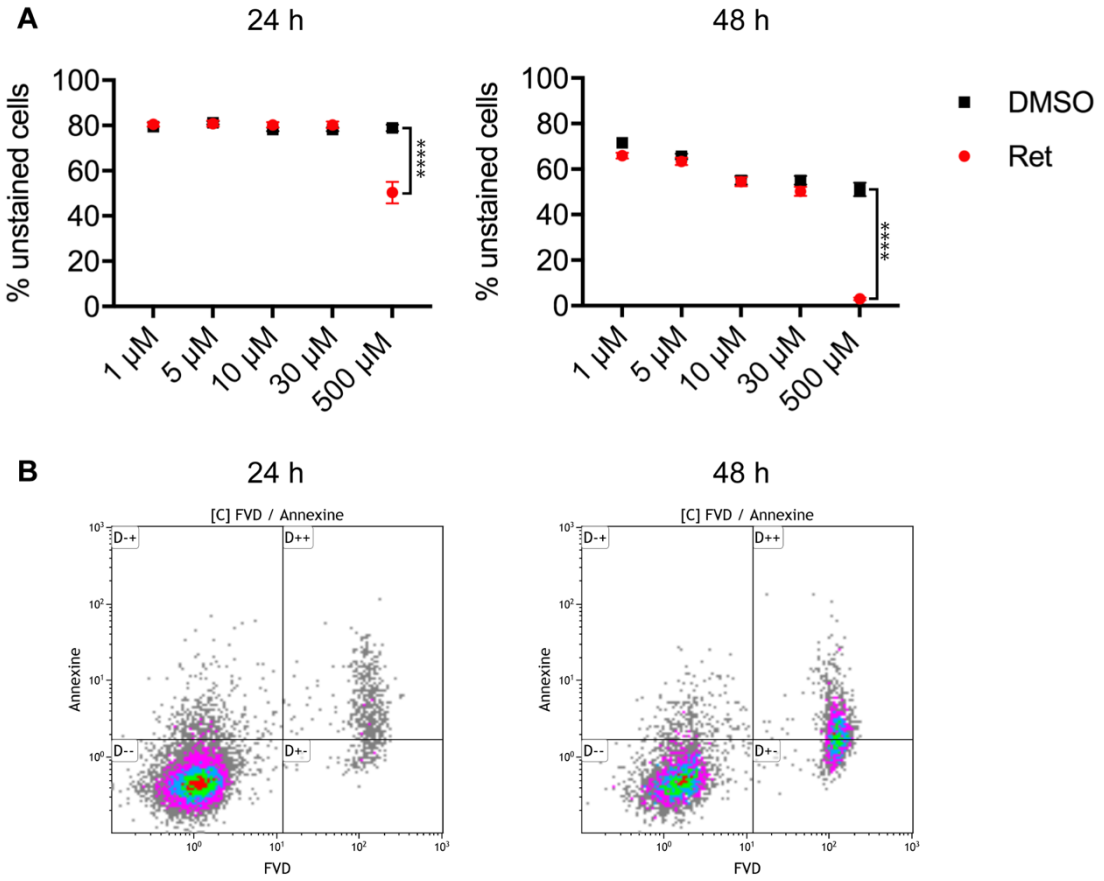

Figure 4: Effect of different retigabine concentrations on the viability of stimulated splenocytes. **A** Dot graph comparing the viable cells (as percentage of unstained cells from a viability staining using annexin V and FVD) of stimulated splenocytes treated with different concentrations of retigabine (red dots) and the vehicle DMSO (black dots) at two different time points. **B** Exemplary FACS scatter plots showing viability of splenocytes treated with 30 µM retigabine after 24 h and 48 h. The x axis shows the FVD staining and the y axis the annexin V staining. Unstained cells are presented in the section D--.

4.5 The Effect of Retigabine Administration on Splenocyte Proliferation

Based on the viability staining described above (see chapter 4. Results, abstract 4.4 Retigabine Titration) we concluded, that retigabine may interact with stimulated splenocytes. Taken together with the expression of KNCQ-channels in immune related organs (see chapter 4. Results, abstract 4.3 Expression Pattern of KCNQ-Channels in Different Organs, Fig. 3) and the ability of the KCNQ-channel opener retigabine to ameliorate EAE disease course, we wanted to investigate if retigabine influences the proliferation of stimulated splenocytes. Therefore, we performed an eFlour670 staining, where a higher proliferation is characterized by lower fluorescence signals as shown in Fig. 5A (see chapter 3. Methods, abstract 3.3.4 Proliferation Assay). Based on the

results obtained from the titration experiments (described in chapter 4. Results, abstract 4.4 Retigabine Titration), we performed the assay using two concentrations of retigabine, namely, 1 µM (Ret 1 µM, silver bars, n = 4) and 30 µM (Ret 30 µM, light gray bars, n = 8). Stimulated cells without additional treatment (stim, black bars, n = 12) and splenocytes treated with DMSO as vehicle (veh, dark gray bars, n = 12) were used as control. There is no significant difference between the proliferation intensity of stimulated splenocytes (71.72 ± 1.08 %), splenocytes treated with the vehicle (71.56 ± 1.01 %) and with 1 µM of retigabine (75.16 ± 1.12 %, Kruskal-Wallis test: p = 0.001, Dunn's multiple comparisons test: stim vs. Ret 1 µM, p = 0.92, veh vs. Ret 1 µM p = 0.64; Fig. 5B). This indicates that at a low concentration retigabine does not influence the immune system. In comparison, splenocytes treated with 30 µM retigabine underwent a lower percentage of proliferation (Ret 30 µM: 63.51 ± 1.67; stim vs. Ret 30 µM: p = 0.02, veh vs. Ret 30 µM: p = 0.04, Ret 1 µM vs. Ret 30 µM: p = 0.002; Fig. 5B), indicating that retigabine might reduce splenocyte proliferation.

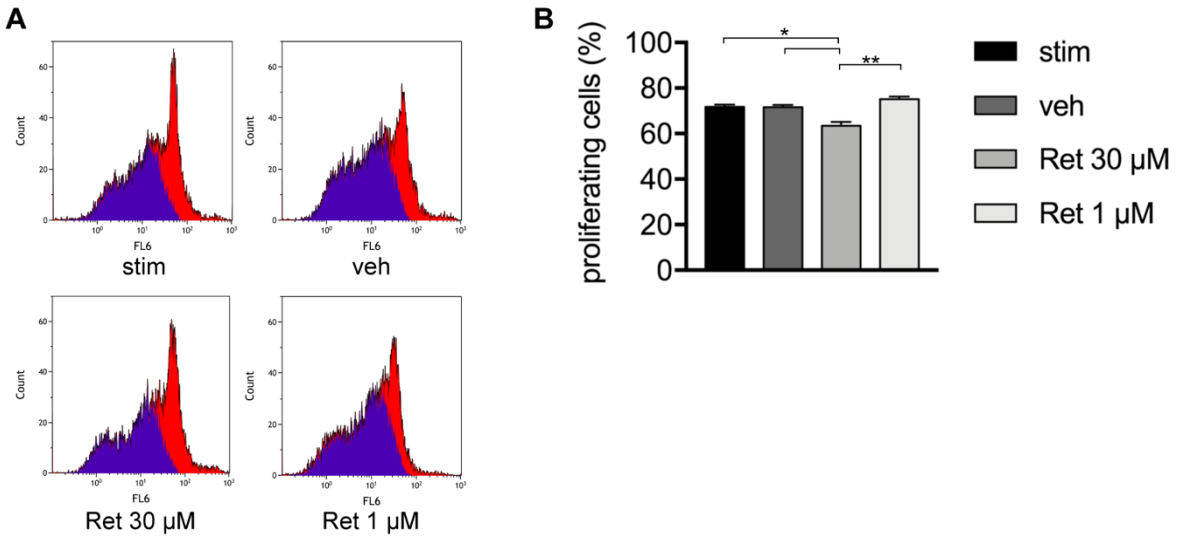

Figure 5: Effect of retigabine on the proliferation of stimulated splenocytes. **A** Exemplary FACS plots showing proliferation cycles of stimulated splenocytes with or without an additional treatment. The red area represents all detected splenocytes, the purple area shows all splenocytes that underwent mitosis as sign of splenocyte proliferation. **B** Bar graph showing the percentage of proliferating cells from stimulated splenocytes with or without additional treatment.

4.6 The Effect of Retigabine on Cytokine Production

To investigate if the lower percentage of proliferation observed at a concentration of 30 µM retigabine influences the immune cells response by altering the cytokine

production, we performed a flowcytometric quantification of IL-2, IL-6, IL-10, IL-17 and TNFα in stimulated splenocytes (stim, black bars, n = 5, Fig. 6), in the presence of 30 µM retigabine (Ret, light grey bars, n = 5, Fig. 6) and of the vehicle (veh, dark grey bars, n = 5, Fig. 6). The different concentrations (in pg/ml) of the cytokines for the 3 conditions as well as the p value of the Kruskal-Wallis Test are presented in table 8. No significant difference in the cytokine production was observed, which indicates that retigabine treatment does not alter the cytokine production of stimulated splenocytes.

	Stimulated	Vehicle	Retigabine	Kruskal-Wallis Test
IL-2	13076 ± 538	12518 ± 439	13239 ± 498	p = 0.65
IL-6	398 ± 78	447 ± 95	502 ± 87	p = 0.6
IL-10	264 ± 38	323 ± 32	385 ± 47	p = 0.99
IL-17	377 ± 62	662 ± 123	422 ± 108	p = 0.11
TNFα	744 ± 170	869 ± 253	1004 ± 231	p = 0.56

Table 8: Concentrations (in pg/ml) of the different cytokines produced by stimulated splenocytes, vehicle and retigabine treated stimulated splenocytes with the p value of the corresponding Kruskal-Wallis Test. No significant differences were observed.

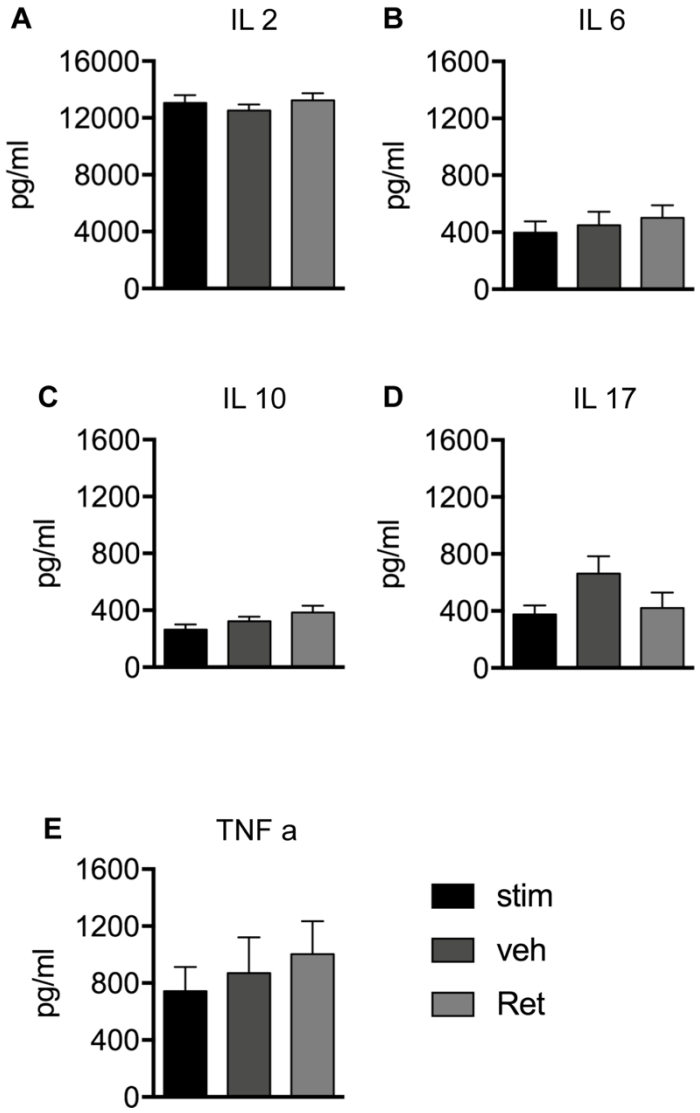

Figure 6: Effect of retigabine treatment on the cytokine production by stimulated splenocytes. **A-F** Bar graphs presenting the concentration (in pg/nl) of different cytokines produced by stimulated splenocytes with or without an additional treatment with retigabine/vehicle.

4.7 The Effect of XE991 Administration on Splenocyte Proliferation

Retigabine showed a slight effect on splenocyte proliferation with no effect on the resulting cytokine production. Therefore, we concluded that the drug has no significant influence on immune system modulation. To corroborate these findings and exclude an involvement of KCNQ-channels in the immune system, we repeated an eFlour 670 proliferation assay blocking KCNQ-channels, which seemed to be expressed in immune related organs (see chapter 4. Results, abstract 4.3 Expression Pattern of KCNQ-Channels in Different Organs, Fig. 3), by using the specific KCNQ-channel blocker XE991. In the eFlour670 assay a higher proliferation is characterized by lower

fluorescence signals as shown in Fig. 7A. We used the following concentrations of XE991: 10 µM (XE 10 µM, dark gray bars, n = 8) and 1µM (XE 1 µM, light gray bars, n = 4). Splenocytes treated with 1 µM of XE991 (74.24 ± 0.59 %) showed a similar average proliferation percentage to the stimulated splenocytes (indicated by the red horizontal line, the corresponding bar graph can be seen in Fig. 5A, 71.72 ± 1.08 %, n = 12, Kruskal-Wallis test: p = 0.0007, Dunn's multiple comparisons test: stim vs. XE 1 µM: p > 0.9999, Fig. 7B). Splenocytes which were exposed to 10 µM XE991 (63.32 ± 1.22 %) proliferated significantly less compared to stimulated splenocytes and those treated with 1 µM XE991 (Dunn's multiple comparisons test: stim vs. Ret 10 µM: p = 0.002, Ret 1 µM vs. Ret 10 µM: p = 0.005, Fig. 7B). These results indicate a possible influence of KCNQ-channel blocking on splenocyte proliferation.

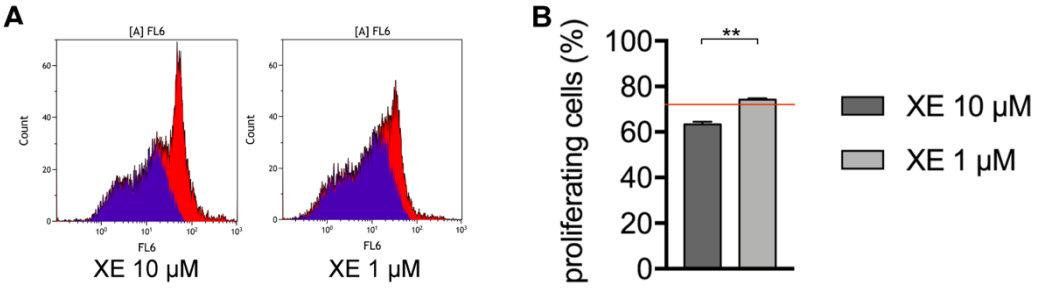

Figure 7: Effect of XE991 on the proliferation of stimulated splenocytes. **A** Exemplary FACS plots showing the proliferation cycles of stimulated splenocytes treated with different concentrations of XE991. The red area represents all detected splenocytes, the purple area shows all splenocytes that underwent mitosis as sign of splenocyte proliferation. **B** Bar graph showing the percentage of proliferating cells treated with different concentrations of XE991. The proliferation rate of stimulated splenocytes without an additional treatment is indicated by the horizontal red line.

4.8 Expression Pattern of KCNQ-Channels in CNS Resident Cells

MS is a multifactorial disease with two main components: the immune system activation and neurodegeneration characterized by demyelination and axonal damage. The immune assays described in the chapters above were focusing on understanding the inflammatory component of the disease, but to consider both sides, further investigations focusing on the involvement of the neuronal system is needed. Therefore, the expression pattern of the different KCNQ-channel subtypes was analyzed by performing conventional PCR with 18s RNA as expression control in neurons, oligodendrocyte progenitor cells (OPC), oligodendrocytes differentiated for 24 h (oligo 24h) and 48 h (oligo 48h), microglia and astrocytes. KCNQ1 was not

expressed in any of the tested cell types, which corroborates our previous findings (see chapter 4. Results, abstract 4.3 Expression Pattern of KCNQ-Channels in Different Organs, Fig. 3A), where KCNQ1 is not expressed in the brain, as well as the literature (Fig. 8A) (104,105). The KCNQ2 subtype was expressed in neurons, as well as in OPC and weaker bands were observed for oligodendrocytes differentiated for 24h and 48h. No signal for an expression of this subtype was detected in microglia and astrocytes (Fig. 8A). The KCNQ3 subtype was expressed in all tested cell types, with a strong signal for neurons, OPC, oligodendrocytes differentiated for 24h and 48h and astrocytes and a weaker signal for the expression in microglia (Fig. 8A). The KCNQ4 subtype was expressed in neurons and astrocytes, but with a lower intensity of the signals compared to the other subtypes which fits the results from paragraph 4.3, where this subtype was not expressed in the brain (Fig. 8A and see chapter 4. Results, abstract 4.3 Expression Pattern of KCNQ-Channels in Different Organs, Fig. 3A). The KCNQ5 subtype is expressed in neurons, OPCs, oligodendrocytes differentiated for 24h and 48h and astrocytes. The signal for an expression of this subtype in microglia was weaker compared to the other cell types (Fig. 8A).

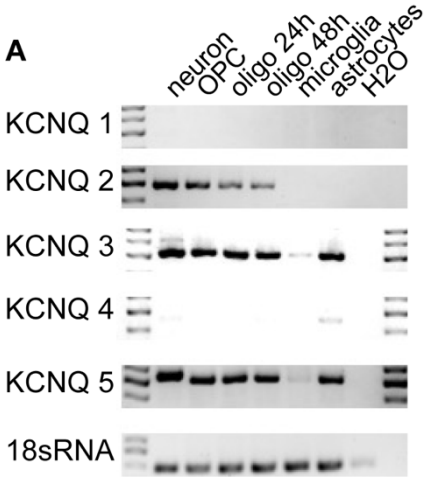

Figure 8: **A** Expression pattern of the KCNQ-channel subtypes in different cell types of the CNS.

4.9 Open Field Test of Cuprizone Mice treated with Retigabine

Based on the expression of KCNQ2, 3 and 5 in neurons and oligodendrocytes, further experiments focusing on the role of KCNQ-channels in neurodegeneration were performed. To focus on the neurodegenerative part of MS we took advantage of the cuprizone model of de- and remyelination, which allows analysis of neurodegenerative

processes without involvement of the activated adaptive immune system (compare chapter 1. Introduction, abstract 1.3.2. Cuprizone Model of De- and Remyelination, Fig. 9A). The cuprizone diet is known to alter the behavior of mice, as mice at 3-4 weeks after cuprizone induction show a less anxiety-like and more exploratory behavior (76). After 5 weeks of cuprizone diet, an impaired motor coordination was observed in the literature (76).Therefore, we performed several behavior experiments to assess these changes in our experimental animals and investigate if a treatment with retigabine influences the behavioral changes of cuprizone mice. During the OF test, which assesses locomotor deficits and anxiety-like behavior, no alterations between the different groups of mice, with or without treatment were observed analyzing the distance traveled by the mice (Kruskal-Wallis test: $p = 0.96$, Fig. 9B). Moreover, the average speed that the mice of the different groups reached was similar (Kruskal-Wallis test: $p = 0.96$, Fig. 9C) suggesting no locomotor impairment. No significant differences were found between the different groups considering the time the animals spent in the center (Kruskal-Wallis test: $p = 0.71$, Fig. 9D) and in the periphery (Kruskal-Wallis test: $p = 0.71$, Fig. 9E) suggesting no anxiety-like behavior. By analyzing the number of grooming, namely self-cleaning behaviors, we observed that cuprizone treated mice at full demyelination (cuprizone, gray bar, n = 5, number of grooming: 5.2 ± 0.73) showed a significantly higher number compared to mice of the late remyelination phase, which received a treatment with the vehicle DMSO (remy 25 days + veh, orange bars, n = 10, number of grooming: 1.4 ± 0.27, Kruskal-Wallis test: $p = 0.006$, Dunn's multiple comparisons test: cuprizone vs. remy 25 days + veh: $p = 0.001$, Fig. 9F). There were differences concerning the number of vertical behaviors observed between the different groups, but they failed to reach significant threshold (Kruskal-Wallis test: $p = 0.04$, Fig. 9G). Taken together our results did not show any obvious altered behavior of cuprizone mice, independent from the status of de- and remyelination.

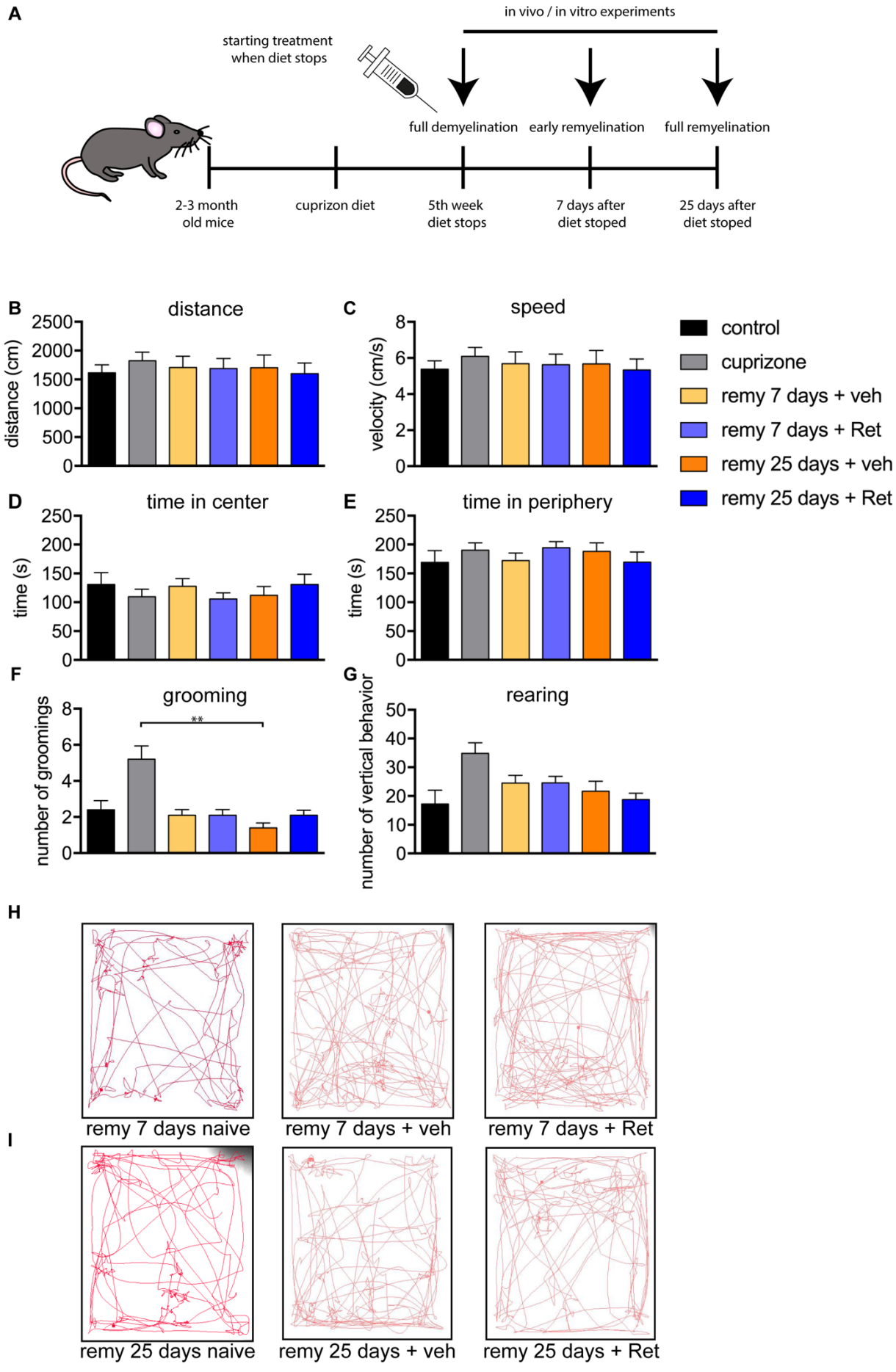
A
in vivo / in vitro experiments
starting treatment
when diet stops
full demyelination
early remyelination
full remyelination
2-3 month
old mice
cuprizon diet
5th week
diet stops
7 days after
diet stoped
25 days after
diet stoped
B
distance
distance (cm)
2500
2000
1500
1000
500
0
C
speed
velocity (cm/s)
8
6
4
2
0
control
cuprizone
remy 7 days + veh
remy 7 days + Ret
remy 25 days + veh
remy 25 days + Ret
D
time in center
time (s)
250
200
150
100
50
0
E
time in periphery
time (s)
250
200
150
100
50
0
F
grooming
number of groomings
**
8
6
4
2
0
G
rearing
number of vertical behavior
50
40
30
20
10
0
H
remy 7 days naive
remy 7 days + veh
remy 7 days + Ret
I
remy 25 days naive
remy 25 days + veh
remy 25 days + Ret

Figure 9: OF of cuprizone mice treated with retigabine. **A** Schematic representation of the experimental outline. The horizontal black arrow represents the timeline. The syringe marks the starting of retigabine/vehicle treatment coherent to changing from cuprizone diet to normal rodent chow after 5 weeks. The different time points of *in vitro* and *in vivo* experiments are marked by vertical black arrows. **B** Bar graph showing the distance, that the different groups of cuprizone mice traveled during the OF. **C** Bar graph showing the speed of the different groups during the OF. **D** Bar graph showing the time the different groups spent in the center during the OF. **E** Bar graph showing the time the different groups spent in the periphery during the OF. **F** Bar graph showing the numbers of grooming of the different groups in the OF. **G** Bar graph showing the number of rearing of the different groups during the OF. **H, I** Exemplary graphs representing the distance that a mouse of the corresponding group traveled during the OF. Naïve mice received no additional treatment and only underwent the cuprizone diet, while the groups remy 7 / remy 25 days +veh and + Ret received the corresponding treatment with retigabine/DMSO.

4.10 Elevated Plus Maze of Cuprizone Mice treated with Retigabine

Another test to assess anxiety-like behavior in mice is the EPM. Naïve C57BL/6J mice, which received no treatment at all, spent similar times in the open and closed arms of the EPM maze (control, black bars, n = 10, time open arms: 77.59 ± 15.96 s, time closed arms: 103.68 ± 10.64 s, Tukey's multiple comparisons test: p = 0.99, Fig. 10A). Cuprizone treated mice at full demyelination also show no significant difference (cuprizone, grey bars, n = 5, time open arms: 83.5 ± 9.06 s, time closed arms: 118.1 ± 13.28 s, p = 0.99, Fig. 10A). However, mice in the remyelination phase that received no additional treatment, spent most of the time in the closed arms, which indicates a higher anxiety level. This effect is stronger in mice remyelinated for 7 days, than for 25 days (remy 7 days naïve: light green bars, n = 5, time open arms: 32.62 ± 8.77 s, time closed arms: 195.47 ± 22.08 s, $p < 0.0001$, remy 25 days naïve: dark green bars, n = 5, time open arms: 53.54 ± 14.51 s, time closed arms: 187.14 ± 33.99 s, p = 0.0009, Fig. 10A). Mice at the early remyelination phase (7 days) treated with the vehicle spent more time in the closed arms (remy 7 days + veh: yellow bars, n = 9, time open arms: 65.06 ± 6.8 s, time closed arms: 151.2 ± 8.33 s, p = 0.0091, Fig. 10B). Mice which received a retigabine treatment during the early remyelination phase, showed a tendency to stay in the closed arms, but compared to the time they spent in the open arms this was not significant (remy 7 days + Ret: light blue bars, n = 10, time open arms: 74.8 ± 11.27 s, time closed arms: 134.14 ± 22.27 s, p = 0.22, Fig. 10B). After full remyelination both treated groups preferred staying in the closed arms, but this effect was stronger on animals receiving the vehicle treatment (remy 25 days + veh: orange bars, n = 10, time open arms: 44.40 ± 7.51 s, time closed arms: 153.72 ± 20.71 s, p <

0.0001, remy 25 days + Ret: dark blue bars, n = 10, time open arms: 48.9 ± 11.03 s, time closed arms: 131.64 ± 19.25 s, p = 0.008, Fig. 10B). Taken together, mice tested during the early remyelination phase explored the arena with a tendency to stay in the closed arms (exemplary tracks shown in Fig. 10C), while mice at the late remyelination phase preferred to stay in the closed arms (exemplary tracks shown in Fig. 10D). This indicates, that there is no general effect of the treatment in this experiment, remyelinated animals with or without treatment present a higher anxiety level compared to demyelinated and naïve C57BL/6J mice.

To support these results, we analyzed the number of entries into the open and close arms (Fig. 11). By comparing them, there was no significant effect of the conditions (open and closed arms; Two-Way ANOVA, condition: $F_{(1,112)} = 2.34$, $p = 0.13$). However, the treatment had an effect on the outcome of the experiment (Two-Way ANOVA, treatment: $F_{(7,112)} = 2.62$, $p = 0.02$). Naïve C57BL/6J mice show similar number of entries into the open and closed arms of the EPM arena (entries open arms: 14.1 ± 1.71, entries closed arms: 12.3 ± 1.8, Tukey's multiple comparisons test: $p > 0.99$, Fig. 11A). Demyelinated animals as well as animals in the early remyelination phase and fully remyelinated without treatment, showed no significant difference between the number of entries into the open arms or closed arms of the EPM arena (Fig. 11A). Treatment with retigabine or the vehicle during the remyelination phase lead to similar numbers of entries into the open and closed arms (Fig. 11B).

These results demonstrated, that the mice explored the maze similarly to what we observed in the OF test (see chapter 4. Results Abstract 4.9 Open Field Test of Cuprizone Mice treated with Retigabine). A general difference between naïve C57BL/6J mice, cuprizone treated mice at full demyelination and mice of the remyelination phase could be observed, but there was no difference in the anxiety-like behavior of the different remyelination groups with or without treatment.

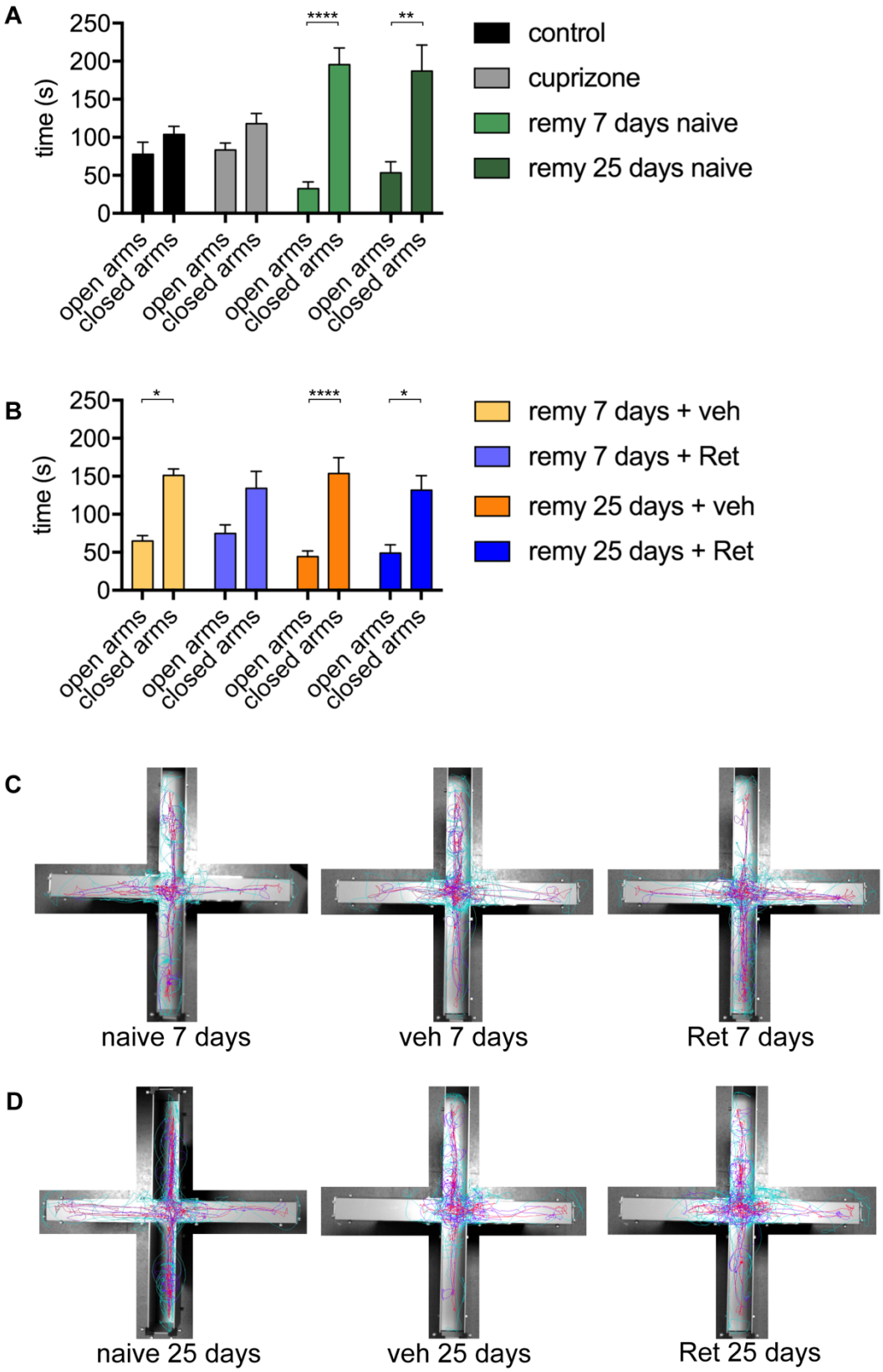

Figure 10: EPM test of cuprizone mice treated with retigabine. **A, B** Bar graph showing the time the different groups of cuprizone mice spent in the open and closed arms. **C, D** Exemplary pictures from the tracking system showing the activity of cuprizone mice remyelinated for 7 and 25 days, which received different treatments. The blue line indicates position of the nose of the mice, the red line the middle of the back and the purple line the beginning of the tail.

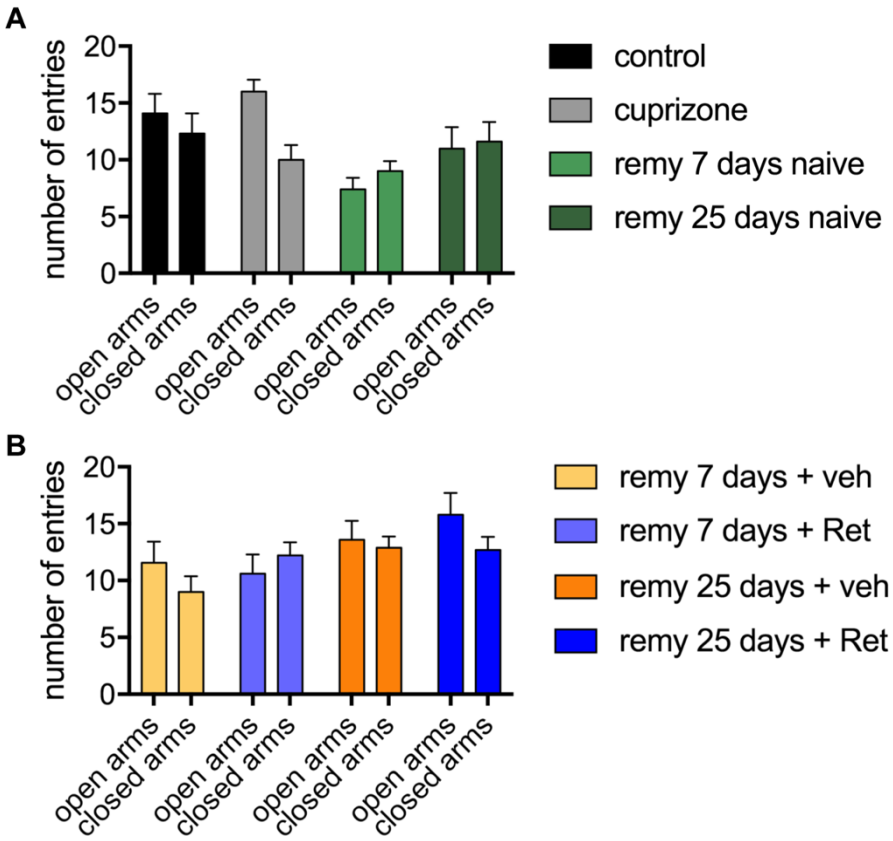

Figure 11: **A, B** Number of entries of the different treatment groups of cuprizone mice in the open and closed arms of the EPM.

4.11 Open Field Test of Cuprizone Mice treated with XE991

Demyelination, induced by feeding the mice cuprizone for 5 weeks, can cause anxiety-like behavior and cognition impairment in mice. A treatment with the KCNQ-channel opener retigabine did not affect the behavior of mice with cuprizone induced de- and remyelination, as they performed similar to control mice during behavior experiments (see chapter 4. Results, abstract 4.9 Open Field Test of Cuprizone Mice treated with Retigabine and 4.10 Elevated Plus Maze of Cuprizone Mice treated with Retigabine). To confirm these data, we repeated the behavior experiments on mice treated with the KCNQ-channel blocker XE991, which should ideally also not affect the behavior. During OF, which assesses locomotor deficits and anxiety-like behavior, no difference between the groups was observed analyzing the distance that the animals traveled within the arena in 5 minutes (Kruskal-Wallis test: p = 0.55, Dunn's multiple comparison: ns, Fig.12A). Moreover, the average speed of the mice of the different groups was similar between groups (Kruskal-Wallis test: p = 0.55, Dunn's multiple

comparison: ns, Fig. 12B). Mice treated with XE991 for 7 days spent more time in the center (remy 7 days + XE: rosa bars, n = 10, time in center: 146.3 ± 6.57 s) compared to mice treated with XE991 for 25 days (remy 25 days +XE, red bars, n = 10, time in center: 100.9 ± 11.83 s, Kruskal-Wallis test: p = 0.04, Dunn's multiple comparisons test: remy 7 days + XE vs. remy 25 days + XE, p = 0.04, Fig. 12C), while both groups were not significantly different compared to the control mice. Coherent to this, mice treated with XE991 for 25 days spent more time in the periphery (199.1 ± 11.83 s) compared to the group treated with XE991 for 7 days (153.8 ± 6.57 s, Kruskal-Wallis test: p = 0.04, Dunn's multiple comparisons test: remy 7 days + XE vs. remy 25 days + XE: p = 0.04, Fig. 12D), but there was no significant difference for both groups compared with the control mice. By comparing the number of groomings, cuprizone mice at full demyelination showed a higher number (5.2 ± 0.73) than the other groups with statistical significance reached when compared to mice of the early remyelination phase treated with XE991 (2.1 ± 0.35, Kruskal-Wallis test: p = 0.06, Dunn's multiple comparisons test: cuprizone vs. remy 7 days + XE: p = 0.05, Fig. 12E). No significant difference between the groups was observed comparing number of vertical behaviors (Kruskal-Wallis test: p = 0.05, Dunn's multiple comparison: ns, Fig. 12F).

Taken together, these results indicate that the locomotor activity and anxiety-like behavior of the mice is not affected by cuprizone and/or treatment with XE991.

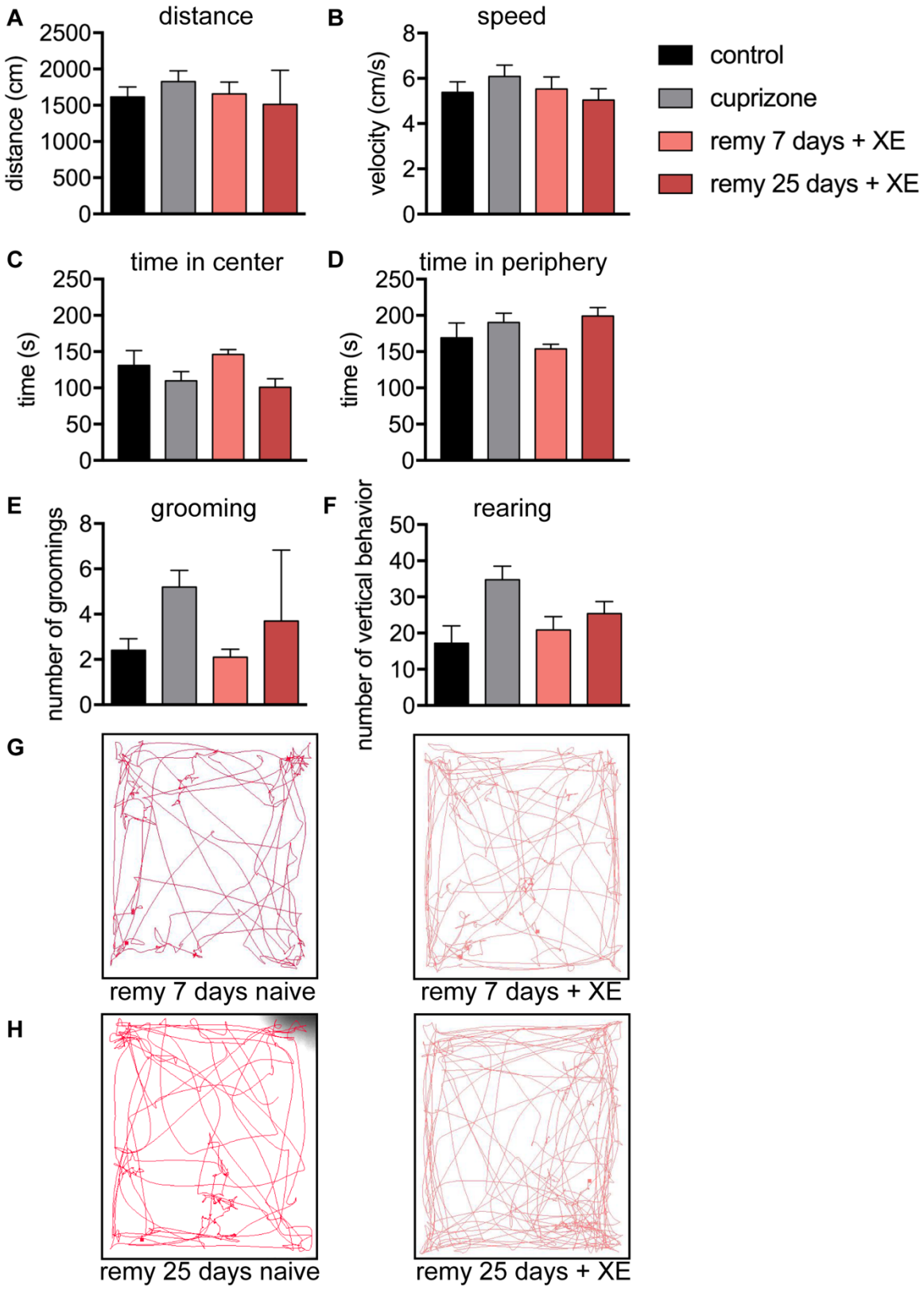

Figure 12: Open field test of cuprizone mice treated with XE991. **A** Bar graph showing the distance, that the different groups of cuprizone mice traveled during the OF. **B** Bar graph showing the speed of the different groups during the OF. **C** Bar graph showing the time the different groups spent in the center during the OF. **D** Bar graph showing the time the different groups spent in the periphery during the OF. **E** Bar graph showing the numbers of grooming of the different groups in the OF. **F** Bar graph showing the number of rearing of the different groups during the OF. **G,**

H Exemplary graphs representing the distance that a mouse of the corresponding group traveled during the OF. Naïve mice received no additional treatment and only underwent the cuprizone diet, while the groups remy 7 / remy 25 days +XE and received the corresponding treatment with XE991.

4.12 Elevated Plus Maze of Cuprizone Mice treated with XE991

Another test to assess the behavior of mice is the EPM, which measures the anxiety level. Treatment with the KCNQ-channel opener retigabine did not affect the behavior of mice undergoing cuprizone induced de- and remyelination. To confirm these findings, we repeated the behavior experiments on mice treated with the KCNQ-channel blocker XE991.

Naïve C57BL/6J mice, which received no treatment at all, spent similar times in the open and closed arms of the EPM maze (control, black bars, n = 10, time open arms: 77.59 ± 15.96 s, time closed arms: 103.68 ± 10.64 s, Tukey's multiple comparisons test: p = 0.98, Fig. 14A). Cuprizone treated mice at full demyelination also showed no significant difference (cuprizone, grey bars, n = 5, time open arms: 83.5 ± 9.06 s, time closed arms: 118.1 ± 13.28 s, p = 0.99, Fig. 13A). However, mice in the remyelination phase that received no additional treatment, spent most of the time in the closed arms, suggesting a higher anxiety level. This effect is stronger in mice remyelinated for 7 days than for 25 days (remy 7 days naïve: light green bars, n = 5, time open arms: 32.62 ± 8.77 s, time closed arms: 195.46 ± 22.08 s, $p < 0.0001$, remy 25 days naïve: dark green bars, n = 5, time open arms: 53.54 ± 14.51 s, time closed arms: 187.14 ± 33.99 s, p = 0.001, Fig. 13A). By adding an additional treatment with XE991 starting with the beginning of the remyelination phase, the tendency of the mice to stay in the closed arms was not altered (remy 7 days + XE, rose bars, n = 10, time open arms: 54.07 ± 4.23 s, time closed arms: 165.78 ± 15.92 s, Tukey's multiple comparisons test: p = 0.0002, remy 25 days + XE, red bars, n = 10, time open arms: 40.56 ± 11.04 s, time closed arms: 189.76 ± 25.96 s, Tukey's multiple comparisons test: $p < 0.0001$, Fig. 13B). Taken together, mice tested during the early remyelination phase explored the arena with a tendency to stay in the closed arms (exemplary tracks are demonstrated in Fig. 13C), while fully remyelinated mice preferred to stay in the closed arms (exemplary tracks shown in Fig. 13D). This indicates, that there is no general effect of the treatment in this experiment, remyelinated mice with or without treatment present a higher anxiety level compared to demyelinated and naïve C57BL/6J mice.

To support these results, we analyzed the number of entries of the animals in the open and closed arms (Fig. 14). There was no statistical significance by comparing the conditions of exploration (open or closed arms; Two-Way ANOVA, condition: $F_{(1,76)}$ = 0.38, p = 0.54). However, the treatment affected the outcome of the experiment (Two-Way ANOVA, treatment: $F_{(5,76)}$ = 2.69, p = 0.03). Naïve C57BL/6J mice showed a similar number of entries both in the open and closed arms of the EPM arena (entries open arms: 14.1 ± 1.71, entries closed arms: 12.3 ± 1.8, Tukey's multiple comparisons test: p = 0.99, Fig. 14A). Demyelinated animals as well as animals in the early remyelination phase and fully remyelinated without treatment showed no significant difference between the number of entries into the open and closed arms of the EPM arena (Fig. 14A). Mice treated with XE991 during the remyelination phase showed similar numbers of entries into the open and closed arms (Tukey's multiple comparisons test: remy 7 days + XE, p > 0.9999, remy 25 days + XE, p > 0.9999, Fig. 14B). These results demonstrated, that the mice showed an explorative behavior. A general anxiety-like behavior difference could be observed between naïve C57BL/6J mice, cuprizone treated mice at full demyelination and mice of the remyelination phase, as cuprizone treated mice spent more time in the closed arms, but there was no difference in the anxiety-like behavior of the different remyelination groups with or without treatment.

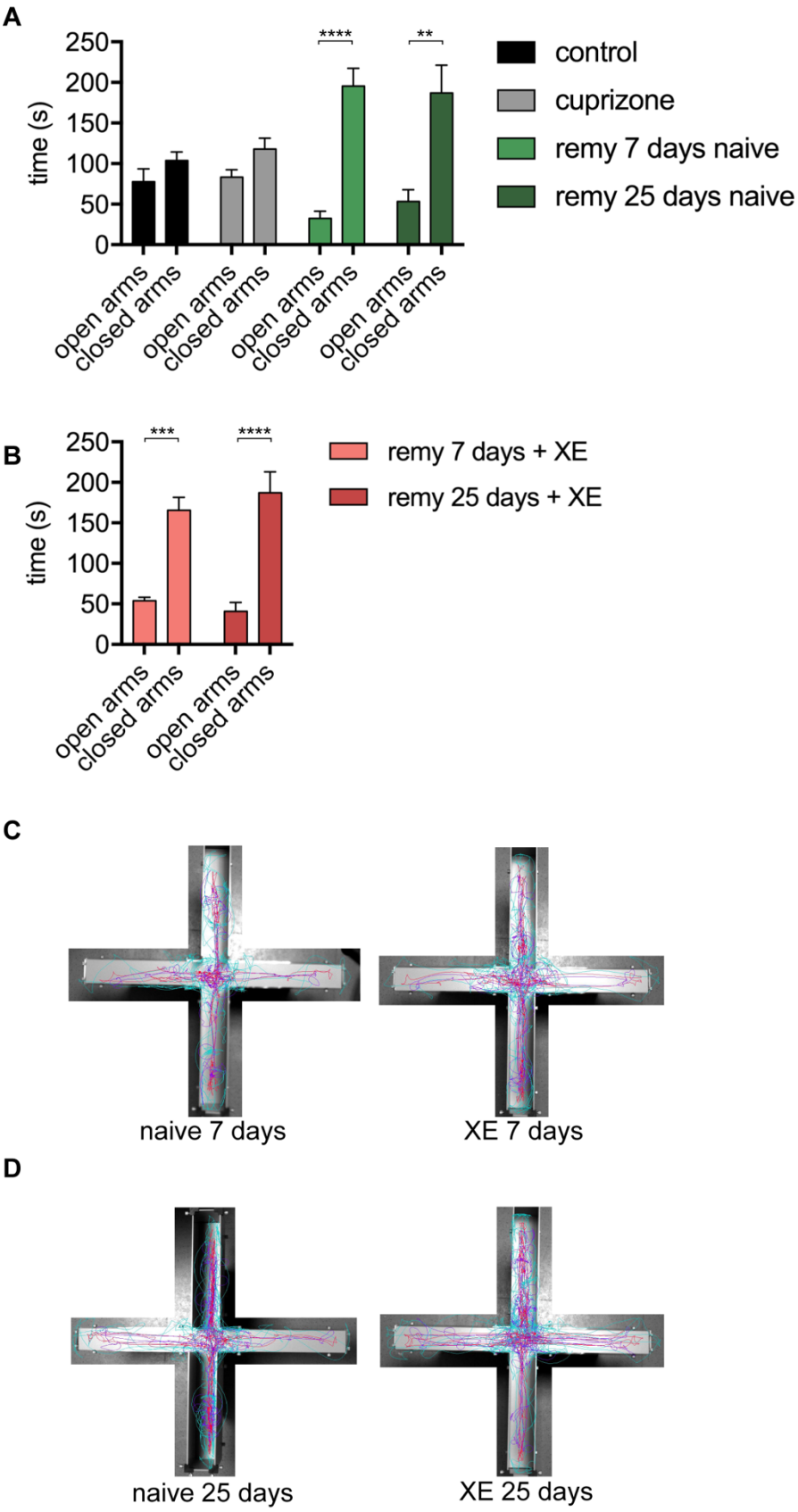

Figure 13: EPM test in cuprizone mice treated with XE991. **A, B** bar graph showing the time the different groups of cuprizone mice spent in the open and closed arms. **C, D** Exemplary pictures from the tracking system showing the activity of cuprizone mice remyelinated for 7 and 25 days, which received different treatments. The blue line

indicates the position of the nose of the mice, the red line the middle of the back and the purple line the beginning of the tail.

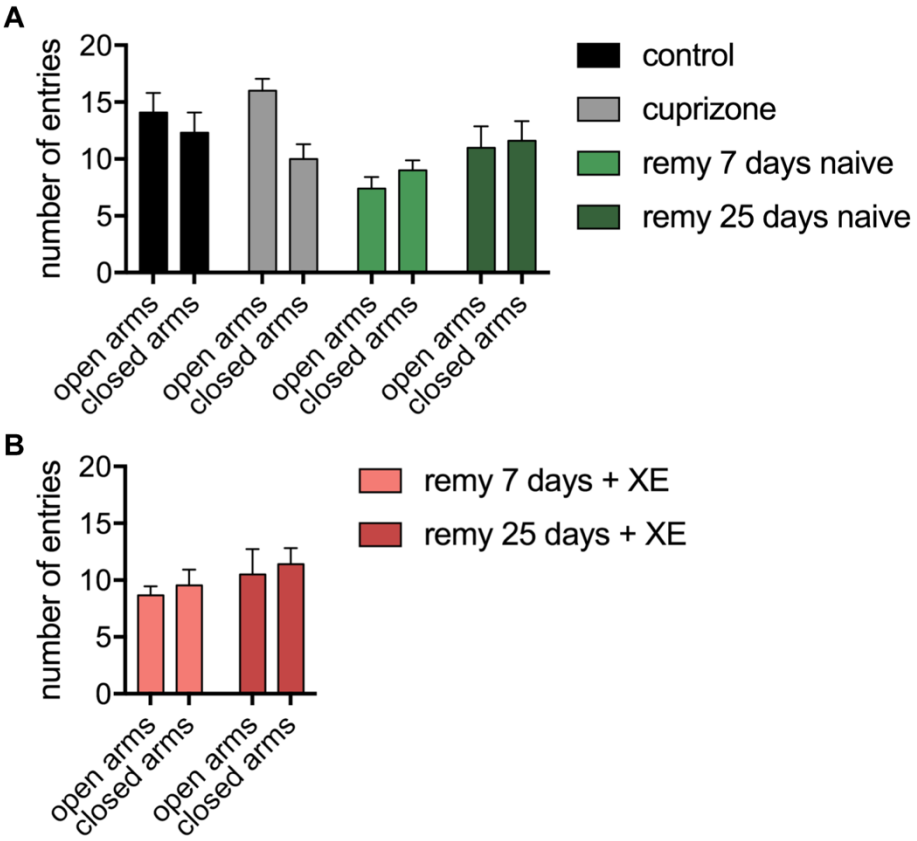

Figure 14: **A, B** Number of entries of the different treatment groups of cuprizone mice in the open and closed arms of the EPM.

4.13 The Effect of a Pharmacological Treatment of KCNQ-Channel on the Novel Object Recognition Test performed with Cuprizone Mice

The cuprizone model of de- and remyelination is known to alter the behavior of mice (76). Since retigabine improved the long-term memory impairment of EAE mice (see chapter 4. Results, abstract 4.2 Novel Object Recognition of EAE Mice treated with Retigabine), we wanted to investigate if this can be translated to cuprizone treated mice. Therefore, we repeated the novel object recognition test as described above (see chapter 3. Methods, abstract 3.2.3 Novel Object Recognition, Fig. 15A) with cuprizone mice which were treated with either retigabine or XE991 during the remyelination period of 7 days (early remyelination, remy 7 days + veh: yellow bars, n = 10, remy 7 days + Ret: light blue bars, n = 8, remy 7 days + XE, rose bar, n = 10, Fig. 15B+C). The mice of the different groups spent a similar time exploring the figures

during the adaptation phase (Kruskal-Wallis test: p = 0.63, Fig. 15B), and while testing the short-term memory 30 minutes after the adaptation phase, no group of the early remyelination phase was able to distinguish between the novel and old object (NOR index remy 7 days + veh: 0.48 ± 0.06, NOR index remy 7 days + Ret: 0.5 ± 0.07, NOR index remy 7 days + XE: 0.5 ± 0.06, Tukey's multiple comparisons test: p > 0.97, Fig. 15C). There was no significant difference between the groups when performing the NOR test 60 minutes after the adaptation phase (NOR index remy 7 days + veh: 0.52 ± 0.09, NOR index remy 7 days + Ret: 0.36 ± 0.06, NOR index remy 7 days + XE: 0.5 ± 0.05, p > 0.29, Fig. 15C). Performing the NOR 24 h after the adaptation phase revealed that mice treated with retigabine (NOR index remy 7 days+ Ret: 0.39 ± 0.1) showed a tendency to spend more time with the old object than mice of the early remyelination phase treated with the vehicle or XE991 (NOR index remy 7 days + veh: 0.62 ± 0.08, NOR index remy 7 days + XE: 0.54 ± 0.08) but this difference was not statistically significant (Tukey's multiple comparisons test: remy 7 days + veh vs. remy 7 days + Ret: p = 0.09, remy 7 days + Ret vs. remy 7 days + XE: p = 0.33, Fig. 15C).

To test the cognition abilities during the full remyelination phase, the mice received an additional treatment with either the vehicle, retigabine or XE991 for 25 days starting with the change to normal rodent chow after the cuprizone diet (late remyelination phase, remy 25 days + veh: orange bars, n = 10, remy 25 days + Ret: dark blue bars, n = 9, remy 25 days + XE, red bars, n = 10, Fig. 15D+E). Mice treated with the vehicle (83.78 ± 11.16 s) spent significantly more time exploring the figures during the adaptation time in comparison to mice treated with retigabine (35.03 ± 6.57 s, Kruskal-Wallis test: p = 0.003, Dunn's multiple comparisons test: remy 25 days+ veh vs. remy 25 days + Ret: p = 0.002, Fig. 15D). While testing the short-term memory 30 minutes after the adaptation phase, mice treated with the vehicle showed more interest in the old object (NOR index remy 25 days + veh: 0.38 ± 0.07), while mice treated with retigabine spent similar time exploring both objects (NOR index remy 25 days + Ret: 0.47 ± 0.07) and mice treated with XE991 showed more interest in the novel object (NOR index remy 25 days + XE: 0.5 ± 0.06), but this tendency was not statistically significant (Tukey's multiple comparisons test: remy 25 days + veh vs. remy 25 days + Ret: p = 0.72, remy 25 days + veh vs. remy 25 days + XE: p = 0.19, remy 25 days + Ret vs. remy 25 days + XE: p = 0.61, Fig. 15E). There was no significant difference between the groups performing the NOR test 60 minutes after the adaptation phase

(NOR index remy 25 days + veh: 0.6 ± 0.09, NOR index remy 25 days + Ret: 0.61 ± 0.09, remy 25 days + XE: 0.46 ± 0.08, Fig. 15E), with a tendency of retigabine treated mice to spent more time exploring the novel object (Tukey's multiple comparisons test: remy 25 days + veh vs. remy 25 days + Ret: p = 0.99, remy 25 days + veh vs. remy 25 days + XE: p = 0.51, remy 25 days + Ret vs. remy 25 days + XE: p = 0.46, Fig. 15E). Considering the long-term memory impairment, by performing the NOR 24h after the adaptation phase, mice treated with the vehicle showed a tendency to spend more time with the old object than mice treated with retigabine or XE991 (NOR index remy 25 days + veh: 0.34 ± 0.09, NOR index remy 25 days + Ret: 0.58 ± 0.12, NOR index remy 25 days + XE: 0.56 ± 0.1), but this difference was not significant (Tukey's multiple comparisons test: remy 25 days + veh vs. remy 25 days + Ret: p = 0.16, remy 25 days + veh vs. remy 25 days + XE: p = 0.18, remy 25 days + Ret vs. remy 25 days + XE: p = 0.99, Fig. 15E).

Taken together, the pharmacological treatment of KCNQ-channels showed no effect on the short- and long-term memory of cuprizone mice during the early or full remyelination phase (Two-Way ANOVA, time: $F_{(2,102)} = 0.14$, p = 0.87, treatment: $F_{(5,51)} = 1.3$, p = 0.28).

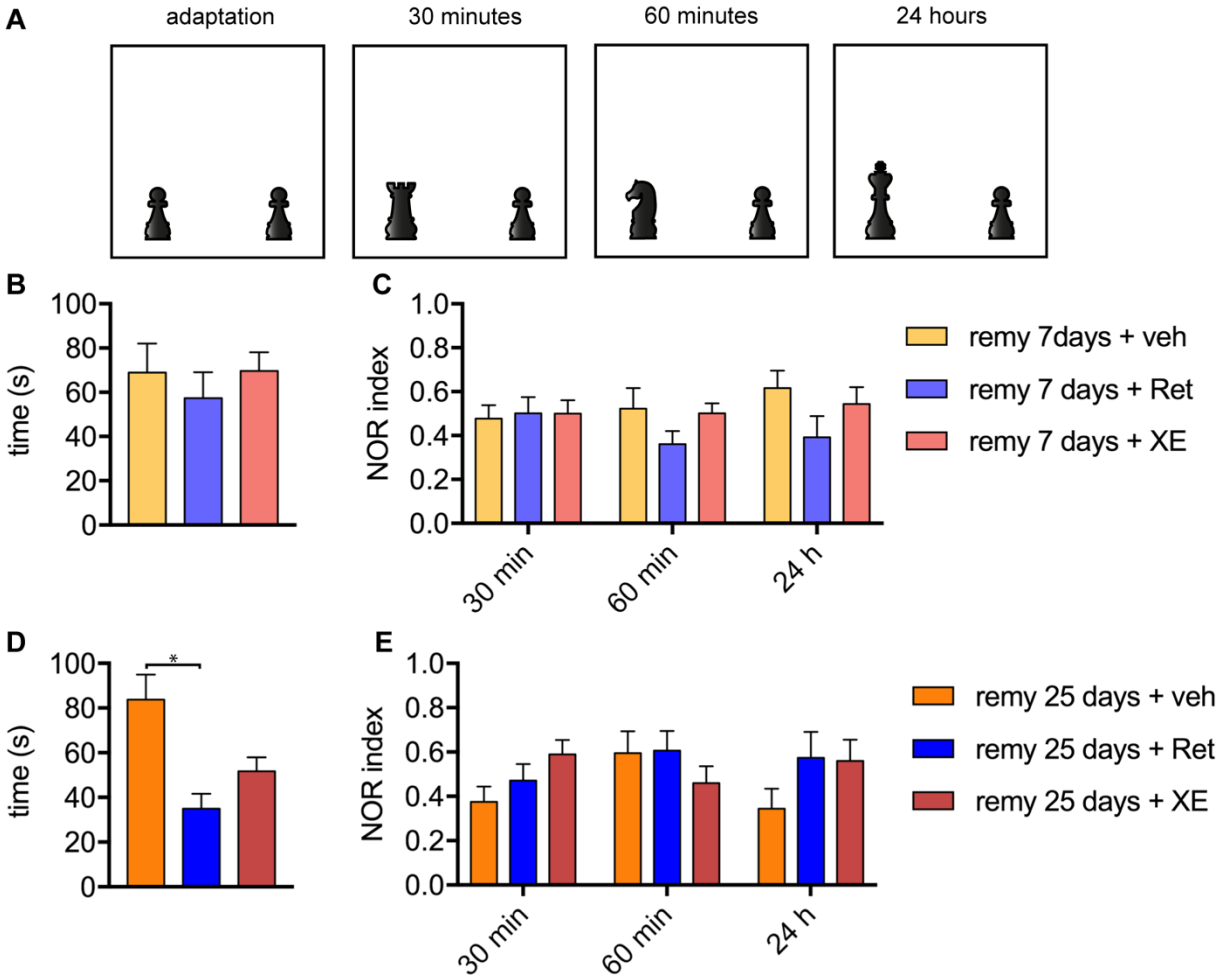

Figure 15: Effect of a pharmacological modulation of KCNQ-channels on the NOR experiments of cuprizone mice. **A** schematic representation of the experimental setting. **B** Bar graph showing the average time the mice of the early remyelination phase spent exploring the objects during the adaptation trial. **C** Bar graph showing the NOR indexes for the different time points of mice from the early remyelination phase. An index of 0.5 indicates, that the mouse spent the same time exploring the novel and old object, an index < 0.5 says that the mouse spent more time with the old object and an index > 0.5 says that the mouse spent more time with the novel object. **D** Bar graph showing the average time the mice of the late remyelination phase spent exploring the objects during the adaptation trial. **D** Bar graph showing the NOR indexes for the different time points of mice from the early remyelination phase.

4.14 Different Learning Abilities of Cuprizone Mice under the Influence of Retigabine or XE991 Treatment tested in an Auditory Pavlovian Conditioning Paradigm

It is known that a cuprizone diet induces changes the learning behavior of mice (49,76). Since previously described behavior tests showed no effect of the cuprizone diet or of additional treatment on the learning abilities of mice, we wanted to investigate a more complex learning mechanism involving different brain circuits (71). Therefore, we

performed an auditory Pavlovian conditioning on cuprizone mice treated with retigabine or XE991 (see chapter 3. Methods, abstract 3.2.4 Auditory Pavlovian Conditioning, Fig. 16A).

In this experiment both factors, frequency of the tones as well as the different treatments of the groups influenced the results significantly (Two-Way ANOVA, frequency: $F_{(1,120)} = 57.56$, $p < 0.0001$, treatment: $F_{(9,120)} = 5.05$, $p < 0.0001$). Naïve C57BL/6J mice were able to distinguish between the conditioned and the unconditioned sound, the percentage of freezing was more than 5 folds higher at a frequency of 10 kHz compared with the percentage of freezing at the unconditioned tone of 2.5 kHz (control, black bars, n = 5, 2.5 kHz = 11.78 ± 1.3 %, 10 kHz = 62.46 ± 1.71 %, Tukey's multiple comparisons test: $p < 0.0001$, Fig. 16B). After undergoing 5 weeks of cuprizone and reaching full demyelination, the animals lost their ability to discriminate between the two frequencies (cuprizone, grey bars, n = 5, 2.5 kHz = 57.65 ± 2.09 %, 10 kHz = 66.45 ± 2.32 %, Tukey's multiple comparisons test: $p > 0.9999$ Fig.16B). After a remyelination period of 7 days, without an additional treatment, the mice did not regain the ability to distinguish between the conditioned and unconditioned frequency, which resulted in similar percentage of freezing at 2.5 kHz and 10 kHz (remy 7 days naïve, light green bars, n = 5, 2.5 kHz = 47.19 ± 4.16 %, 10 kHz = 43.22 ± 3.55 %, Tukey's multiple comparisons test: $p > 0.9999$, Fig.16B). Moreover, after a full remyelination period of 25 days without an additional treatment the mice showed a similar freezing percentage at both frequencies (remy 25 days naïve, dark green bars, n = 5, 2.5 kHz = 38.73 ± 6.44 %, 10 kHz = 32.58 ± 7 %, Tukey's multiple comparisons test: $p > 0.9999$, Fig. 16B). This effect could be altered by introducing a pharmacological modulation starting with the remyelination phase. After a remyelination period of 7 days, with an additional retigabine treatment, the mice showed a significant higher percentage of freezing after being exposed to the conditioned sound compared with the unconditioned frequency (remy 7 days + Ret, light blue bars, n = 6, 2.5 kHz = 34.82 ± 6.52 %, 10 kHz = 66 ± 3.09 %, Tukey's multiple comparisons test: $p = 0.03$, Fig. 16C). A treatment during this period with the corresponding vehicle DMSO did not show this effect, the percentage of freezing was similar for both frequencies with no significant difference (remy 7 days + veh, yellow bars, n = 5, 2.5 kHz = 46.87 ± 6.92 %, 10 kHz = 55.81 ± 6.17 %, Tukey's multiple comparisons test: $p > 0.9999$, Fig. 16C). A treatment with XE991 (remy 7 days + XE,

rose bars, n = 10) during the early remyelination period indeed strengthened the learning abilities of the animals, so that there was a bigger difference between the percentage of freezing at 2.5 kHz (27.21 ± 7.08 %) and at 10 kHz (58.55 ± 4.5 %, Tukey's multiple comparisons test: $p < 0.0001$ Fig. 16C).

Treatment with retigabine for a period of 25 days after cuprizone withdrawal from the diet strengthened the ability of the mice to discriminate between the two frequencies, resulting in a significantly higher percentage of freezing for the 10 kHz sound compared to the 2.5 kHz sound (remy 25 days + Ret, blue bars, n = 10, 2.5 kHz = 17.18 ± 3.12 %, 10 kHz = 59.1 ± 2.52 %, Tukey's multiple comparisons test: $p < 0.0001$, Fig 16D). A treatment with the corresponding vehicle DMSO over the same period of time did not change the outcome of the test (remy 25 days + veh, orange bars, n = 10, 2.5 kHz = 49.03 ± 3.8 %, 10 kHz = 57.76 ± 3.66 %, Tukey's multiple comparisons test: $p = 0.99$, Fig. 16D). The ameliorative effect of a treatment with XE991 observed after 7 days remyelination did not persist when animals were treated for 25 days (remy 25 days + XE, red bars, n = 10, 2.5 kHz = 42.11 ± 5 %, 10 kHz = 45.34 ± 4.58 %, Tukey's multiple comparisons test: $p > 0.99$, Fig. 16D).

Taken together, these results demonstrate that the learning abilities of cuprizone mice are impaired during both de- and remyelination phases. An additional treatment with retigabine ameliorated the cognition impairment in both phases of the remyelination, while XE991 ameliorated only the cognition impairment during the early remyelination phase and not during the full remyelination phase.

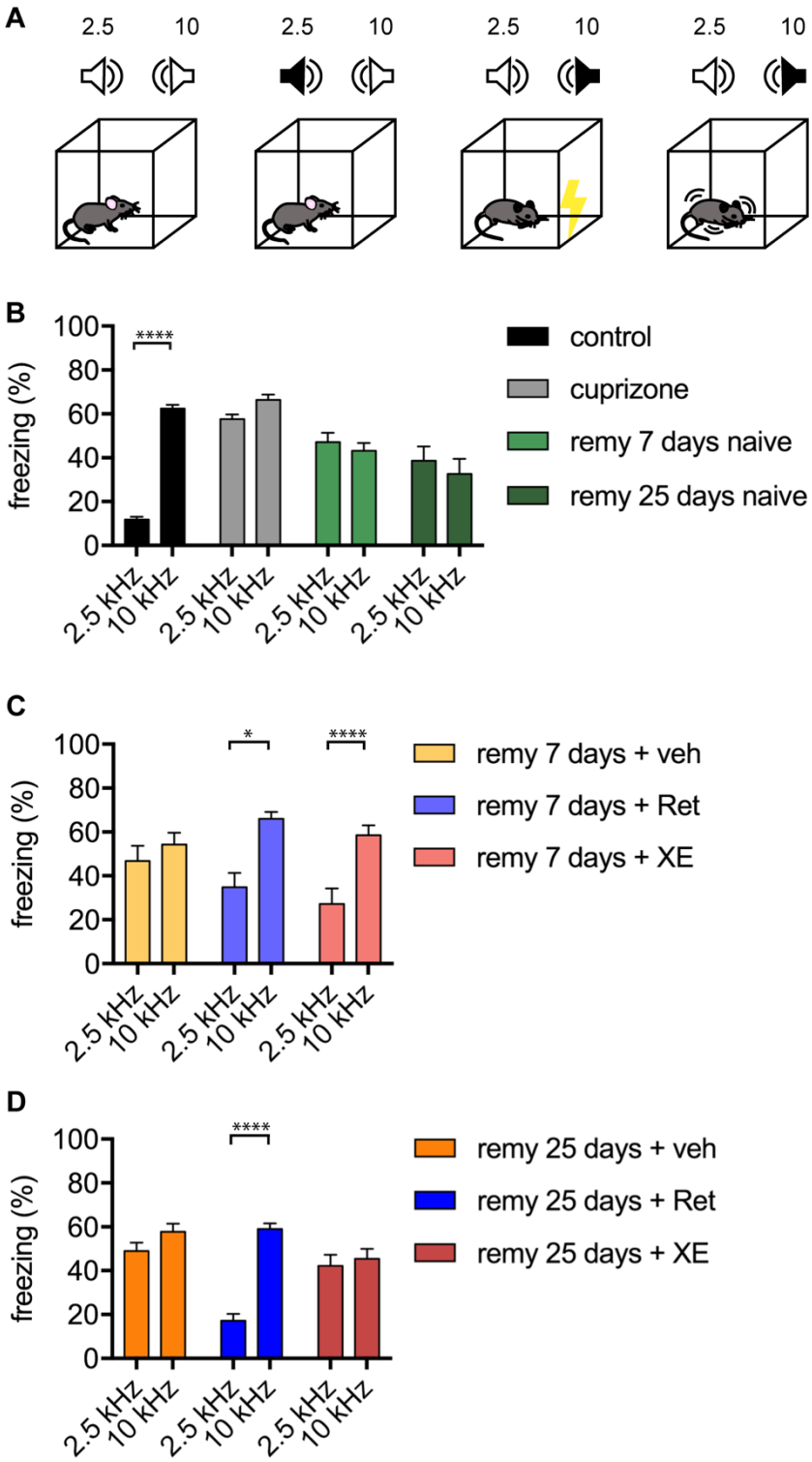

Figure 16: Effect of a pharmacological modulation of the KCNQ-channels on a Pavlovian conditioning paradigm of cuprizone mice. **A** Schematic representation of the experimental outline. **B** Bar graph showing the percentage of freezing of control mice (black graph), cuprizone mice at full demyelination (grey graph) and mice of the different remyelination phases without an additional treatment (green bars). **C** Bar graph showing the percentage of freezing of mice from the early remyelination phase with different additional treatments. **D** Bar graph showing the percentage of freezing of mice from the full remyelination phase with different additional treatments.

5. Discussion

5.1 Summary of the results

Our experiments indicate an involvement of KCNQ-channels in the pathophysiology of neurodegenerative diseases like MS. We could show that a prophylactic treatment with the KCNQ-channel opener retigabine ameliorated the outcome of EAE experiments. In more detail, EAE mice treated with retigabine showed the same onset of clinical symptoms as controls (untreated mice), but the progression of symptoms was less severe, and the mice showed improved learning abilities. Thus, retigabine might influence the clinical course and the cognitive impairment characterizing EAE mice. Moreover, in vitro immune assays showed no changes in the proliferation and cytokine production of stimulated splenocytes upon retigabine treatment. Hence, we concluded that the drug does not significantly influence the immune component and that an effect on neurodegeneration in EAE is a more likely one. To evaluate this neurodegenerative process, we took advantage of the cuprizone mouse model of de- and remyelination which is characterized by the absence of adaptive immunity. The ameliorative effect of retigabine was confirmed, as retigabine treatment improved the cognitive impairment which characterizes cuprizone-treated mice. Taken together with findings from the literature showing an altered expression pattern of KCNQ-channels and an increased neuronal excitability upon cuprizone diet (54,84,93), we concluded that KCNQ-channels might play a role in the pathophysiology of MS and that a treatment with retigabine might have neuroprotective effects.

5.2 Interpretation of the Main Findings

5.2.1 Retigabine Treatment Ameliorates the Course of EAE

We could demonstrate that a prophylactic treatment with retigabine improved the outcome of an EAE experiment. The drug ameliorated the progression of symptoms and decreased the cumulative score of EAE mice (compare chapter 4. Results, abstract 4.1 the Effect of KCNQ-channels on Experimental Autoimmune Encephalitis, Figure 1). In addition, retigabine treatment improved the cognitive abilities of EAE mice, which are known to suffer from memory impairment (73,147). The mechanisms underlying such amelioration can only be hypothesized by involving KCNQ-channels,

which are directly regulated by retigabine and that were previously indicated as players in the onset of hyperexcitability in other models of MS (93). This hyperexcitability was accompanied by altered ion-channel expression and it is known, that demyelination leads to modified KCNQ3 expression as this subtype redistributes into the demyelinated internodes in acute and chronically demyelinated neurons (93). Disruption of physiologic excitability levels is associated with impairment of proper neuronal and network functioning both *in vitro* and *in vivo* (40,54,56,80,81). Since retigabine exerts an hyperpolarizing effect on neurons controlling neuronal excitability (111,127,134), a prophylactic treatment with this drug might have neuroprotective effects. In EAE hyperexcitability is observed in neurons of the remission phase which is known to be characterized by neurodegeneration (40). After all, others K^+-channels physiologically involved in maintaining the RMP, like TASK and TREK were already shown to play major roles in the disease onset and course (148,149). Therefore, animal experiments and human studies indicate an involvement of ion channels, respectively K^+-channels, in MS, marking them possible targets for therapeutic strategies (88).

5.2.2 KCNQ-channels are not Involved in Inflammation

MS pathophysiology consists of neurodegeneration and inflammation like the respective animal model EAE (1,2). To investigate the underlying mechanisms of the ameliorative effect of retigabine in our EAE experiment, we performed different immune assays using stimulated splenocytes to represent the role of T lymphocytes. We did find KCNQ3 expression in the spleen (compare chapter 4. Results, abstract 4.3 Expression Pattern of KCNQ-channels in different organs) but retigabine administration showed no significant effect in immune cell experiments (proliferation and cytokine production), and, therefore, the function of this subtype remains unclear. The observed decrease in proliferation of retigabine treated splenocytes (compare chapter 4. Results, abstract 4.5 The Effect of Retigabine Administration on Splenocyte Proliferation), could be induced by a decline in splenocyte viability (compare chapter 4. Results, abstract 4.4 Retigabine Titration), and therefore, no clear antiproliferative effect of retigabine could be established. Furthermore, retigabine did not influence cytokine production of stimulated splenocytes (compare chapter 4. Results, abstract, Figure 6). Therefore, it is unlikely that the effect of retigabine observed in our EAE is

based on an involvement of KCNQ-channels in inflammation. For further confirmation of this thesis, *ex vivo* experiments comparing immune related tissue of EAE mice receiving a retigabine treatment are needed, as at this time point, we can only consider no effect of retigabine on isolated splenocytes. The overall immune reaction in MS/EAE involves reaction pathways that are not represented in our experiments and since there is little known in the literature, no clear statement about the role of KCNQ-channels in the immune system can be done.

5.2.3 Retigabine Treatment Influences Neurodegenerative Processes in Cuprizone Animal Experiments

Based on our findings from the immune assays and the literature, we concluded that KCNQ-channels play a more prominent role in neurodegeneration than neuroinflammation. Cuprizone mice treated with retigabine showed reduced learning impairment and better memory function than the corresponding vehicle control and therefore, we hypothesize a neuroprotective potential of retigabine. It was demonstrated, that changes in memory function are accompanied by altered neurotransmission and excitability of hippocampal neurons (150,151). Several studies using invertebrates could demonstrate an involvement of voltage gated K^+-channels in learning and memory consolidation (150). As XE991 enhanced learning and memory mechanisms in healthy mice (152), an influencing role of KCNQ-channels on memory function in mammalians was reported. Demyelination as consequence of neurodegeneration leads to a reduced neuronal excitability while the early phase of remyelination induces hyperexcitability in neurons. This results in a generally reduced excitability at full remyelination with impaired signal transduction and therefore the remyelinating process does not recover normal neuronal function (54). Retigabine shifts the activation potential of KCNQ2/3 to a hyperpolarized membrane potential and therefore, more channels stay open at the RMP preventing hyperexcitability (106,127). We hypothesize a neuroprotective effect on retigabine based on regulating neuronal excitability with consequently less learning and memory impairment. This thesis is supported by reports of neuroprotective effects of retigabine in animal models of other neurodegenerative disease. Amyotrophic lateral sclerosis and ischemic stroke mechanisms working against excitotoxic effects and hyperexcitability could be shown (153,154). Based on these findings, retigabine might moderate the hyperexcitability

during the early remyelination which might improve the remyelination process in general. Another mode of action could also relate to evidence showing that retigabine administration reduces the cell loss by preventing the production of reactive oxygen species (ROS) (153). The generally reduced neuronal network activity caused by demyelination results in reduced excitotoxity (153), indicating an indirect effect of retigabine administration on ROS production. As astrocytes play an important role in ROS production (4,155) and KCNQ3 and 5 are expressed in astrocytes, a direct effect of retigabine on ROS production cannot be excluded and should be subject to further investigations.

Taken together, KCNQ-channels and a pharmacological treatment with retigabine showed neuroprotective features in neurodegenerative disease highlighting the importance of K^+ balance for physiological neuronal function.

5.3 Limitations and Critique of Methodology

All animal experiments where performed with female C57BL/6J mice and all experimental groups were matched for sex and age. Hereby, the number of confounding factors was minimized, but animal experiments remain dependent from a number of other heterogeneous factors as individuality between the mice. In addition, not all influencing factors were established and could therefore be counteracted. To overcome these limitations and strengthen the significance, we increased the number of animals undergoing the immunization and behavior experiments.

To reduce the failure rate of our *in vitro* experiments, we increased the number of the repetitions of experiments always according to power calculation. Moreover, each experiment *in vitro* was performed with technical duplicates or triplicates. Nevertheless, mistakes in stimulation, culturing and handling of *in vitro* experiments can occur. To minimize stimulation differences, the cultured splenocytes were checked under the microscope (Inverted Zeiss Axioexaminer, Germany) prior to use.

Moreover, we detected irregularities in the expression of different KCNQ-channel subtypes in different tissue. Therefore, we changed the manufacturer company of our primers and adapted the sequence. This thesis only presents the data obtained with

our latest primers (see table 3). Nevertheless, splice variants of different KCNQ-channels (especially KCNQ2 and 3) were detected. Only little is known about the function of those splice variants and this limits the significance of the importance of the different subtypes for cell function.

6. Conclusions and Perspectives:

The work presented in this thesis suggests an involvement of KCNQ-channels in the pathophysiology of neurodegenerative diseases like MS. However, our results do not allow to understand if these channels play a role in the onset or in the maintenance of the disease. Given the findings indicating increased neuronal excitability and the effects of the EAE disease score, we would be oriented towards suggesting a role played by these channels in the neurodegenerative phase of the disease. Moreover, relating our findings with the literature, we hypothesize a neuroprotective role played by retigabine. In order to corroborate this conclusion EAE experiments should be repeated and animals should be observed for a longer period of time (in this study it was 25 days). In this way, the disease score course could be followed up long after d_{max}.

Moreover, in order to make the study more translational and to better mimic the clinical condition of a MS patient, an EAE with a therapeutic retigabine treatment should be planned. In this way, treatment would start at the onset of symptoms. Furthermore, histological staining of brain and spinal cord from EAE mice treated either with vehicle or retigabine are needed to assess differences in number and location of lesions of the different treatment groups. As we hypothesize a neuroprotective effect of retigabine by counteracting hyperexcitability, electrophysiological measures using brain slices from the EAE and cuprizone mice treated with retigabine/XE991 are required.

The role of KCNQ-channels in the immune component of MS remains unclear. First of all, our analysis of the KCNQ expression pattern could neither confirm nor exclude an KCNQ expression in splenocytes. To elucidate this, further PCR experiments on the different cell populations of splenocytes (e.g. B-cells, T-cells) are needed. If an expression can be confirmed, additional immune assays focusing on the role of KCNQ-channels in these cell populations are required. The same applies to investigating the

role of KCNQ-channels in the innate immune system of the brain, as our PCR could demonstrate an expression of KCNQ3 in astrocytes.

For further insights into the role of KCNQ-channels it is necessary to explore the different subtypes separately. Unfortunately, KCNQ2 knock out (KO) strains suffer from lethal seizures in the perinatal period, and therefore, it is not possible to use them in further experiments as full KOs (156,157). Alternatively, a KCNQ3 KO strain based on C57BL/6J mice is available and EAE experiments with these KO mice are in progress.

Taken together, the work provided in this thesis demonstrates an involvement of KCNQ-channels in neurodegenerative disease like MS, but further investigations clarifying the role in the pathophysiology are needed.

7. Bibliography

1. Trapp BD, Peterson J, Ransohoff RM, Rudick R, Mörk S, Bö L. Axonal transection in the lesions of multiple sclerosis. N Engl J Med. 1998;338(5):278–285. doi: 10.1056/NEJM199801293380502
2. Vogt J, Paul F, Aktas O, Müller-Wielsch K, Dörr J, Dörr S, Bharathi BS, Glumm R, Schmitz C, Steinbusch H, Raine CS, Tsokos M, Nitsch R, Zipp F. Lower motor neuron loss in multiple sclerosis and experimental autoimmune encephalomyelitis. Ann Neurol. 2009;66(3):310–322. doi: 10.1002/ana.21719
3. Herz J, Zipp F, Siffrin V. Neurodegeneration in autoimmune CNS inflammation. Exp Neurol. 2010;225(1):9–17. doi: 10.1016/j.expneurol.2009.11.019
4. Miljković D, Spasojević I. Multiple sclerosis: molecular mechanisms and therapeutic opportunities. Antioxid Redox Signal. 2013 Dec 20;19(18):2286–2334. doi: 10.1089/ars.2012.5068
5. Confavreux C, Vukusic S. Age at disability milestones in multiple sclerosis. Brain. 2006 Mar 1;129(3):595–605. doi: 10.1093/brain/awh714
6. Compston A, Coles A. Multiple sclerosis. Lancet. 2008;372(9648):1502–1517. doi: 10.1016/S0140-6736(08)61620-7
7. Friese MA, Schattling B, Fugger L. Mechanisms of neurodegeneration and axonal dysfunction in multiple sclerosis. Nat Rev Neurol. 2014;10:225–238. doi: 10.1038/nrneurol.2014.37
8. Brownlee WJ, Swanton JK, Altmann DR, Ciccarelli O, Miller DH. Earlier and more frequent diagnosis of multiple sclerosis using the McDonald criteria. J Neurol Neurosurg Psychiatry. 2015 May;86(5):584–585. doi: 10.1136/jnnp-2014-308675
9. Polman CH, Reingold SC, Banwell B, Clanet M, Cohen JA, Filippi M, Fujihara K, Havrdova E, Hutchinson M, Kappos L, Lublin FD, Montalban X, O'Connor P, Sandberg-Wollheim M, Thompson AJ, Waubant E, Weinshenker B, Wolinsky JS. Diagnostic criteria for multiple sclerosis: 2010 revisions to the McDonald criteria. Ann Neurol. 2011 Feb;69(2):292–302. doi: 10.1002/ana.22366
10. Hart FM, Bainbridge J. Current and emerging treatment of multiple sclerosis. Am J Manag Care. 2016;22(6 Suppl):159–170.
11. Frohman EM, Racke MK, Raine CS. Multiple sclerosis-the plaque and its pathogenesis. N Engl J Med. 2006;354:942–955. doi: 10.1056/NEJMra052130
12. La Mantia L, Di Pietrantonj C, Rovaris M, Rigon G, Frau S, Berardo F, Gandini A, Longobardi A, Weinstock-Guttman B, Vaona A. Interferons-beta versus glatiramer acetate for relapsing-remitting multiple sclerosis. Cochrane Database Syst Rev. 2016;24(11):1–67. doi: 10.1002/14651858.cd009333.pub3
13. Barnett MH, Henderson AP, Prineas JW. The macrophage in MS: just a scavenger after all? Pathology and pathogenesis of the acute MS lesion. Mult Scler J. 2006 Apr 2;12(2):121–132. doi: 10.1191/135248506ms1304rr
14. Barnett MH, Prineas JW. Relapsing and remitting multiple sclerosis: Pathology of the newly forming lesion. Ann Neurol. 2004 Apr 1;55(4):458–468. doi: 10.1002/ana.20016
15. Steinman L, Martin R, Bernard C, Conlon P, Oksenberg JR. Multiple sclerosis: deeper understanding of its pathogenesis reveals new targets for therapy. Annu Rev Neurosci. 2002 Mar 28;25(1):491–505. doi: 10.1146/annurev.neuro.25.112701.142913
16. Henderson APD, Barnett MH, Parratt JDE, Prineas JW. Multiple sclerosis: Distribution of inflammatory cells in newly forming lesions. Ann Neurol. 2009 Dec 1;66(6):739–753.

doi: 10.1002/ana.21800

17. McFarland HF, Martin R. Multiple sclerosis: a complicated picture of autoimmunity. Nat Immunol. 2007 Sep 1;8(9):913–919. doi: 10.1038/ni1507

18. Gay F, Drye T, Dick G, Esiri M. The application of multifactorial cluster analysis in the staging of plaques in early multiple sclerosis. Identification and characterization of the primary demyelinating lesion. Brain. 1997 Aug 1;120(8):1461–1483. doi: 10.1093/brain/120.8.1461

19. Hauser SL, Oksenberg JR. The neurobiology of multiple sclerosis: Genes, inflammation, and neurodegeneration. Neuron. 2006 Oct 5;52(1):61–76. doi: 10.1016/J.NEURON.2006.09.011

20. Podbielska M, Banik N, Kurowska E, Hogan E. Myelin recovery in multiple sclerosis: The challenge of remyelination. Brain Sci. 2013;3(3):1282–1324. doi: 10.3390/brainsci3031282

21. Minagar A, Alexander JS. Blood-brain barrier disruption in multiple sclerosis. Mult Scler J. 2003;9:540–549. doi: 10.1191/1352458503ms965oa

22. Babbe H, Roers A, Waisman A, Lassmann H, Goebels N, Hohlfeld R, Friese M, Schröder R, Deckert M, Schmidt S, Ravid R, Rajewsky K. Clonal expansions of CD8(+) T cells dominate the T cell infiltrate in active multiple sclerosis lesions as shown by micromanipulation and single cell polymerase chain reaction. J Exp Med. 2000 Aug 7;192(3):393–404. doi: 10.1084/JEM.192.3.393

23. Sobottka B, Harrer MD, Ziegler U, Fischer K, Wiendl H, Hünig T, Becher B, Goebels N. Collateral bystander damage by myelin-directed CD8 T cells causes axonal loss. Am J Pathol. 2009;175(3):1160–1166. doi: 10.2353/ajpath.2009.090340

24. Lucchinetti C, Brück W, Parisi J, Scheithauer B, Rodriguez M, Lassmann H. Heterogeneity of multiple sclerosis lesions: implications for the pathogenesis of demyelination. Ann Neurol. 2000;47(6):707–717. doi: 10.1002/1531-8249(200006)47:6<707::aid-ana3>3.0.co;2-q

25. Lassmann H, Van Horssen J. The molecular basis of neurodegeneration in multiple sclerosis. FEBS Lett. 2011;585(23):3715–3723. doi: 10.1016/j.febslet.2011.08.004

26. Nikić I, Merkler D, Sorbara C, Brinkoetter M, Kreutzfeldt M, Bareyre FM, Brück W, Bishop D, Misgeld T, Kerschensteiner M. A reversible form of axon damage in experimental autoimmune encephalomyelitis and multiple sclerosis. Nat Med. 2011 Apr 27;17(4):495–499. doi: 10.1038/nm.2324

27. Craner MJ, Newcombe J, Black JA, Hartle C, Cuzner ML, Waxman SG. Molecular changes in neurons in multiple sclerosis: altered axonal expression of Nav1.2 and Nav1.6 sodium channels and Na+/Ca2+ exchanger. Proc Natl Acad Sci U S A. 2004 May 25;101(21):8168–8173. doi: 10.1073/pnas.0402765101

28. Paling D, Golay X, Wheeler-Kingshott C, Kapoor R, Miller D. Energy failure in multiple sclerosis and its investigation using MR techniques. J Neurol. 2011 Dec 10;258(12):2113–2127. doi: 10.1007/s00415-011-6117-7

29. Gonsette RE. Oxidative stress and excitotoxicity: a therapeutic issue in multiple sclerosis? Mult Scler J. 2008 Jan 1;14(1):22–34. doi: 10.1177/1352458507080111

30. Musella A, Mandolesi G, Mori F, Gentile A, Centonze D. Linking synaptopathy and gray matter damage in multiple sclerosis. Mult Scler J. 2016 Feb 28;22(2):146–149. doi: 10.1177/1352458515581875

31. Chang A, Staugaitis SM, Dutta R, Batt CE, Easley KE, Chomyk AM, Yong VW, Fox RJ, Kidd GJ, Trapp BD. Cortical remyelination: a new target for repair theraies in multiple sclerosis. Ann Neurol. 2012;72(6):918–926. doi: 10.1002/ana.23693.

32. Denic A, Johnson AJ, Bieber AJ, Warrington AE, Rodriguez M, Pirko I. The relevance of animal models in multiple sclerosis research. Pathophysiology. 2011;18(1):21–29. doi: 10.1016/j.pathophys.2010.04.004

33. Procaccini C, De Rosa V, Pucino V, Formisano L, Matarese G. Animal models of Multiple Sclerosis. Eur J Pharmacol. 2015;759:182–191. doi: 10.1016/j.ejphar.2015.03.042

34. Gudi V, Gingele S, Skripuletz T, Stangel M. Glial response during cuprizone-induced de- and remyelination in the CNS: lessons learned. Front Cell Neurosci. 2014 Mar 13;8:1–24. doi: 10.3389/fncel.2014.00073

35. Rivers TM, Sprunt DH, Berry GP. Observations on attempts to produce acute disseminated encephalomyelitis in monkeys. J Exp Med. 1933 Jun 30;58(1):39–53. doi: 10.1084/jem.58.1.39

36. Bittner S, Afzali AM, Wiendl H, Meuth SG. Myelin oligodendrocyte glycoprotein (MOG35-55) induced experimental autoimmune encephalomyelitis (EAE) in C57BL/6 mice. J Vis Exp. 2014 Apr 15;(86). doi: 10.3791/51275

37. Pollak Y, Ovadia H, Goshen I, Gurevich R, Monsa K, Avitsur R, et al. Behavioral aspects of experimental autoimmune encephalomyelitis. J Neuroimmunol. 2000;104(1):31–36. doi: 10.1016/s0165-5728(99)00257-x

38. Marques KB, Santos LMB, Oliveira ALR. Spinal motoneuron synaptic plasticity during the course of an animal model of multiple sclerosis. Eur J Neurosci. 2006;24(11):3053–3062. doi: 10.1111/j.1460-9568.2006.05184.x

39. Mandolesi G, Gentile A, Musella A, Fresegna D, De Vito F, Bullitta S, Sepman H, Marfia GA, Centonze D. Synaptopathy connects inflammation and neurodegeneration in multiple sclerosis. Nat Rev Neurol. 2015 Dec 20;11(12):711–724. doi: 10.1038/nrneurol.2015.222

40. Ellwardt E, Pramanik G, Luchtman D, Novkovic T, Jubal ER, Vogt J, Arnoux I, Vogelaar CF, Mandal S, Schmalz M, Barger Z, Ruiz de Azua I, Kuhlmann T, Lutz B, Mittmann T, Bittner S, Zipp F, Stroh A. Maladaptive cortical hyperactivity upon recovery from experimental autoimmune encephalomyelitis. Nat Neurosci. 2018 Oct 26;21(10):1392–1403. doi: 10.1038/s41593-018-0193-2

41. Mix E, Meyer-Rienecker H, Hartung H-P, Zettl UK. Animal models of multiple sclerosis - potentials and limitations. Prog Neurobiol. 2010;92:386–404. doi: 10.1016/j.pneurobio.2010.06.005

42. Gold R, Linington C, Lassmann H. Understanding pathogenesis and therapy of multiple sclerosis via animal models: 70 years of merits and culprits in experimental autoimmune encephalomyelitis research. Brain. 2006 Jul 1;129(8):1953–1971. doi: 10.1093/brain/awl075

43. ’t Hart BA, Gran B, Weissert R. EAE: imperfect but useful models of multiple sclerosis. Trends Mol Med. 2011;17(3):119–125. doi: 10.1016/j.molmed.2010.11.006

44. Sun D, Whitaker JN, Huang Z, Liu D, Coleclough C, Wekerle H, et al. Myelin antigen-specific CD8+ T Cells are encephalitogenic and produce severe disease in C57BL/6 mice. J Immunol. 2001 Aug 1;166(12):7579–7587. doi: 10.4049/jimmunol.166.12.7579

45. Huseby ES, Liggitt D, Brabb T, Schnabel B, Öhlén C, Goverman J. A pathogenic role for myelin-specific CD8(+) T cells in a model for multiple sclerosis. J Exp Med. 2001 Sep 3;194(5):669–676. doi: 10.1084/jem.194.5.669

46. Mix E, Meyer-Rienecker H, Zettl UK. Animal models of multiple sclerosis for the development and validation of novel therapies – potential and limitations. J Neurol. 2008 Dec;255(S6):7–14. doi: 10.1007/s00415-008-6003-0

47. Sriram S, Steiner I. Experimental allergic encephalomyelitis: A misleading model of multiple sclerosis. Ann Neurol. 2005 Dec 1;58(6):939–945. doi: 10.1002/ana.20743

48. Skripuletz T, Gudi V, Hackstette D, Stangel M. De- and remyelination in the CNS white and grey matter induced by cuprizone: the old, the new, and the unexpected. Histol Histopathol. 2011;26(12):1585–1597. doi: 10.14670/HH-26.1585

49. Cerina M, Narayanan V, Göbel K, Bittner S, Ruck T, Meuth P, Herrmann AM, Stangel M, Gudi V, Skripuletz T, Daldrup T, Wiendl H, Seidenbecher T, Ehling P, Kleinschnitz C, Pape H-C, Budde T, Meuth SG. The quality of cortical network function recovery depends on localization and degree of axonal demyelination. Brain Behav Immun. 2016 Jan;59:103–117. doi: 10.1016/j.bbi.2016.08.014

50. Gudi V, Moharregh-Khiabani D, Skripuletz T, Koutsoudaki PN, Kotsiari A, Skuljec J, Trebst C, Stangel M. Regional differences between grey and white matter in cuprizone induced demyelination. Brain Res. 2009 Aug 4;1283:127–138. doi: 10.1016/j.brainres.2009.06.005

51. Tagge I, O'Connor A, Chaudhary P, Pollaro J, Berlow Y, Chalupsky M, Bourdette D, Woltjer R, Johnson M, Rooney W. Spatio-temporal patterns of demyelination and remyelination in the cuprizone mouse model. Stangel M, editor. PLoS One. 2016 Apr 7;11(4):e0152480. doi: 10.1371/journal.pone.0152480

52. Crawford DK, Mangiardi M, Tiwari-Woodruff SK. Assaying the functional effects of demyelination and remyelination: Revisiting field potential recordings. J Neurosci Methods. 2009 Aug;182(1):25–33. doi: 10.1016/j.jneumeth.2009.05.013

53. Kipp M, Clarner T, Dang J, Copray S, Beyer C. The cuprizone animal model: new insights into an old story. Acta Neuropathol. 2009 Dec 18;118(6):723–736. doi: 10.1007/s00401-009-0591-3

54. Cerina M, Narayanan V, Delank A, Meuth P, Graebenitz S, Göbel K, Herrmann AM, Albrecht S, Daldrup T, Seidenbecher T, Gorji A, Kuhlmann T, Wiendl H, Kleinschnitz C, Speckmann EJ, Pape H-C, Meuth SG, Budde T. Protective potential of dimethyl fumarate in a mouse model of thalamocortical demyelination. Brain Struct Funct. 2018 Sep 9;223(7):3091–3106. doi: 10.1007/s00429-018-1680-7

55. Vega-Riquer JM, Mendez-Victoriano G, Morales-Luckie RA, Gonzalez-Perez O. Five decades of cuprizone, an updated model to replicate demyelinating diseases. Curr Neuropharmacol. 2019 Jan 7;17(2):129–141. doi: 10.2174/1570159x15666170717120343

56. Narayanan V, Cerina M, Göbel K, Meuth P, Herrmann AM, Fernandez-Orth J, Stangel M, Gudi V, Skripuletz T, Daldrup T, Lesting J, Schiffler P, Wiendl H, Seidenbecher T, Meuth SG, Budde T, Pape H-C. Impairment of frequency-specific responses associated with altered electrical activity patterns in auditory thalamus following focal and general demyelination. Exp Neurol. 2018 Nov;309(February):54–66. doi: 10.1016/j.expneurol.2018.07.010

57. Benedict RHB, Cookfair D, Gavett R, Gunther M, Munschauer F, Garg N, Weinstock-Gutman B. Validity of the minimal assessment of cognitive function in multiple sclerosis (MACFIMS). J Int Neuropsychol Soc. 2006 Jul 27;12(04):549–558. doi: 10.1017/S1355617706060723

58. Chiaravalloti ND, DeLuca J. Cognitive impairment in multiple sclerosis. Lancet Neurol. 2008 Dec;7(12):1139–1151. doi: 10.1016/S1474-4422(08)70259-X

59. Sumowski JF, Benedict R, Enzinger C, Filippi M, Geurts JJ, Hamalainen P, Hulst H, Inglese M, Leavitt VM, Rocca MA, Rosti-Otajarvi EM, Rao S. Cognition in multiple sclerosis: State of the field and priorities for the future. Neurology. 2018 Feb;90(6):278–288. doi: 10.1212/WNL.0000000000004977

60. van Munster CEP, Jonkman LE, Weinstein HC, Uitdehaag BMJ, Geurts JJG. Gray matter damage in multiple sclerosis: Impact on clinical symptoms. Neuroscience. 2015 Sep 10;303:446–461. doi: 10.1016/j.neuroscience.2015.07.006

61. Sen MK, Mahns DA, Coorssen JR, Shortland PJ. Behavioural phenotypes in the cuprizone model of central nervous system demyelination. Neurosci Biobehav Rev. 2019 Dec;107(May):23–46. doi: 10.1016/j.neubiorev.2019.08.008

62. Karl T, Pabst R, von Hörsten S. Behavioral phenotyping of mice in pharmacological and toxicological research. Exp Toxicol Pathol. 2003 Jan;55(1):69–83. doi: 10.1078/0940-2993-00301

63. Hånell A, Marklund N. Structured evaluation of rodent behavioral tests used in drug discovery research. Front Behav Neurosci. 2014 Jul;8(252). doi: 10.3389/fnbeh.2014.00252

64. Deacon RMJ. Measuring motor coordination in mice. J Vis Exp. 2013;(75). doi: 10.3791/2609

65. Carter RJ, Morton J, Dunnett SB. Motor coordination and balance in rodents. Curr Protoc Neurosci. 2001;15(1):8.12.1-8.12.14. doi: 10.1002/0471142301.ns0812s15

66. Lezak KR, Missig G, Carlezon WA. Behavioral methods to study anxiety in rodents. Dialogues Clin Neurosci. 2017;19(2):181–191.

67. Ennaceur A. One-trial object recognition in rats and mice: Methodological and theoretical issues. Behav Brain Res. 2010 Dec 31;215(2):244–254. doi: 10.1016/j.bbr.2009.12.036

68. Antunes M, Biala G. The novel object recognition memory: neurobiology, test procedure, and its modifications. Cogn Process. 2012 May 9;13(2):93–110. doi: 10.1007/s10339-011-0430-z

69. Falls WA. Fear-potentiated startle in mice. Curr Protoc Neurosci. 2002;Chapter 8:1–16. doi: 10.1002/0471142301.ns0811bs19

70. LeDoux J. The emotional brain, fear, and the amygdala. Cell Mol Neurobiol. 2003;23(4–5):727–738. doi: 10.1023/A:1025048802629

71. Izquierdo I, Furini CRG, Myskiw JC. Fear memory. Physiol Rev. 2016 Apr 1;96(2):695–750. doi: 10.1152/physrev.00018.2015

72. Acharjee S, Nayani N, Tsutsui M, Hill MN, Ousman SS, Pittman QJ. Altered cognitive-emotional behavior in early experimental autoimmune encephalitis – Cytokine and hormonal correlates. Brain Behav Immun. 2013 Oct 1;33:164–172. doi: 10.1016/J.BBI.2013.07.003

73. Olechowski CJ, Tenorio G, Sauve Y, Kerr BJ. Changes in nociceptive sensitivity and object recognition in experimental autoimmune encephalomyelitis (EAE). Exp Neurol. 2013;241:113–121. doi: 10.1016/j.expneurol.2012.12.012

74. Ziehn MO, Avedisian AA, Tiwari-Woodruff S, Voskuhl RR. Hippocampal CA1 atrophy and synaptic loss during experimental autoimmune encephalomyelitis, EAE. Lab Invest. 2010 May;90(5):774–786. doi: 10.1038/labinvest.2010.6

75. Liebetanz D, Merkler D. Effects of commissural de- and remyelination on motor skill behaviour in the cuprizone mouse model of multiple sclerosis. Exp Neurol. 2006;202(1):217–224. doi: 10.1016/j.expneurol.2006.05.032

76. Franco-Pons N, Torrente M, Colomina MT, Vilella E. Behavioral deficits in the cuprizone-induced murine model of demyelination/remyelination. Toxicol Lett. 2007 Mar 30;169(3):205–213. doi: 10.1016/j.toxlet.2007.01.010

77. Han SR, Kang YH, Jeon H, Lee S, Park S-J, Song D-Y, Min SS, Yoo S-M, Lee M-S,

Lee S-H. Differential expression of miRNAs and behavioral change in the cuprizone-induced demyelination mouse model. Int J Mol Sci. 2020 Jan 18;21(2):646. doi: 10.3390/ijms21020646

78. Tomas-Roig J, Torrente M, Cabré M, Vilella E, Colomina MT. Long lasting behavioural effects on cuprizone fed mice after neurotoxicant withdrawal. Behav Brain Res. 2019 May;363:38–44. doi: 10.1016/j.bbr.2019.01.036

79. Hibbits N, Pannu R, Wu TJ, Armstrong RC. Cuprizone demyelination of the corpus callosum in mice correlates with altered social interaction and impaired bilateral sensorimotor coordination. ASN Neuro. 2009 May 6;1(3):153–164. doi: 10.1042/AN20090032

80. Caramia MD, Palmieri MG, Desiato MT, Boffa L, Galizia P, Rossini PM, Centonze D, Bernardi G. Brain excitability changes in the relapsing and remitting phases of multiple sclerosis: a study with transcranial magnetic stimulation. Clin Neurophysiol. 2004 Apr 1;115(4):956–965. doi: 10.1016/j.clinph.2003.11.024

81. Conte A, Lenzi D, Frasca V, Gilio F, Giacomelli E, Gabriele M, Marini Bettolo C, Iacovelli E, Pantano P, Pozzilli C, Inghilleri M. Intracortical excitability in patients with relapsing-remitting and secondary progressive multiple sclerosis. J Neurol. 2009 Jun;256(6):933–938. doi: 10.1007/s00415-009-5047-0

82. Stampanoni Bassi M, Mori F, Buttari F, Marfia GA, Sancesario A, Centonze D, Lezzi E. Neurophysiology of synaptic functioning in multiple sclerosis. Clin Neurophysiol. 2017 Jul;128(7):1148–1157. doi: 10.1016/j.clinph.2017.04.006

83. Centonze D, Muzio L, Rossi S, Cavasinni F, De Chiara V, Bergami A, Musella A, D'Amelio M, Cavallucci V, Martorana A, Bergamaschi A, Cencioni MT, Diamantini A, Butti E, Comi G, Bernardi G, Cecconi F, Battistini L, Furlan R, Martino G. Inflammation triggers synaptic alteration and degeneration in experimental autoimmune encephalomyelitis. J Neurosci. 2009 Mar 18;29(11):3442–3452. doi: 10.1523/JNEUROSCI.5804-08.2009

84. Ghaffarian N, Mesgari M, Cerina M, Göbel K, Budde T, Speckmann E-J, Meuth SG, Gorji A. Thalamocortical-auditory network alterations following cuprizone-induced demyelination. J Neuroinflammation. 2016 Jun 22;13(1):160. doi: 10.1186/s12974-016-0629-0

85. Bista P, Pawlowski M, Cerina M, Ehling P, Leist M, Meuth P, Aissaoui A, Borsotto M, Heurteaux C, Decher N, Pape H-C, Oliver D, Meuth SG, Budde T. Differential phospholipase C-dependent modulation of TASK and TREK two-pore domain K + channels in rat thalamocortical relay neurons. J Physiol. 2015 Jan 1;593(1):127–144. doi: 10.1113/jphysiol.2014.276527

86. Busche MA, Konnerth A. Neuronal hyperactivity - A key defect in Alzheimer's disease? BioEssays. 2015 Jun;37(6):624–632. doi: 10.1002/bies.201500004

87. Bean BP. The action potential in mammalian central neurons. Nat Rev Neurosci. 2007 Jun;8(6):451–465. doi: 10.1038/nrn2148

88. Ehling P, Bittner S, Budde T, Wiendl H, Meuth SG. Ion channels in autoimmune neurodegeneration. FEBS Lett. 2011 Dec 1;585(23):3836–3842. doi: 10.1016/j.febslet.2011.03.065

89. Bittner S, Meuth SG. Targeting ion channels for the treatment of autoimmune neuroinflammation. Ther Adv Neurol Disord. 2013 Sep 28;6(5):322–336. doi: 10.1177/1756285613487782

90. Moll C, Mourre C, Lazdunski M, Ulrich J. Increase of sodium channels in demyelinated lesions of multiple sclerosis. Brain Res. 1991 Aug;556(2):311–316. doi: 10.1016/0006-8993(91)90321-L

91. Waxman SG. Axonal conduction and injury in multiple sclerosis: the role of sodium channels. Nat Rev Neurosci. 2006 Dec 1;7(12):932–941. doi: 10.1038/nrn2023

92. Bostock H, Sears TA. The internodal axon membrane: electrical excitability and continuous conduction in segmental demyelination. J Physiol. 1978 Jul 1;280(1):273–301. doi: 10.1113/jphysiol.1978.sp012384

93. Hamada MS, Kole MHP. Myelin loss and axonal ion channel adaptations associated with gray matter neuronal hyperexcitability. J Neurosci. 2015 May 6;35(18):7272–7286. doi: 10.1523/JNEUROSCI.4747-14.2015

94. Dutta R, McDonough J, Yin X, Peterson J, Chang A, Torres T, Gudz T, Macklin WB, Lewis DA, Fox RJ, Rudick R, Mirnics K, Trapp BD. Mitochondrial dysfunction as a cause of axonal degeneration in multiple sclerosis patients. Ann Neurol. 2006 Mar 1;59(3):478–489. doi: 10.1002/ana.20736

95. Ellwardt E, Zipp F. Molecular mechanisms linking neuroinflammation and neurodegeneration in MS. Exp Neurol. 2014 Dec;262:8–17. doi: 10.1016/j.expneurol.2014.02.006

96. Stys P, Waxman S, Ransom B. Ionic mechanisms of anoxic injury in mammalian CNS white matter: role of Na+ channels and Na(+)-Ca2+ exchanger. J Neurosci. 1992 Feb 1;12(2):430–439. doi: 10.1523/JNEUROSCI.12-02-00430.1992

97. Kapoor R, Furby J, Hayton T, Smith KJ, Altmann DR, Brenner R, Chataway J, Hughes RA, Miller DH. Lamotrigine for neuroprotection in secondary progressive multiple sclerosis: a randomised, double-blind, placebo-controlled, parallel-group trial. Lancet Neurol. 2010 Jul 1;9(7):681–688. doi: 10.1016/S1474-4422(10)70131-9

98. Jukkola PI, Lovett-Racke AE, Zamvil SS, Gu C. K+ channel alterations in the progression of experimental autoimmune encephalomyelitis. Neurobiol Dis. 2012 Aug;47(2):280–293. doi: 10.1016/j.nbd.2012.04.012

99. Sedehizadeh S, Keogh M, Maddison P. The use of aminopyridines in neurological disorders. Clin Neuropharmacol. 2012 Jul 1;35(4):191–200. doi: 10.1097/WNF.0b013e31825a68c5

100. Battefeld A, Tran BT, Gavrilis J, Cooper EC, Kole MHP. Heteromeric Kv7.2/7.3 channels differentially regulate action potential initiation and conduction in neocortical myelinated axons. J Neurosci. 2014 Mar 5;34(10):3719–3732. doi: 10.1523/JNEUROSCI.4206-13.2014

101. Hill AS, Nishino A, Nakajo K, Zhang G, Fineman JR, Selzer ME, Okamura Y, Cooper EC. Ion channel clustering at the axon initial segment and node of Ranvier evolved sequentially in early chordates. Frankel WN, editor. PLoS Genet. 2008 Dec 26;4(12):e1000317. doi: 10.1371/journal.pgen.1000317

102. Pan Z, Kao T, Horvath Z, Lemos J, Sul J-Y, Cranstoun SD, Bennett V, Scherer SS, Cooper EC. A common ankyrin-G-based mechanism retains KCNQ and NaV channels at electrically active domains of the axon. J Neurosci. 2006 Mar 8;26(10):2599–2613. doi: 10.1523/JNEUROSCI.4314-05.2006

103. Greene DL, Hoshi N. Modulation of Kv7 channels and excitability in the brain. Cell Mol Life Sci. 2017 Feb 19;74(3):495–508. doi: 10.1007/s00018-016-2359-y

104. Robbins J. KCNQ potassium channels: physiology, pathophysiology, and pharmacology. Pharmacol Ther. 2001 Apr 1;90(1):1–19. doi: 10.1016/S0163-7258(01)00116-4

105. Jentsch TJ. Neuronal KCNQ potassium channels:physislogy and role in disease. Nat Rev Neurosci. 2000 Oct 1;1(1):21–30. doi: 10.1038/35036198

106. Brown DA, Passmore GM. Neural KCNQ (Kv7) channels. Br J Pharmacol. 2009 Apr

6;156(8):1185–1195. doi: 10.1111/j.1476-5381.2009.00111.x

107. Cooper EC, Harrington E, Jan YN, Jan LY. M channel KCNQ2 subunits are localized to key sites for control of neuronal network oscillations and synchronization in mouse brain. J Neurosci. 2001 Dec 15;21(24):9529–9540. doi: 10.1523/JNEUROSCI.21-24-09529.2001

108. Geiger J, Weber YG, Landwehrmeyer B, Sommer C, Lerche H. Immunohistochemical analysis of KCNQ3 potassium channels in mouse brain. Neurosci Lett. 2006 May 29;400(1–2):101–104. doi: 10.1016/j.neulet.2006.02.017

109. Zhou X, Wei J, Song M, Francis K, Yu SP. Novel role of KCNQ2/3 channels in regulating neuronal cell viability. Cell Death Differ. 2011 Mar 1;18(3):493–505. doi: 10.1038/cdd.2010.120

110. Grigorov A, Moskalyuk A, Kravchenko M, Veselovsky N, Verkhratsky A, Fedulova S. Kv7 potassium channel subunits and M currents in cultured hippocampal interneurons. Pflügers Arch - Eur J Physiol. 2014 Sep 11;466(9):1747–1758. doi: 10.1007/s00424-013-1406-x

111. Cerina M, Szkudlarek HJ, Coulon P, Meuth P, Kanyshkova T, Nguyen XV, Göbel K, Seidenbecher T, Meuth SG, Pape H-C, Budde T. Thalamic K v 7 channels: pharmacological properties and activity control during noxious signal processing. Br J Pharmacol. 2015 Jun;172(12):3126–3140. doi: 10.1111/bph.13113

112. Schroeder BC, Hechenberger M, Weinreich F, Kubisch C, Jentsch TJ. KCNQ5, a novel potassium channel broadly expressed in brain, mediates M-type currents. J Biol Chem. 2000 Aug 4;275(31):24089–24095. doi: 10.1074/jbc.M003245200

113. Allen NM, Mannion M, Conroy J, Lynch SA, Shahwan A, Lynch B, King MD. The variable phenotypes of KCNQ-related epilepsy. Epilepsia. 2014 Sep 1;55(9):e99–105. doi: 10.1111/epi.12715

114. Pascual FT, Wierenga KJ, Ng Y-T. Contiguous deletion of KCNQ2 and CHRNA4 may cause a different disorder from benign familial neonatal seizures. Epilepsy Behav Case Reports. 2013;1:35–38. doi: 10.1016/j.ebcr.2013.01.004

115. Fister P, Soltirovska-Salamon A, Debeljak M, Paro-Panjan D. Benign familial neonatal convulsions caused by mutation in KCNQ3, exon 6: A European case. Eur J Paediatr Neurol. 2013 May;17(3):308–310. doi: 10.1016/j.ejpn.2012.10.007

116. Dedek K, Fusco L, Teloy N, Steinlein OK. Neonatal convulsions and epileptic encephalopathy in an italian family with a missense mutation in the fifth transmembrane region of KCNQ2. Epilepsy Res. 2003 Apr 1;54(1):21–27. doi: 10.1016/S0920-1211(03)00037-8

117. Singh NA, Westenskow P, Charlier C, Pappas C, Leslie J, Dillon J, Anderson VE, Sanguinetti MC, Leppert MF. KCNQ2 and KCNQ3 potassium channel genes in benign familial neonatal convulsions: expansion of the functional and mutation spectrum. Brain. 2003 Sep 23;126(12):2726–2737. doi: 10.1093/brain/awg286

118. Saitsu H, Kato M, Koide A, Goto T, Fujita T, Nishiyama K, Tsurusaki Y, Doi H, Miyake N, Hayasaka K, Matsumoto N. Whole exome sequencing identifies KCNQ2 mutations in Ohtahara syndrome. Ann Neurol. 2012 Aug;72(2):298–300. doi: 10.1002/ana.23620

119. Weckhuysen S, Mandelstam S, Suls A, et al. KCNQ2 encephalopathy: Emerging phenotype of a neonatal epileptic encephalopathy. Ann Neurol. 2012 Jan 1;71(1):15–25. doi: 10.1002/ana.22644

120. Wang H-S, Pan Z, Shi W, Brown BS, Wymore RS, Cohen IS, Dixon JE, McKinnon D. KCNQ2 and KCNQ3 potassium channel subunits: molecular correlates of the M-channel. Science. 1998 Dec 4;282(5395):1890–1893. doi:

10.1126/science.282.5395.1890

121. Brown DA, Adams PR. Muscarinic suppression of a novel voltage-sensitive K+ current in a vertebrate neurone. Nature. 1980 Feb;283(5748):673–676. doi: 10.1038/283673a0

122. Miceli F, Soldovieri MV, Martire M, Taglialatela M. Molecular pharmacology and therapeutic potential of neuronal Kv7-modulating drugs. Curr Opin Pharmacol. 2008 Feb 1;8(1):65–74. doi: 10.1016/j.coph.2007.10.003

123. Zaczek R, Chorvat RJ, Saye JA, Pierdomenico ME, Maciag CM, Logue AR, Fisher BN, Rominger DH, Earl RA. Two new potent neurotransmitter release enhancers, 10,10-bis(4-pyridinylmethyl)-9(10H)-anthracenone and 10,10-bis(2- fluoro-4-pyridinylmethyl)-9(10H)-anthracenone: comparison to linopirdine. J Pharmacol Exp Ther. 1998;285:724–730.

124. Fontana DJ, Inouye GT, Johnson RM. Linopirdine (DuP 996) improves performance in several tests of learning and memory by modulation of cholinergic neurotransmission. Pharmacol Biochem Behav. 1994 Dec;49(4):1075–1082. doi: 10.1016/0091-3057(94)90267-4

125. Rockwood K, Beattie BL, Eastwood MR, Feldman H, Mohr E, Pryse-Phillips W, Gauthier S. A randomized, controlled trial of linopirdine in the treatment of Alzheimer's disease. Can J Neurol Sci. 1997 May 18;24(2):140–145. doi: 10.1017/S031716710002148X

126. Greene DL, Kang S, Hoshi N. XE991 and linopirdine are state-dependent inhibitors for Kv7/KCNQ channels that favor activated single subunits. J Pharmacol Exp Ther. 2017 Jul 1;362(1):177–185. doi: 10.1124/jpet.117.241679

127. Stafstrom CE, Grippon S, Kirkpatrick P. Ezogabine (retigabine). Nat Rev Drug Discov. 2011 Oct 30;10(10):729–730. doi: 10.1038/nrd3561

128. Porter RJ, Nohria V, Rundfeldt C. Retigabine. Neurotherapeutics. 2007 Jan;4(1):149–154. doi: 10.1016/j.nurt.2006.11.012

129. Main MJ, Cryan JE, Dupere JRB, Cox B, Clare JJ, Burbidge SA. Modulation of KCNQ2/3 potassium channels by the novel anticonvulsant retigabine. Mol Pharmacol. 2000 Aug 1;58(2):253–262. doi: 10.1124/mol.58.2.253

130. Rundfeldt C. The new anticonvulsant retigabine (D-23129) acts as an opener of K+ channels in neuronal cells. Eur J Pharmacol. 1997 Oct;336(2–3):243–249. doi: 10.1016/S0014-2999(97)01249-1

131. Wickenden AD, Yu W, Zou A, Jegla T, Wagoner PK. Retigabine, a novel anti-convulsant, enhances activation of KCNQ2/Q3 potassium channels. Mol Pharmacol. 2000 Sep 1;58(3):591–600. doi: 10.1124/mol.58.3.591

132. Straub H, Köhling R, Höhling J-M, Rundfeldt C, Tuxhorn I, Ebner A, Wolf P, Pannek H, Speckmann E-J. Effects of retigabine on rhythmic synchronous activity of human neocortical slices. Epilepsy Res. 2001 May;44(2–3):155–165. doi: 10.1016/S0920-1211(01)00193-0

133. Roza C, Lopez-Garcia JA. Retigabine, the specific KCNQ channel opener, blocks ectopic discharges in axotomized sensory fibres. Pain. 2008 Sep;138(3):537–345. doi: 10.1016/j.pain.2008.01.031

134. Passmore GM, Selyanko AA, Mistry M, Al-Qatari M, Marsh SJ, Matthews EA, Dickenson AH, Brown TA, Burbidge SA, Main M, Brown DA. KCNQ/M currents in sensory neurons: significance for pain therapy. J Neurosci. 2003 Aug 6;23(18):7227–7236. doi: 10.1523/JNEUROSCI.23-18-07227.2003

135. Brodie MJ, Lerche H, Gil-Nagel A, Elger C, Hall S, Shin P, Nohria V, Mansbach H. Efficacy and safety of adjunctive ezogabine (retigabine) in refractory partial epilepsy. Neurology. 2010 Nov 16;75(20):1817–1824. doi: 10.1212/WNL.0b013e3181fd6170

136. Surur AS, Bock C, Beirow K, Wurm K, Schulig L, Kindermann MK, Siegmund W, Bednarski PJ, Link A. Flupirtine and retigabine as templates for ligand-based drug design of K V 7.2/3 activators. Org Biomol Chem. 2019 May 8;17(18):4512–4522. doi: 10.1039/C9OB00511K

137. Clark S, Antell A, Kaufman K. New antiepileptic medication linked to blue discoloration of the skin and eyes. Ther Adv Drug Saf. 2015 Feb 20;6(1):15–19. doi: 10.1177/2042098614560736

138. European Medicines Agency. Withdrawal of pain medicine flupirtine endorsed. 2018. [accessed 5 Apr 2020] https://www.ema.europa.eu/en/news/withdrawal-pain-medicine-flupirtine-endorsed

139. Kilkenny C, Browne W, Cuthill IC, Emerson M, Altman DG. Animal research: reporting in vivo experiments: the ARRIVE guidelines. Br J Pharmacol. 2010 Aug;160(7):1577–1579. doi: 10.1111/j.1476-5381.2010.00872.x

140. Hofstetter HH, Shive CL, Forsthuber TG. Pertussis toxin modulates the immune response to neuroantigens injected in incomplete Freund's Adjuvant: Induction of Th1 cells and experimental autoimmune encephalomyelitis in the presence of high frequencies of Th2 cells. J Immunol. 2002 Jul 1;169(1):117–125. doi: 10.4049/jimmunol.169.1.117

141. Hammond RS, Tull LE, Stackman RW. On the delay-dependent involvement of the hippocampus in object recognition memory. Neurobiol Learn Mem. 2004 Jul 1;82(1):26–34. doi: 10.1016/j.nlm.2004.03.005

142. Narayanan V, Heiming RS, Jansen F, Lesting J, Sachser N, Pape H-C, Seidenbecher T. Social defeat: impact on fear extinction and amygdala-prefrontal cortical theta synchrony in 5-HTT deficient mice. Meuth SG, editor. PLoS One. 2011 Jul 27;6(7):e22600. doi: 10.1371/journal.pone.0022600

143. Daldrup T, Remmes J, Lesting J, Gaburro S, Fendt M, Meuth P, Kloke V, Pape H-C, Seidenbecher T. Expression of freezing and fear-potentiated startle during sustained fear in mice. Genes, Brain Behav. 2015 Mar;14(3):281–291. doi: 10.1111/gbb.12211

144. Thermo Fisher Scientific - DE. Annexin V Staining. 2015. [accessed 24 Feb 2020] https://www.thermofisher.com/de/de/home/life-science/cell-analysis/cell-viability-and-regulation/apoptosis/annexin-v-staining.html

145. Thermo Fisher Scientific - DE. eBioscience™ Cell Proliferation Dye eFluor™ 670. 2017. [accessed 28 Mar 2020] https://www.thermofisher.com/order/catalog/product/65-0840-90?ICID=search-product#/65-0840-90?ICID=search-product

146. Thermo Fisher Scientific - DE. So funktionieren TaqMan Assays. 2018.[accessed 25 Feb 2020] https://www.thermofisher.com/de/de/home/life-science/pcr/real-time-pcr/real-time-pcr-learning-center/real-time-pcr-basics/how-taqman-assays-work.html#expression

147. Aharoni R, Schottlender N, Bar-Lev DD, Eilam R, Sela M, Tsoory M, Arnon R. Cognitive impairment in an animal model of multiple sclerosis and its amelioration by glatiramer acetate. Sci Rep. 2019 Dec 11;9(1):4140. doi: 10.1038/s41598-019-40713-4

148. Bittner S, Meuth SG, Göbel K, Melzer N, Herrmann AM, Simon OJ, Weishaupt A, Budde T, Bayliss DA, Bendszus M, Wiendl H. TASK1 modulates inflammation and neurodegeneration in autoimmune inflammation of the central nervous system. Brain. 2009 Sep;132(9):2501–2516. doi: 10.1093/brain/awp163

149. Bittner S, Ruck T, Fernández-Orth J, Meuth SG. TREK-King the Blood-Brain-Barrier. J Neuroimmune Pharmacol. 2014 Jun;9(3):293–301. doi: 10.1007/s11481-014-9530-8

150. Giese KP, Peters M, Vernon J. Modulation of excitability as a learning and memory

mechanism: A molecular genetic perspective. Physiol Behav. 2001 Aug 1;73(5):803–810. doi: 10.1016/S0031-9384(01)00517-0

151. Grüter T, Wiescholleck V, Dubovyk V, Aliane V, Manahan-Vaughan D. Altered neuronal excitability underlies impaired hippocampal function in an animal model of psychosis. Front Behav Neurosci. 2015 May 20;9. doi: 10.3389/fnbeh.2015.00117

152. Fontán-Lozano Á, Suárez-Pereira I, Delgado-García JM, Carrión ÁM. The M-current inhibitor XE991 decreases the stimulation threshold for long-term synaptic plasticity in healthy mice and in models of cognitive disease. Hippocampus. 2011 Jan 1;21(1):22–32. doi: 10.1002/hipo.20717

153. Ghezzi F, Monni L, Nistri A. Functional up-regulation of the M-current by retigabine contrasts hyperexcitability and excitotoxicity on rat hypoglossal motoneurons. J Physiol. 2018 Jul 1;596(13):2611–2629. doi: 10.1113/JP275906

154. Barrese V, Taglialatela M, Greenwood IA, Davidson C. Protective role of Kv7 channels in oxygen and glucose deprivation-induced damage in rat caudate brain slices. J Cereb Blood Flow Metab. 2015 Oct 13;35(10):1593–1600. doi: 10.1038/jcbfm.2015.83

155. Smith KJ. Newly lesioned tissue in multiple sclerosis - a role for oxidative damage? Brain. 2011 Jul;134(7):1877–1881. doi: 10.1093/brain/awr144

156. Watanabe H, Nagata E, Kosakai A, Nakamura M, Yokoyama M, Tanaka K, Sasai H. Disruption of the epilepsy KCNQ2 gene results in neural hyperexcitability. J Neurochem. 2000 Dec 25;75(1):28–33. doi: 10.1046/j.1471-4159.2000.0750028.x

157. Soh H, Pant R, LoTurco JJ, Tzingounis A V. Conditional deletions of epilepsy-associated KCNQ2 and KCNQ3 channels from cerebral cortex cause differential effects on neuronal excitability. J Neurosci. 2014 Apr 9;34(15):5311–5321. doi: 10.1523/JNEUROSCI.3919-13.2014

8. List of Figures

9. List of Abbreviations

ACK	Ammonium-Chlorid-Potassium
AIS	Axon initial segment
AP	Action potential
ATP	Adenosintrisphosphate
AUT	Austria
BBB	Blood brain barrier
BSA	Bovine serum albumin
BW	Bodyweight
Ca^{2+}	Calcium
CC	Corpus callosum
cDNA	Complementary DNA
CHE	Switzerland
CIS	Clinical isolated syndrome
CNS	Central nervous system
ddH2O	Distillated Water
DMEM	Dulbeccos modified eagle serum
DMSO	Dimethyl sulfoxide
DMT	Disease modifying therapy
d_{max}	Day of maximum score
DNA	Deoxyribonucleic acid

dNTPs	Deoxyribonucleic acid trisphosphates
EAE	Experimental autoimmune encephalitis
EDTA	Ethylendiaminetetraacetic acid
EPM	Elevated plus maze
FACS	Fluresence activated cell sorting
FCS	Fetal calf serum
Fig.	Figure
FVD	Fixable viability dye
GABA	Gamma butyl acid
GER	Germany
h	Hour(s)
HEPES	(4-(2-hydroxyethyl)-1-piperazineethanesulfonic acid)
IL	Interleukin
K^+	Potassium
KO	Knock out
LN	Lymph node
LUX	Luxemburg
MACS	Magnetic activated cell sorting
MBP	Myelin basic protein
MHC	Major Histocompatibility complex

min	Minute(s)
MOG	Myelin oligodendrocyte glycoprotein
MRI	Magnet resonance imaging
mRNA	Messenger RNA
MS	Multiple Sclerosis
Na^+	Sodium
NLD	The Netherlands
NOR	Novel object recognition
ns	Not significant
OF	Open field
OPC	Oligodendrocyte progenitor cells
P/S	Penicillin/Streptomycin
PBS	Phosphate-buffered saline
PCR	Polymerase chain reaction
PLP	Phospholipid protein
PNS	Peripheral nervous system
Remy	Remyelinated
Ret	Retigabine
RNA	Ribonucleic acid
ROS	Reactive oxygen species
RRMS	Relapsing remitting MS

Rpm	Rounds per minute
RT-PCR	Real time polymerase chain reaction
s	Second(s)
SA-PE	Streptavidin-phycoerythrin
SEM	Standard error of the mean
stim	stimulated
TNFα	Tumor necrosis factor α
USA	United States of America
Veh	vehicle
Vs.	versus

10. Lebenslauf

11. Danksagung

Mein aufrichtigster Dank gilt Herrn Prof. Dr. Dr. Meuth für die Bereitstellung des Themas sowie die überaus freundliche Aufnahme in seine Arbeitsgruppe. Ich fand mich stets in einem produktiven und sehr freundlichen Umfeld wieder, welches mich allzeit unterstützt und gefördert hat. Mir hat die Zusammenarbeit wirklich Freude bereitet und ich bin froh, mir die Zeit für ein Forschungssemester genommen zu haben.

Ein besonderer Dank geht hierbei an Manuela Cerina, die mir mit ihrer kompetenten Unterstützung und Beratung jederzeit zur Seite stand. Sie hat mich maßgeblich bei der Umsetzung dieses Projektes sowie der Anfertigung meiner Dissertation unterstützt, hatte aber auch stets in privaten Angelegenheiten ein offenes Ohr für mich. Sie hat mich mit ihrer Begeisterung für die Wissenschaft und unser Projekt angesteckt und mich somit auch über die Zeit meines Forschungssemesters hinaus für die Forschung begeistert.

Des Weiteren möchte ich mich herzlich bei Herrn Alexander Herrmann, Juncal Fernández-Orth sowie Tobias Ruck bedanken, welche mich bei der Umsetzung von diversen Experimenten tatkräftig unterstützt haben.

Ich bedanke mich bei Monika Wart und Jeanette Budde für die praktische Anleitung und Hinweise zu Labortechniken sowie der Unterstützung und Hilfe beim Umsetzen verschiedener Experimente.

Frank Kurt möchte ich für seine Unterstützung und Mitorganisation bei der Umsetzung unserer tierexperimentellen Versuchsreihen danken.

Bei Heike Blum möchte ich mich gerne für die illustrative Inspiration bezüglich der Präsentation unserer Figuren und Darstellung der Ergebnisse bedanken.

Ich bedanke mich bei der Medizinischen Fakultät Münster über die Förderung dieser Dissertation im Rahmen des Promotionsstipendiums „Mediziner Kolleg Münster“.

Und natürlich bedanke ich mich bei meiner Familie und meinen Freunden, die mich während meines Studiums sowie dem Fertigstellen dieser Arbeit jederzeit unterstützt haben und mir mit wichtigen Ratschlägen sowie einer rettenden Tasse Kaffee beiseite standen.

12. Anhang

Table 1: Instruments

Instrument	**Manufacturer**
Autoclaver VX-95	Systec GmbH, GER
Axio Examiner	Zeiss, GER
Behavior Setup (Open Field + EPM)	Ethovision, Noldus IT, NLD
Casy Model TT cell counter	OLS Omni Life Science, GER
Centrifuge 5415R	Eppendorf, GER
Centrifuge 5810R	Eppendorf, GER
Centrifuge minister silverline	VWR, GER
Clean Bench, Hera Safe KS 12, 1/PE Ac	Thermo Scientific, Thermo Fisher Scientific, MA, USA
Distillery	
Electrophoresis chamber	Bio-Rad Hercules, USA
Fear Conditioning apparatus	TSE System GmbH Bad Homburg, GER
Gallios™ Flow Cytometer, 10 Colors/ 3 Laser	Beckmann Coulter, CA, GER
Incubator T5042 E	Heraeus, GER
Microplate Reader, Infinite M200 Pro Multimode	Tecan Life Science, CHE
NanoDrop™ 1000, spectrophotometer	Peq Lab Biotechnology, VWR, GER
pH-meter, S20 – SevenEasy™ pH	Mettler, Toledo, OH, USA

Pipette Controler, accu-jet pro	Brand GmbH & CoKG, GER
Pipette Research plus 0.5-10 µl, 10-100 µl, 20-200 µl, 100-1000 µl single channel	Eppendorf, GER
Pipette Research Plus, 30-300 µl, 12-channel	Eppendorf, GER
Pump 11 Elite	Havard Apparatus, MA, USA
StepOnePlus™ RT-PCR system	Applied Biosystem, Thermo Fisher Scientific, MA, USA
Titramax 101 platform shaker	Heidolph, GER
Thermocycler, Biometra Tprofessional TRIO	Analytik Jena, GER
Vortex mixer 7-2020	neoLab Migge GmbH, GER
Water bath	Memmert, GER

Table 2: Expandable Material and Reagents

Expendable Material	**Manufacturer**
6/12/24 well plates, flat bottom with lid	Corning costars, Corning, NJ, USA
96 well plate, flat bottom with lid	Cellstar Greiner bio-one, AUT
96 well plate, flat bottom with lid, white	Cellstar Greiner bio-one, AUT
96 well plate, U-bottom with lid	Cellstar Greiner bio-one, AUT
Adhesive qPCR seal	Sarstedt, GER
Agarose powder	Sigma-Aldrich St. Louis, USA

Biosphere filter tip, 0.1-20 µl ,2-20 µl, 2-100 µl, 2-200 µl, 100-1000 µl	Sarstedt, GER
CASYcups	OLS Omni Life Science, GER
Cell strainer, 40 µm mesh size	Falcon, Corning, NJ, USA
Discadit Luer slip syringe 2/5/10/20 ml	BD Bioscience, NJ, USA
Gloves, classic nitril, powder free	Abena, Denmark
Micro amp Fast-optical reaction plate with barcode	Applied Biosystem, Thermo Fisher Scientific, MA, USA
Multichannel Pipette	Eppendorf Hamburg, GER
PCR Tubes	
Pipette Tips	Eppendorf Hamburg, GER
Polyprophylene Conical Tube, 50 ml	Falcon, Corninh, NJ, USA
Protective Glove	Braun Melsungen, GER
Safe-Lock Tubes, 0.5/1.5/2.0 ml	Eppendorf, GER
Serological pipettes 5/10/25 ml, Stripette	Corning Costar, Corning, NJ, USa
Single-use hypodermic needles, Sterican	Braun, GER
Spin away filter	ZYMO Research Irvine, USA
Reagents	**Manufacturer**
5x Buffer (cDNA)	Thermo Fisher Scientific, MA, USA
Annexin V	Thermo Fisher Scientific, USA

Annexin Binding Buffer (5x)	Thermo Fischer Scientific Waltham, USA
Assay Buffer	BioLegend SAN Diego, USA
Bis-Cyclohexanone Oxaldihydrazone	Sigma-Aldrich Inc. Hamburg GER
Bovine serum albumin	Sigma-Aldrich, Merck, GER
CASYton	OLS O,ni Life Science, GER
Cell proliferation dye eFlour™ 670	Thermo Fisher Scientific, USA
Chloroform	Sigma-Aldrich Schnelldorf, GER
Dulbecco's Modified Eagle Medium (DMEM)	Gibco, Thermo Fisher Scientific, MA, USA
DEPC-H20	Thermo Fischer Scientific Waltham, USA
Detection Antibodies	BioLegend SAN Diego, USA
Dimethylsulfoxid (DMSO)	Carl Roth Karlsruhe, GER
Desoxyribonucleosidtriphosphate (dNTPs)	Thermo Fischer Scientific Waltham, USA
Ethanol	Merck Darmstadt, GER
Ethylenediaminetetra-acetic acid (EDTA) disodium salt dihydrate	Sigma-Aldrich, Merck, GER
Fixable viability dye eFlour™ 780	Thermo Fisher Scientific, USA
GeneRuler 50 bp DNA ladder	Thermo Fischer Scientific Waltham, USA
HEPES Buffer Solution (1M)	Gibco, Thermo Fisher Scientific, MA, USA
Isopropanol	Merck Darmstadt, GER

Maxima RT	Thermo Fisher Scientific, MA, USA
Penicillin/Streptomycin (P/S)	Sigma-Aldrich, Merck, GER
Phosphate-buffered Saline (PBS)	Sigma-Aldrich Schnelldorf, GER
qPCR MasterMix	Thermo Fisher Scientific, MA, USA
Random Hexamer	Thermo Fischer Scientific Waltham, USA
RedSafe™ Nuclear Acid Staining Solution	iNtRON Bio, Burlington USA
Retigabine	Cayman Chemicals (item No. 21449)
RiboLock RNase Inhibitor	Thermo Fisher Scientific, MA, USA
RNA Lysis Buffer	ZYMO Research Irvine, USA
RNA Prep Buffer	ZYMO Research Irvine, USA
RNAse Inhibitor	Thermo Fischer Scientific Waltham, USA
Sodium Azide (NaN_3)	Sigma-Aldrich, Merck, GER
Streptavidin-phycoerythrin (SA-PE)	BioLegend SAN Diego, USA
Standard Cocktail	BioLegend SAN Diego, USA
Taqman® reverse Transcriptase	Applied Biosystems Foster City, USA
Taq-Polymerase	Thermo Fischer Scientific Waltham, USA
Trizol	Invitrogen Carlsbad, USA
Washing Buffer for LegendPlex	BioLegend SAN Diego, USA
Washing Buffer for RNA Isolation	ZYMO Research Irvine, USA
XE991	Tocris (Catalog number: 2000)

Table 3: Antibodies and Primer

Antibody	**Clone/Isotype**	**Manufacturer**
Anti-mouse CD 3 purified	145-2C11	eBiosc. Frankfurt, GER
Anti-mouse CD 28 purified	37.51	Biolgened, CA, USA
Primer		Manufacturer
KCNQ 1 forward: 5´-GCC ACC GGG ACC CTC TTC TG-3´		Eurofins Scientific, LUX
KCNQ 1 reverse: 5´-GAT GCG GCC GGA CTC ATT CA-3´		Eurofins Scientific, LUX
KCNQ 2 forward: 5´-CAA GTA CCC TCA GAC CTG GAA C-3´		Eurofins Scientific, LUX
KCNQ 2 reverse: 5´-CAG CTC TTG GGC ACC TTG CT-3´		Eurofins Scientific, LUX
KCNQ 3 forward: 5´-CCA AGG ATG AAC CAT ATG TAG CC-3´		Eurofins Scientific, LUX
KCNQ 3 reverse: 5´-CAG AAG AGT CCA GAT GGG CAG GAC-3´		Eurofins Scientific, LUX
KCNQ 4 forward: 5´-CAT CGG GTT CCT GGT GCT CAT CTT-3´		Eurofins Scientific, LUX
KCNQ 4 reverse: 5´-TAG GCC CGG CTC GTG TCA GTG-3´		Eurofins Scientific, LUX
KCNQ 5 forward 1: 5´-CAT TGT TCT CAT CHC TTC A-3´		Eurofins Scientific, LUX
KCNQ 5 forward 2: 5´-CCA TTG TCA TCG CTT CA-3´		Eurofins Scientific, LUX

KCNQ 5 reverse: 5´-TCC AAT GTA CCA GGC TGT GA-3´	Eurofins Scientific, LUX

Table 4: Software

Software	**Manufacturer**
Adobe Illustrator	Adobe Inc. Mountain View, USA
EthoVision XT	Noldus, Wageningen, The Netherlands
GraphPad PRISM	Graphpadsoftware Inc. San Diego, USA
Kaluza Analysis Software	Beckman Coulter Life Science Brea, USA
LegenPlex analysis software	BioLegend SAN Diego, USA

Table 6: cytokine detection beats

Cytokine detection beat	**Manufacturer**
TNF a	BioLegend SAN Diego, USA
IFN y	BioLegend SAN Diego, USA
IL-2	BioLegend SAN Diego, USA
IL-6	BioLegend SAN Diego, USA
IL-10	BioLegend SAN Diego, USA
IL-17	BioLegend SAN Diego, USA

Table 7: TaqMan Primers

KCNQ subtype	**Primer**	**Manufacturer**
KCNQ1	Mm00434640_m1	Thermo Fisher Scientific USA
KCNQ2	Mm00440080_m1	Thermo Fisher Scientific USA
KCNQ3	Mm00548884_m1	Thermo Fisher Scientific USA
KCNQ4	Mm01185500_m1	Thermo Fisher Scientific USA
KCNQ5	Mm01226041_m1	Thermo Fisher Scientific USA

Landesamt für Natur,
Umwelt und Verbraucherschutz
Nordrhein-Westfalen

LANUV NRW, Postfach 10 10 52, 45610 Recklinghausen

Herrn
Prof. Dr. Dr. Sven G. Meuth
Institut f. Neuropathophysiologie u. Klinik f.
Neurologie, Universität Münster
Domagkstr. 13
48149 Münster

Auskunft erteilt:
Herr Skoff
Direktwahl 02361-305-3478
Fax 02361/305-3062
fachbereich84@lanuv.nrw.de

Aktenzeichen
84-02.04.2015.A585
bei Antwort bitte angeben
Ihre Nachricht vom:
Ihr Aktenzeichen:

Datum: 04.08.2016

Tierschutz
Genehmigung von Versuchen an Wirbeltieren gemäß § 8 Abs. 1 TierSchG i.V.m. § 33 TierSchVersV
Ihr Antrag vom 05.11.2015; mein Schreiben vom 30.03.2016; Ihre Antwort vom 12.04.2016; mein Schreiben vom 01.07.2016; Ihre Antwort vom 08.07.2016; eingegangen am 15.07.2016

Sehr geehrter Herr Prof. Dr. Dr. Meuth,

I. Gemäß § 8 Abs. 1 des Tierschutzgesetzes (TierSchG) in der derzeit gültigen Fassung i. V. m. § 33 der Verordnung zum Schutz von zu Versuchszwecken oder zu anderen wissenschaftlichen Zwecken verwendeten Tieren (Tierschutz-Versuchstierverordnung - TierSchVersV) vom 01. August 2013 (BGBl I, S.3125) erteile ich Ihnen unter dem Vorbehalt des jederzeitigen Widerrufs die Genehmigung zur Durchführung des nachstehenden Tierversuches:

„Funktionelle Charakterisierung demyelinisierender und inflammatorischer Läsionen in verschiedenen Tiermodellen der Multiplen Sklerose".

II. Die Verantwortung für die Durchführung des Tierversuchsvorhabens obliegt folgenden Personen:

Verantwortlicher Leiter: **Prof. Dr. Dr. Sven Meuth**
Stellvertretender Leiter: **Dr. Kerstin Göbel**

III. An der Durchführung des Tierversuchsvorhabens dürfen neben dem Leiter und dem Stellvertreter des Versuchsvorhabens folgende Personen beteiligt werden:

Hauptsitz:
Leibnizstraße 10
45659 Recklinghausen
Telefon 02361 305-0
Fax 02361 305-3215
poststelle@lanuv.nrw.de
www.lanuv.nrw.de

Dienstgebäude:
Hauptsitz Recklinghausen

Öffentliche Verkehrsmittel:
Ab Recklinghausen Hbf mit Buslinie 236 bis Haltestelle "Siemensstraße" und 5 Min. Fußweg oder mit Buslinie SB 20 bis Haltestelle "Hohenhorster Weg" und 15 Min. Fußweg in Richtung Trabrennbahn bis Leibnizstraße

Bankverbindung:
Landeskasse Düsseldorf
Konto-Nr.: 41 000 12
West LB AG
(BLZ 300 500 00)
BIC-Code: WELADEDD
IBAN-Code: DE 41 3005
0000 0004 1000 12

- Die in Ihrem Antrag unter Punkt 2.4.1-2.5 genannten Personen

IV. Die Versuche dürfen nur in den in Ihrem Antrag unter Punkt 1.2.1 genannten Räumlichkeiten durchgeführt werden.

V. Eine rückblickende Bewertung nach § 35 TierSchVersV ist nicht vorzunehmen.

VI. Die Genehmigung erstreckt sich auf Versuche mit :

Maus : 3816

VII. Sie haben folgende Auflagen zu beachten:

1. Ist ein Transport der Versuchstiere zwischen Operations- und Tierhaltungsraum unvermeidbar, so ist dafür Sorge zu tragen, dass mit Hilfe geeigneter Behältnisse dieser Transport so durchgeführt wird, dass negative Beeinflussungen durch äußere Einflüsse (z. B. Witterung, Lärm etc.) ausgeschlossen sind. Es ist insbesondere darauf zu achten, dass die Tiere keinen Temperaturschwankungen ausgesetzt sind.
2. Unabhängig von den im Antrag angeführten Abbruchkriterien ist der Versuch abzubrechen und das betroffene Tier tierschutzgerecht zu töten, wenn dies aufgrund des Zustandes des Tieres nach der Einschätzung des Tierschutzbeauftragten aus Tierschutzgründen unerlässlich ist.
3. Sie werden gebeten, nach Erhalt der Genehmigung eine aktualisierte Zusammenfassung elektronisch zu übersenden, die den Inhalt der Genehmigung vollständig und richtig darstellt.

VIII. Diese Genehmigung ist bis zum **31.08.2021** befristet.

IX. Dieser Bescheid ergeht gebührenfrei.

X

zu VIII.:
Diese Genehmigung ist zeitlich bis zum dem o. g. Termin befristet, so dass mir vor Ablauf der Genehmigungsfrist ggf. der Abschluss des Tierversuchsvorhabens mitzuteilen ist. Sollte das Tierversuchsvorhaben innerhalb des zeitlichen Genehmigungsrahmens noch nicht abgeschlossen sein, ist rechtzeitig vor Ablauf der Genehmigungsfrist - über den zuständigen Tierschutzbeauftragten - ein Antrag auf Verlängerung des Tierversuchsvorhabens zu stellen.

Rechtsbehelfsbelehrung:
Gegen diesen Bescheid kann innerhalb eines Monats nach Bekanntgabe Widerspruch bei dem Landesamt für Natur, Umwelt und Verbraucherschutz NRW, Leibnizstr. 10, 45659 Recklinghausen erhoben werden.

Mit freundlichen Grüßen
Im Auftrag

(Köbrich)

EINGEGANGEN 10. Mai 2017

Landesamt für Natur,
Umwelt und Verbraucherschutz
Nordrhein-Westfalen

LANUV NRW, Postfach 10 10 52, 45610 Recklinghausen

Herrn
Prof. Dr. Dr. Sven G. Meuth
c/o Dr. Hundehege Neurologie, ICB
Universitätsklinikum Münster
Mendelstr.7
48149 Münster

Auskunft erteilt:
Herr Skoff
Direktwahl 02361-305-3478
Fax 02361/305-3062
fachbereich84@lanuv.nrw.de

Aktenzeichen
84-02.04.2016.A307
bei Antwort bitte angeben
Ihre Nachricht vom:
Ihr Aktenzeichen:

Datum: 08.05.2017

Hauptsitz:
Leibnizstraße 10
45659 Recklinghausen
Telefon 02361 305-0
Fax 02361 305-3215
poststelle@lanuv.nrw.de
www.lanuv.nrw.de

Dienstgebäude:
Hauptsitz Recklinghausen

Öffentliche Verkehrsmittel:
Ab Recklinghausen Hbf mit Buslinie 236 bis Haltestelle "Siemensstraße" und 5 Min. Fußweg oder mit Buslinie SB 20 bis Haltestelle "Hohenhorster Weg" und 15 Min. Fußweg in Richtung Trabrennbahn bis Leibnizstraße

Bankverbindung:
Landeskasse Düsseldorf
Konto-Nr.: 41 000 12
West LB AG
(BLZ 300 500 00)
BIC-Code: WELADEDD
IBAN-Code: DE 41 3005
0000 0004 1000 12

Tierschutz
Genehmigung von Versuchen an Wirbeltieren gemäß § 8 Abs. 1 TierSchG i.V.m. § 33 TierSchVersV
Ihr Antrag vom 10.06.2016; mein Schreiben vom 10.01.2017; mein Schreiben vom 03.04.2017; Ihre Antwort vom 06.04.2017

Sehr geehrter Herr Prof. Dr. Dr. Meuth,

I. Gemäß § 8 Abs. 1 des Tierschutzgesetzes (TierSchG) in der derzeit gültigen Fassung i. V. m. § 33 der Verordnung zum Schutz von zu Versuchszwecken oder zu anderen wissenschaftlichen Zwecken verwendeten Tieren (Tierschutz-Versuchstierverordnung - TierSchVersV) vom 01. August 2013 (BGBl I, S.3125) erteile ich Ihnen unter dem Vorbehalt des jederzeitigen Widerrufs die Genehmigung zur Durchführung des nachstehenden Tierversuches:

„Zeit- und zelltypabhängige Regulation der Ionenhomöostase in der experimentellen autoimmunen Enzephalomyelitis als Tiermodell der Multiplen Sklerose".

II. Die Verantwortung für die Durchführung des Tierversuchsvorhabens obliegt folgenden Personen:

Verantwortlicher Leiter: **Herr Prof. Dr. Dr. Sven Meuth**
Stellvertretender Leiter: **Herr Prof. Dr. Heinz Wiendl**

III. An der Durchführung des Tierversuchsvorhabens dürfen neben dem Leiter und dem Stellvertreter des Versuchsvorhabens folgende Personen beteiligt werden:

- Die in Ihrem Antrag unter Punkt 2.4.1 -2.4.3 genannten Personen

IV. Die Versuche dürfen nur in den in Ihrem Antrag unter Punkt 1.2.1 genannten Räumlichkeiten durchgeführt werden.

V. Eine rückblickende Bewertung nach § 35 TierSchVersV ist nicht vorzunehmen.

VI. Die Genehmigung erstreckt sich auf Versuche mit :

Maus : 2430

VII. Sie haben folgende Auflagen zu beachten:

1. Ist ein Transport der Versuchstiere zwischen Operations- und Tierhaltungsraum unvermeidbar, so ist dafür Sorge zu tragen, dass mit Hilfe geeigneter Behältnisse dieser Transport so durchgeführt wird, dass negative Beeinflussungen durch äußere Einflüsse (z. B. Witterung, Lärm etc.) ausgeschlossen sind. Es ist insbesondere darauf zu achten, dass die Tiere keinen Temperaturschwankungen ausgesetzt sind.
2. Unabhängig von den im Antrag angeführten Abbruchkriterien ist der Versuch abzubrechen und das betroffene Tier tierschutzgerecht zu töten, wenn dies aufgrund des Zustandes des Tieres nach der Einschätzung des Tierschutzbeauftragten aus Tierschutzgründen unerlässlich ist.
3. Sie werden gebeten, nach Erhalt der Genehmigung eine aktualisierte Zusammenfassung elektronisch zu übersenden, die den Inhalt der Genehmigung vollständig und richtig darstellt.

VIII. Diese Genehmigung ist bis zum **31.05.2020** befristet.

IX. Für diesen Bescheid wird eine Gebühr erhoben. Hierzu ergeht ein gesonderter Gebührenbescheid.

Erläuterungen und Begründung:

zu I.:
Der Inhalt Ihrer Antragsunterlagen ist Gegenstand dieser Genehmigung. Änderungen sind dem Landesamt für Natur, Umwelt und Verbraucherschutz NRW unverzüglich - unter Angabe des Aktenzeichens - anzuzeigen (§ 34

Abs. 1 Nr. 4 TierSchVersV). Es wird empfohlen, allen an der Tierversuchsdurchführung beteiligten Personen diese Genehmigung zur Kenntnis zu geben. Der Tierschutzbeauftragte Dr. Martin Lücke und das zuständige Veterinäramt der Stadt Münster erhalten eine Durchschrift dieser Genehmigung.

Der Widerruf dieser Genehmigung kann erfolgen, wenn gegen diese Genehmigung verstoßen wird.
Außerdem kann die Einstellung des Tierversuchs gemäß § 16 a TierSchG angeordnet werden, wenn Tierversuche ohne die erforderliche Genehmigung oder entgegen tierschutzrechtlicher Bestimmungen durchgeführt werden.

Eventuell erforderliche Ausnahmegenehmigungen nach dem Tierschutzgesetz oder anderen gesetzlichen Bestimmungen bleiben von dieser Genehmigung unberührt.

zu II.:
Für die Einhaltung der Vorschriften des Tierschutzgesetzes sowie der in dieser Genehmigung angeführten Voraussetzungen ist der bzw. die oben bezeichnete Leiter/in des Tierversuchsvorhabens oder im Falle dessen/deren Verhinderung sein/ihr in dieser Genehmigung bezeichnete/r Vertreter/in verantwortlich (§ 30 TierSchVersV). Dabei ist jeder beabsichtigte Wechsel der Versuchsleiter- oder Stellvertreterposition dem Landesamt für Natur, Umwelt und Verbraucherschutz NRW unverzüglich anzuzeigen (§ 34 Abs. 2 TierSchVersV).

zu III.:
Die bezeichneten Personen dürfen ausschließlich die im Genehmigungsantrag aufgeführten Eingriffe oder Behandlungen im Rahmen der zulässigen Verantwortlichkeitsstufe durchführen. Zu beachten ist, dass Personen, die Eingriffe und Behandlungen innerhalb des Versuchsvorhabens durchführen sollen und die Voraussetzungen nach § 16 Abs. 1 Sätze 2 und 3 der TierSchVersV nicht erfüllen, erst nach Erteilung einer Ausnahmegenehmigung gem. § 16 Abs. 1 Satz 5 TierSchVersV durch die zuständige Kreisordnungsbehörde eingesetzt werden dürfen.

zu VIII.:
Diese Genehmigung ist zeitlich bis zum dem o. g. Termin befristet, so dass mir vor Ablauf der Genehmigungsfrist ggf. der Abschluss des Tierversuchsvorhabens mitzuteilen ist. Sollte das Tierversuchsvorhaben innerhalb des zeitlichen Genehmigungsrahmens noch nicht abgeschlossen

sein, ist rechtzeitig vor Ablauf der Genehmigungsfrist - über den zuständigen Tierschutzbeauftragten - ein Antrag auf Verlängerung des Tierversuchsvorhabens zu stellen.

Rechtsbehelfsbelehrung:
Gegen diesen Bescheid kann innerhalb eines Monats nach Bekanntgabe Widerspruch bei dem Landesamt für Natur, Umwelt und Verbraucherschutz NRW, Leibnizstr. 10, 45659 Recklinghausen erhoben werden.

Mit freundlichen Grüßen
Im Auftrag

(Köbrich)

Landesamt für Natur,
Umwelt und Verbraucherschutz
Nordrhein-Westfalen

LANUV NRW, Postfach 10 10 52, 45610 Recklinghausen

Herrn
Prof. Dr. Dr. Sven G. Meuth
Klinik für Allgemeine Neurologie
Universitätsklinikum Münster
Albert-Schweitzer-Campus 1, Gebäude A1
48149 Münster

Auskunft erteilt:
Frau Kögel
Direktwahl 02361 305-3255
Fax 02361 305-3062
fachbereich81@lanuv.nrw.de

DE-MAIL:
fachbereich81@lanuv-nrw.de-mail.de

Aktenzeichen
81-02.04.2018.A266
bei Antwort bitte angeben

Ihre Nachricht vom:
Ihr Aktenzeichen:

Datum: 26.02.2019

Hauptsitz:
Leibnizstraße 10
45659 Recklinghausen
Telefon 02361 305-0
Fax 02361 305-3215
poststelle@lanuv.nrw.de
www.lanuv.nrw.de

Dienstgebäude:
Hauptsitz Recklinghausen

Öffentliche Verkehrsmittel:
Ab Recklinghausen Hbf mit Buslinie 236 oder 237 bis Haltestelle "LANUV" und 5 Min. Fußweg oder mit Buslinie SB 20 bis Haltestelle "Hohenhorster Weg" und 15 Min. Fußweg in Richtung Trabrennbahn bis Leibnizstraße

Bankverbindung:
Landeshauptkasse NRW
Helaba
BIC-Code: WELADEDD
IBAN-Code:
DE 41 3005 0000 0004 1000 12

Tierversuche
Ihr Antrag auf Genehmigung eines Versuchsvorhabens gemäß § 8 Abs. 1 Tierschutzgesetz (TierSchG) i. V. m. § 31 Tierschutz-Versuchstierverordnung (TierSchVersV) vom 12.07.2018, eingegangen am 18.07.2018;
Rückfragen vom 08.10.2018
Ihr Schreiben vom 08.01.2019, eingegangen am 21.01.2019
Erneute Rückfragen vom 30.01.2019
Ihr Schreiben vom 07.02.2019, eingegangen am 18.02.2019

Sehr geehrter Herr Prof. Dr. Dr. Meuth,

I. Gemäß § 8 Abs. 1 Tierschutzgesetz (TierSchG) in der Fassung der Bekanntmachung vom 18.05.2006 (BGBL.I, S.1206,1313) in der derzeit geltenden Fassung i. V. m. § 33 der Verordnung zum Schutz von zu Versuchszwecken oder zu anderen wissenschaftlichen Zwecken verwendeten Tieren (Tierschutz-Versuchstierverordnung – TierSch-VersV) vom 01.08.2013 (BGBl. I, 3125) in der derzeit gültigen Fassung erteile ich Ihnen, unter dem Vorbehalt des jederzeitigen Widerrufs, die Genehmigung zur Durchführung des Tierversuches mit dem Titel:

"Die Rolle von TREK1 und Kv7.3 in der experimentellen autoimmunen Enzephalomyelitis"

LANUV
Kompetenz für ein lebenswertes Land

II. Die Verantwortung für die Durchführung des Tierversuchsvorhabens obliegt folgenden Personen:

Verantwortliche(r) Leiter(in): Herr Prof. Dr. Dr. Sven Meuth
Stellvertretende(r) Leiter(in): Frau Dr. Manuela Cerina

III. An der Durchführung des Tierversuchsvorhabens dürfen neben der/dem Leiter(in) und der/dem Stellvertreter(in) folgende Personen beteiligt werden:

Alle unter 2.4.1 bis einschließlich 2.5 aufgeführten Personen

IV. Die Versuche dürfen nur in der

- ZTE Hauptstelle, Albert-Schweitzer-Campus 1, Gebäude A8, Raum 106
- ZTE Außenstelle, Mendelstr. 7, 48149 Münster, Raum R0.62, R0.63, R0.65, R0.67, R0.68b, R0.69, R206, R0235, R329, R301, R352
- Institut für Physiologie I, Robert-Koch-Str. 27a, Münster, Raum 012 und 012a, Raum 101, Raum 102, Raum 104 und Raum 104c, Raum 309
- S2-Bereich am Institut für klinische Radiologie, Albert-Schweitzer-Campus 1, Gebäude A16

durchgeführt werden.

V. ☒ Eine rückblickende Bewertung nach § 35 TierSchVersV ist nicht vorzunehmen.

VI. Die Genehmigung erstreckt sich auf Versuche mit:

Tierart		Anzahl
Maus	:	**5.256**

VII. Sie haben folgende Auflagen zu beachten:

1. Ist ein Transport der Versuchstiere zwischen Operations- und Tierhaltungsraum unvermeidbar, so ist dafür Sorge zu tragen, dass mit Hilfe geeigneter Behältnisse dieser Transport so

durchgeführt wird, dass negative Beeinflussungen durch äußere Einflüsse (z.B. Witterung, Lärm, etc.) ausgeschlossen sind. Es ist insbesondere darauf zu achten, dass die Tiere keinen Temperaturschwankungen ausgesetzt sind.

2. Unabhängig von den im Antrag angeführten Abbruchkriterien ist der Versuch abzubrechen und das betroffene Tier tierschutzgerecht zu töten, wenn dies aufgrund des Zustandes des Tieres nach der Einschätzung der/des Tierschutzbeauftragten aus Tierschutzgründen unerlässlich ist.
3. Bitte teilen Sie nach Erhalt der Genehmigung mit, ob die von Ihnen eingestellte Nichttechnische Projektzusammenfassung (NTP) immer noch den Inhalt der Genehmigung vollständig und richtig darstellt und somit zur Veröffentlichung freigegeben werden kann. Andernfalls aktualisieren und übersenden Sie bitte die NTP mit der neuen ID-Nummer.

VIII. Diese Genehmigung ist bis zum 28.02.2024 befristet.

IX. Für diesen Bescheid wird eine Gebühr erhoben. Hierzu ergeht ein gesonderter Gebührenbescheid.

Erläuterungen und Begründung:

Zu I.:
Der Inhalt Ihrer Antragsunterlagen ist Gegenstand dieser Genehmigung. Jede Änderung ist dem Landesamt für Natur, Umwelt und Verbraucherschutz NRW (LANUV) unverzüglich - unter Angabe des Aktenzeichens - mitzuteilen (§ 34 Abs. 1 Nr. 4 TierSchVersV).

Es wird empfohlen, allen an der Tierversuchsdurchführung beteiligten Personen diese Genehmigung zur Kenntnis zu geben.
Der Tierschutzbeauftragte, Herr Dr. Martin Lücke, und das zuständige Veterinäramt der Stadt Münster erhalten eine Durchschrift dieser Genehmigung.

Der Widerruf dieser Genehmigung kann erfolgen, wenn gegen diese Genehmigung verstoßen wird.
Außerdem kann die Einstellung des Tierversuchs gemäß § 16a Abs. 1 Nr. 4 TierSchG angeordnet werden, wenn Tierversuche ohne die erforderliche Genehmigung oder entgegen tierschutzrechtlicher Bestimmungen durchgeführt werden.

Zu II.:
Für die Einhaltung der tierschutzrechtlichen Vorschriften zur Durchführung von Tierversuchen ist der bzw. die oben bezeichnete Leiter/in des Tierversuchsvorhabens oder im Falle deren/dessen Verhinderung ihr/sein in dieser Genehmigung bezeichnete/r Vertreter/in verantwortlich (§ 30 TierSchVersV).
Jeder beabsichtigte Wechsel der/des Versuchsleiterin/-leiters oder der Stellvertreterposition ist dem Landesamt für Natur, Umwelt und Verbraucherschutz NRW unverzüglich anzuzeigen (§ 34 Abs. 2 TierSchVersV).

Zu III.:
Die bezeichneten Personen dürfen ausschließlich die im Genehmigungsantrag aufgeführten Eingriffe oder Behandlungen im Rahmen der zulässigen Verantwortlichkeitsstufe durchführen. Zu beachten ist, dass Personen, die Eingriffe und Behandlungen innerhalb des Versuchsvorhabens durchführen sollen und die Voraussetzungen nach § 16 Abs. 1 Sätze 2 und 3 TierSchVersV nicht erfüllen, erst nach Erteilung einer Ausnahmegenehmigung gem. § 16 Abs. 1 Satz 5 TierSchVersV durch die zuständige Kreisordnungsbehörde eingesetzt werden dürfen.

Zu VIII.:
Die Genehmigung ist gem. § 33 Abs. 2 Satz 1 TierSchVersV auf höchstens fünf Jahre zu befristen.
Sofern die Befristung antragsgemäß weniger als fünf Jahre beträgt, kann ein Antrag auf Verlängerung gestellt werden. Der Antrag ist rechtzeitig vor Ablauf der Genehmigungsfrist – über den/die zuständige/n Tierschutzbeauftragte/n – zu stellen. Die Verlängerung kann gem. § 33 Abs. 2 Satz 2 TierSchVersV höchstens zweimal um jeweils bis zu einem Jahr erfolgen, wobei die Gesamtdauer der Genehmigung von fünf Jahren nicht überschritten werden darf.

Hinweis:
Eventuell erforderliche weitere Genehmigungen nach dem Tierschutzgesetz oder anderen gesetzlichen Bestimmungen bleiben von dieser Genehmigung unberührt.

Rechtsbehelfsbelehrung:
Gegen diesen Bescheid kann innerhalb eines Monats nach Bekanntgabe Klage beim Verwaltungsgericht Münster, Piusallee 38, 48147 Münster (Postfach 80 48, 48043 Münster), erhoben werden.

Die Klage ist schriftlich beim Verwaltungsgericht einzureichen oder zur Niederschrift der Urkundsbeamten der Geschäftsstelle zu erklären.

Landesamt für Natur,
Umwelt und Verbraucherschutz
Nordrhein-Westfalen

Die Klage kann auch durch Übertragung eines elektronischen Dokuments an die elektronische Poststelle des Gerichts erhoben werden. Das elektronische Dokument muss für die Bearbeitung durch das Gericht geeignet sein. Es muss mit einer qualifizierten elektronischen Signatur der verantwortenden Person versehen sein oder von der verantwortenden Person signiert und auf einem sicheren Übermittlungsweg gemäß § 55a Absatz 4 VwGO eingereicht werden. Die für die Übermittlung und Bearbeitung geeigneten technischen Rahmenbedingungen bestimmen sich nach näherer Maßgabe der Verordnung über die technischen Rahmenbedingungen des elektronischen Rechtsverkehrs und über das besondere elektronische Behördenpostfach (Elektronischer-Rechtsverkehr-Verordnung - ERVV) vom 24. November 2017 (BGBl. I S. 3803).

Mit freundlichen Grüßen
Im Auftrag

V. Reijak
Dr. Viviane Reijak